United States
Consumer Product Safety Commission

November 2022

CPSC Staff[1] Statement on SEA, Ltd. Report "Evaluation of Anti-Lock Brake System (ABS) Technology on ATV Stability"

The report titled, "Evaluation of Anti-lock Brake System (ABS) Technology on ATV Stability," presents the results of laboratory testing of two all-terrain vehicles (ATVs), one ATV equipped with ABS technology and one standard ATV without ABS technology. This work was conducted for CPSC under Task Order 4 of CPSC contract 61320618D0003.

SEA conducted a series of static and autonomously controlled dynamic tests (on asphalt, dry grass, wet grass, and groomed dirt surfaces) on a model year 2021 ATV model equipped with ABS and on the same model year 2021 ATV model without ABS. This exploratory work examined the potential stability and traction benefits of the ABS technology installed on ATVs. Other physical parameters were measured utilizing the SEA Vehicle Inertia Measurement Facility (VIMF), Tilt Table, and other laboratory equipment.

Although both vehicles performed well under tests, indicating relatively high degrees of stability compared to some other ATVs and good braking performance, the differences do indicate that ABS technology in ATVs provides a foundation for using that technology as part of a comprehensive package for ATV Electronic Stability Control (ESC). ESC has been shown to improve stability in on-road vehicles, and staff is interested in exploring the potential use in off-road vehicles, particularly in combination with ABS.

This report will assist CPSC staff as they continue to collaborate with the Specialty Vehicle Association of America (SVIA) and other interested parties to examine potential ATV safety improvements.

[1] This statement was prepared by the CPSC staff, and the attached report was produced by SEA for CPSC staff. The statement and report have not been reviewed or approved by, and do not necessarily represent the views of, the Commission.

U.S. Consumer Product Safety Commission
4330 East-West Highway
Bethesda, MD 20814

National Product Testing & Evaluation Center
5 Research Place
Rockville, MD 20850

Evaluation of Anti-lock Brake System (ABS) Technology on ATV Stability

Results from Tests on Two 2021 Model Year Vehicles

for:
Consumer Product Safety Commission

September 2021

Vehicle Dynamics Division
7001 Buffalo Parkway
Columbus, Ohio 43229

Evaluation of Anti-lock Brake System (ABS) Technology on ATV Stability

Results from Tests on Two 2021 Model Year Vehicles

for:
Consumer Product Safety Commission

"These comments are those of SEA, Ltd. staff, and they have not been reviewed or approved by, and may not necessarily reflect the views of, the Commission."

Report prepared by Gary J. Heydinger, Ph.D., P.E.,
with primary support from Scott Zagorski, Ph.D., P.E., Jim Nowjack,
Hank Jebode, Joe Yapp, Jon Coyle, and Dale Andreatta, Ph.D., P.E.

Vehicle Dynamics Division
7001 Buffalo Parkway
Columbus, Ohio 43229

TABLE OF CONTENTS

1. OVERVIEW

This report contains results from measurements made by SEA, Ltd. (SEA) for the Consumer Product Safety Commission (CPSC) under CPSC contract 61320618D0003, a contract that covers general testing and evaluation of All-Terrain Vehicles (ATVs).

This report covers work completed under Task Order 4 of contract 61320618D0003. The objective of Task Order 4 is the following:

- The objective of this task order is to evaluate Anti-lock Brake System (ABS) technology in ATVs, and its ability to be used by Electronic Stability Control (ESC) technology to improve vehicle stability. Specifically, the objective is to perform the following:
    - Conduct static and autonomously-controlled dynamic tests (on asphalt and groomed dirt surfaces) on an ATV model equipped with ABS
    - Conduct static and autonomously-controlled dynamic tests (on asphalt and groomed dirt surfaces) on the same model ATV not equipped with ABS

Specific tasks for Task Order 4 include:

1. Obtain and modify test vehicles (one with ABS and one without ABS) as required to adapt autonomous ATV Robotic Test Driver (RTD) to operate vehicle. This may require pneumatic or hydraulic control of brakes and throttle, sensors at each wheel, and modification of data acquisition instrumentation.
2. Measure static metrics and properties in four (4) loading conditions for each test vehicle.
    A. Curb weight
    B. Curb weight plus 95th percentile male
    C. Curb weight plus 95th percentile male plus max cargo load
    D. Curb weight plus instrumentation, RTD, safety outrigger, and driver ballast needed to match overall weight of B. above. This is the Autonomous Ballast to Driver Loading condition.
3. Conduct dynamic tests with ATD to evaluate rollover resistance and vehicle handling. Tests shall be conducted on paved and groomed dirt surfaces. The load condition for the testing is the representative Curb weight plus 95th percentile male condition. Test procedures will include J-turns, constant radius, and yaw rate ratio testing.

In addition to the tasks listed above, dynamic tests were also conducted to evaluate the braking characteristics of both vehicles. These tests included straight-line braking maneuvers on asphalt, groomed dirt, dry grass, and wet grass, as well as braking and turning maneuvers on wet grass.

This report contains test results for measurements made on two 2021 model year (MY) vehicles. The two vehicles are the same make and model. One of the vehicles, designated Vehicle M, does not have ABS, while the other vehicle, designated Vehicle N, is equipped with OEM ABS. The vehicles were selected by CPSC. They have straddle seating, and their intended use is for a single occupant, the driver. Both vehicles have handlebar (tiller) steering, thumb activated throttles, and hand and foot activated brakes.

Under a previous contract, U.S. Department of Health and Human Services (HHS) contract HHSP233201400030I, SEA made laboratory and dynamics measurements for CPSC on twelve MY 2014-2015 vehicles. The vehicles tested we designated Vehicle A through Vehicle L. Vehicles A-J were MY 2014 vehicles, and Vehicles K and L were MY 2015 vehicles.

This report contains results comparing laboratory and dynamic test measurements made on the two MY 2021 vehicles with the twelve MY 2014-2015 vehicles tested previously. Details of the previous laboratory results can be found in the CPSC report titled *Vehicle Characteristics Measurements of All-Terrain Vehicles – Results from Tests on Twelve 2014-2015 Model Year Vehicles*.[1] Details of the previous autonomously-controlled dynamic tests on asphalt can be found in the CPSC report titled *Effects on ATV Vehicle Characteristics of Rider Active Weight Shift – Results from Tests on Twelve 2014-2015 Model Year Vehicles*.[2] Details of the previous autonomously-controlled dynamic tests on groomed dirt can be found in the CPSC report titled *Vehicle Characteristics Measurements of ATVs Tested on Groomed Dirt Results from Tests on Twelve 2014-2015 Model Year Vehicles*.[3]

Table 1 contains a list of assorted vehicle information and tire specifications for the two MY 2021 vehicles tested during this study. Listed are the measured curb weight, measured maximum speed, transmission type, rear suspension type, and OEM driveline setting options. Both vehicles have open rear differentials, and they were tested in two-wheel drive mode. Table 1 also lists the front and rear tire make, tire size, and tire pressure for each vehicle.

The vehicles were evaluated using both laboratory measurements and dynamic tests. The laboratory measurements were made by SEA in Columbus, Ohio using their Vehicle Inertia Measurement Facility (VIMF), Tilt Table, and other laboratory equipment. The dynamic tests were performed by SEA on numerous dates between May 6, 2021 and August 5, 2021. The dynamic tests included steering and braking maneuvers on SEA's asphalt and groomed dirt vehicle dynamics test pads and grass-covered test area.

This report contains four main sections: Overview, Laboratory Testing, Dynamic Testing, and Discussion of Test Results. There are also four appendices containing test results, and one appendix containing photographs of test equipment.

---

[1] *Vehicle Characteristics Measurements of All-Terrain Vehicles – Results from Tests on Twelve 2014-2015 Model Year Vehicles*, HHS Contract HHSP233201400030I, SEA, Ltd. Report to CPSC, November 2016.
https://www.cpsc.gov/s3fs-public/SEA_Report_to_CPSC_Vehicle_Characteristics_Measurements_of_All_Terrain_Vehicles.pdf

[2] *Effects on ATV Vehicle Characteristics of Rider Active Weight Shift – Results from Tests on Twelve 2014-2015 Model Year Vehicles*, HHS Contract HHSP233201400030I, SEA, Ltd. Report to CPSC, January 2018.
https://cpsc-d8-media-prod.s3.amazonaws.com/s3fs-public/SEA-Report-to-CPSC-Rider-Active-ATV-Study-December-2017_0.pdf

[3] *Vehicle Characteristics Measurements of ATVs Tested on Groomed Dirt – Results from Tests on Twelve 2014-2015 Model Year Vehicles*, HHS Contract HHSP233201400030I, SEA, Ltd. Report to CPSC, February 2018.
https://www.cpsc.gov/s3fs-public/SEA-Report-to-CPSC-Groomed-Dirt-ATV-Study.pdf?eK1E6h7IXBtznyCDatWHofAoHHmwD_nr

Table 1: Test Vehicle Information and Tire Specifications		
Vehicle M – No ABS **Curb Weight: 931.4 lb** **Maximum Speed: 66.0 mph**	**Automatic Transmission** **Independent Rear Suspension** **2WD or 4WD**	
	Front Tires	Rear Tires
Tire Make	ITP Terra Cross R/T	ITP Terra Cross R/T
Tire Size	205/75R14 M/C 48M 6 Ply	255/65R14 M/C 55M 6 Ply
Tire Pressure (psi)	10.0	10.0
Vehicle N – ABS Equipped **Curb Weight: 951.0 lb** **Maximum Speed: 70.0 mph**	**Automatic Transmission** **Independent Rear Suspension** **2WD or 4WD**	
	Front Tires	Rear Tires
Tire Make	ITP Terra Cross R/T	ITP Terra Cross R/T
Tire Size	205/75R14 M/C 48M 6 Ply	255/65R14 M/C 55M 6 Ply
Tire Pressure (psi) For Driver plus Cargo < 155 kg (341 lb)	7.0	7.0
Tire Pressure (psi) For Driver plus Cargo > 155 kg (341 lb)	9.0	10.0

2. LABORATORY TESTING

This section describes the laboratory measurements made as well as computations of various rollover resistance metrics and other vehicle characteristics. This section is divided into four parts: one covering the vehicle loading conditions used for the tests, one covering the Vehicle Inertia Measurement Facility (VIMF) tests, one covering the Tilt Table tests, and one covering the steering ratio tests. Tabular results from all the measurements and metrics discussed in this section are contained in Appendix A.

2.1 Vehicle Loading Conditions

The four loading conditions described below were used for the laboratory tests.

1. **Curb (Curb Weight)**
   This loading condition is the curb weight of the vehicle, the as-received vehicle with no driver or ballast load and with full fuel and fluids.

2. **Driver (Curb Weight plus 95th Percentile Male)**
   This loading condition is specified to be the vehicle curb condition plus a 213 lb driver. For tests conducted in this loading condition, a test dummy weighing 213 lb was seated on each vehicle with its feet on the footrests and its hands attached to the handlebars. The vehicle weight for this loading is nominally 213 lb more than the vehicle curb weight.

3. **Gross Vehicle Weight (GVW) (Curb weight plus 95th Percentile Male plus Maximum Cargo Load)**
   This loading condition is referred to here as GVW loading, which includes adding a 213 lb driver and the specified maximum cargo weights allowed on the front and rear racks. GVW loading was achieved by adding maximum front rack ballast (100 lb) and maximum rear rack ballast (200 lb) to both vehicles as loaded in their Driver loading condition.

4. **Autonomous Ballast to Driver Loading**
   This loading condition is Curb weight plus instrumentation, RTD, safety outrigger, and driver ballast needed to match the overall weight of the Driver loading condition.

The VIMF and Tilt Table tests were conducted in all four loading conditions. The dynamic tests were conducted in the Autonomous Ballast to Driver Loading condition.

2.2 Vehicle Inertia Measurement Facility (VIMF) Tests

Laboratory measurements of vehicle weight (including the four corner weights); vehicle center-of-gravity (CG) position (longitudinal, lateral, and vertical (CG height)); vehicle pitch, roll, and yaw moments of inertia; and roll/yaw product of inertia were made by SEA using their Vehicle Inertia Measurement Facility (VIMF).[4] Measurements of front track width, rear track width, and wheelbase were also made.

The vehicle CG longitudinal position is expressed as a distance from the front axle. The vehicle CG lateral position is expressed as a lateral distance from the vehicle centerline; CG positions to

[4] *The Design of a Vehicle Inertia Measurement Facility*, Heydinger, G.J., Durisek, N.J., Coovert, D.A., Guenther, D.A., and Novak, S.J., SAE Paper No. 950309, February 1995.

the right of the centerline are positive. The vehicle CG height is expressed as the distance of the vehicle center of gravity above the road plane.

The moments and product of inertia for a vehicle are computed relative to the vehicle's center of gravity, using an orthogonal coordinate system with its origin at the vehicle center of gravity. The X-axis of the coordinate system is directed forward and parallel to the road plane, the Y-axis is directed to the driver's right and is also parallel to the road plane, and the Z-axis is directed downward.

In addition to the direct measurements provided by the VIMF, two other metrics that are used to characterize vehicle rollover resistance were computed, namely, the Static Stability Factor (SSF) and the lateral stability coefficient (K_{ST}).

SSF is a fundamental rollover resistance metric which equals the lateral acceleration in units of g at which rollover begins in the most simplified rollover analysis of a vehicle represented by a rigid body without suspension movement or tire deflections. SSF is given by:

$$SSF = \frac{T_{AVE}}{2 \times H_{CG}}$$

where: T_{AVE} is the Average Track Width, and
H_{CG} is the Vehicle CG Height.

K_{ST} is similar to SSF in that it represents the acceleration in g's at which rollover begins in the most simplified rollover analysis of a vehicle with different front and rear track widths represented by a rigid body without suspension movement or tire deflections. For vehicles with equal front and rear track widths, K_{ST} and SSF are equal. K_{ST} is given by:

$$K_{ST} = \frac{L \times T_R + L_{CG} \times (T_F - T_R)}{2 \times L \times H_{CG}}$$

where: L is the Vehicle Wheelbase,
T_F is the Front Track Width,
T_R is the Rear Track Width, and
L_{CG} is the Longitudinal Distance from the Rear Axle to the CG, and
H_{CG} is the Vehicle CG Height.

Appendix A contains results from all the VIMF tests conducted on both vehicles in all four loading conditions.

2.3 Tilt Table Tests

SEA built a tilt table consisting of a rigid steel platform mounted on top of a yaw bearing, shown in the photographs on Page 1 of Appendix E (the vehicle shown is not Vehicle M or Vehicle N). The yaw bearing allows the platform to be rotated so that lateral tilts (left-side leading and right-side leading), forward tilts (front-end leading), and rearward tilts (rear-end leading) can be conducted without removing and reloading the vehicle. A hydraulic cylinder was used to tilt the yaw bearing and platform assembly, up to 60 degrees from horizontal.

Tilt Table tests were conducted in all four loading conditions for both vehicles, and tilts were conducted in four directions: left-side leading, right-side leading, front-end leading, and rear-end leading.

For the lateral tilts, the vehicles were tilted in a direction nominally parallel to their longitudinal or roll axis. The outsides of the low side tires were aligned to be parallel to the tilt axis prior to testing. The platform was gradually tilted to the point when both high side tires lifted off the platform. The vehicles were prevented from tilting completely off the platform by straps that restrained further tilting once the high side tires lifted about two to three inches off the platform. A high friction surface, an aluminum plate with its top surface covered with marine grade safety walk paint, was secured to the platform in the areas beneath all four tires. This surface prevented the vehicles from sliding sideways during the lateral tilt table tests.

For the longitudinal tilts (the forward and rearward tilts), the vehicles were tilted in a direction nominally parallel to their pitch axis. To prevent the vehicles for rolling during these tests, the vehicle transmissions were locked (they were put in park or in gear), their hand brakes were applied using a hose clamp, and if necessary, straps were wrapped around the front and/or rear tires and secured to the vehicle chassis. The forward and rearward tilt angles needed to get two-wheel lift are greater than the tilt angles needed to get lateral tilt two-wheel lift. As was done during previous ATV longitudinal tilt table tests conducted by SEA for CPSC, to prevent the ATV tires from sliding off the tilt table platform at high tilt angles, a 2-inch-high trip rail (a 2x2 inch square aluminum tube) was used for all longitudinal tilt table tests. The tires were rolled up against the 2-inch-high trip rail prior to locking the transmissions, setting the brakes, and applying the roll-preventing tire straps.

For the longitudinal tilts, the low side tires were aligned to be parallel to the tilt axis. The platform was gradually tilted to the point when both high side tires lifted off the platform. The vehicles were prevented from pitching completely off the platform by straps that restrained further tilting once the high side tires lifted about two to three inches off the platform.

The important factors involved in accurate tilt table testing include having a rigid and flat platform; having the ability to produce slow, smooth, and consistent tilt rates; and having accurate and repeatable measures of tilt angle and point of wheel lift. The SEA tilt table platform is very rigid, and it was designed to have deflections of less than 0.1 inch for all ATV vehicles tested. It is also very flat, with a flatness tolerance of ±0.1 inch. The hydraulic cylinder used to tilt the platform is controlled to provide for smooth tilting at rates as slow as 0.1 deg/sec.

A high-accuracy, two-axis (one aligned with the right/left tilt axis and one aligned with the fore/aft tilt axis) angle sensor is mounted to the platform to record the tilt angles throughout the tilt table tests. The point of two-wheel lift is determined visually, and the observer generates a signal that is recorded by the data acquisition system by pushing a button on a handheld trigger. Typically, five or six tilts to two-wheel lift were conducted for each vehicle configuration tested. The tests with the closest three angles of two-wheel lift were selected and averaged together to determine the final angle of two-wheel lift. Based on repeatability evaluations conducted using a range of ATVs, SEA thinks that the repeatability of the measurements of two-wheel lift is within ±0.1 degrees.

For left side leading and right side leading tilts, the angle at which two-wheel lift occurs is referred to as the Tilt Table Angle (TTA). In addition to measuring TTA, the tilt table test results provide a measure of the rollover resistance metric Tilt Table Ratio (TTR). TTR is the tangent of the TTA. TTR values are lower than SSF values because suspension and tire deflections during the tilt table tests reduce the effective track widths below the values based on the rigid body concept that is the basis for SSF. During tilt table tests the load perpendicular to the road plane decreases causing the CG to rise, which also contributes to TTR being less than SSF. TTR is computed mathematically using:

$$\mathrm{TTR} = tan\left(\mathrm{TTA}\right)$$

For front end leading tilts, the angle at which two-wheel lift occurs is referred to here as Forward Tilt Table Angle (FTTA); and for rear end leading tilts, the angle at which two-wheel lift occurs is referred to here as Rearward Tilt Table Angle (RTTA). In addition to measuring FTTA and RTTA, the tilt table test results provide measures of a vehicle's pitch-over resistance, metrics referred to here as Froward Tilt Table Ratio (FTTR) and Rearward Tilt Table Angle (RTTR). FTTR and RTTR are computed using:

$$\mathrm{FTTR} = tan\left(\mathrm{FTTA}\right)$$

$$\mathrm{RTTR} = tan\left(\mathrm{RTTA}\right)$$

Appendix A contains results from all the tilt table tests conducted on both vehicles in all four loading conditions.

2.4 Steering Ratio Tests

Steering ratio tests were conducted with the vehicles in their Autonomous Ballast to Driver Loading condition. The steering ratio tests consisted of placing the front tires on commercial low friction wheel alignment pads and placing the rear tires on blocks of the same thickness as the alignment pads. The steering column angle (the handlebar angle) was measured using the RTD's steer angle sensor, and the right and left roadwheel angles are measured using the angle gages on the alignment pads. To conduct the tests, the steering handlebar was moved incrementally from zero degrees, to its full lock position to the right, to its full lock position to the left, and returned back to zero degrees. The handlebar angle increments used were 0°, ±5°, ±10°, ±15°, ±20°, ±30°, ±40°, and full lock in both directions. Both the right side and left side roadwheel angles were recorded at all steering positions. Linear curve fits of the measured data in the range of ±10° of steering column (handlebar) angle were used to compute the overall steering ratios. The overall steering ratios for the two vehicles tested during this study are listed in Appendix A, and graphical results from these tests are contained in Appendix C.

3. DYNAMIC TESTING

This section describes the dynamic tests conducted on numerous dates between May 6, 2021 and August 5, 2021. Both vehicles were tested at SEA in Columbus, Ohio, on their asphalt and groomed dirt vehicle dynamics test pads, and on a grass-covered area adjacent to the parking lot of the office building at SEA. The grass area is relatively flat, and it contains mostly fescue grass mowed weekly to about three inches in height.

Both vehicles tested have automatic transmissions and they were tested in two-wheel drive mode, and in their most-open driveline configuration.

3.1 Vehicle Loading Condition

The loading condition used for the dynamic testing was the Autonomous Ballast to Driver Loading condition, representing a 213 lb driver only loading condition. Pages 2-4 of Appendix E contain photographs of one of the fully loaded and instrumented vehicles.

The Autonomous Ballast to Driver Loading is the vehicle curb weight plus the weight (nominally 213 lb) of the test instrumentation and equipment that included: measurement transducers, SEA's ATV RTD, SEA's ATV safety outrigger, wheel speed sensors, and a driver ballast weight frame.

Page 2 of Appendix E shows the safety outrigger mounted beneath the vehicle, the wheel speed sensors on the left side of the vehicle, and the driver ballast weight frame. The weight frame, constructed of 80/20 T-slot aluminum bars, is used to rigidly hold enough weight to bring the total test weight up to nominally 213 lb above the curb weight for each vehicle. The only weight added to the ballast frame for this study was a 12V battery (used to provide power to the RTD and test equipment) attached to the top of the frame.

The ATV RTD consists of a computer-controlled 24V electric motor (rotary actuator) that mounts to the front rack of an ATV for steering control. A four-bar linkage arrangement is used to connect the motor drive gear to an aluminum rod that is connected to the ATV steering column beneath the ATV handlebars. For throttle control, the ATV RTD includes a computer-controlled 24V electric motor (rotary actuator), with a pulley and wire attachment to the throttle lever, mounted to the aluminum rod. The RTD version used for this study also included a computer-controlled 24V electric motor (linear actuator) to actuate the left hand brake. The left hand brake lever was removed from the its handlebar mount, and replaced on the front base plate in line with the linear actuator. This configuration provided precise control of the braking inputs needed for the tests involving braking. Page 3 of Appendix E contains photographs of the RTD actuators used for this study. The ATV RTD also includes a GPS/IMU (OxTS RT3002), an electronics box (with a National Instruments (NI) cRIO, the on-vehicle computer with the motor controllers and data acquisition software), an auxiliary 24V battery, and antennas for wireless communication. Page 4 of Appendix E contain photographs of these items.

Table 2 lists the nominal weights of the components that comprise the Autonomous Ballast to Driver Loading condition.

Table 2: Autonomous Ballast to Driver Loading	
Component	**Nominal Weight (lb)**
Components Mounted at Front of Each Vehicle Base Plate, Steer Actuator, Throttle Actuator, Brake Actuator, and Associated Mounts and Linkages	46.1
Components Mounted at Rear of Each Vehicle Base Plate, Electronics Box, GPS/IMU (RT3002), 24V Battery, and Antennas	62.3
Standard ATV Outrigger	30.8
Wheel Speed Sensors and Associated Electronics	19.8
Weight Frame and Miscellaneous Ballast	54.0
Total Nominal Driver Only Weight	**213.0**

3.2 Test Instrumentation

The on-vehicle instrumentation used during the dynamic testing is listed in Table 3. The GPS/IMU RT3002 was mounted on the rear base frame of each vehicle. For both vehicles tested, the longitudinal, lateral, and vertical offsets from the center of the RT3002 to the actual vehicle CG location were measured and entered into the RT3002 system software. This information was used to translate the measured quantities to those at the CG of the vehicle. The lateral accelerations measured and reported herein are accelerations parallel to the road plane, as opposed to vehicle body-fixed accelerations.

Table 3: Instrumentation Used During Dynamic Testing			
Transducer	**Measurement**	**Range**	**Accuracy**
Oxford Technical Solutions (OxTS) RT3002 Inertial and GPS Navigation System	Longitudinal, Lateral, and Vertical Accelerations	± 100 m/s^2 (± 10 g)	0.01 m/s^2 (0.001 g)
	Roll, Pitch, and Yaw Rates	± 100 deg/s	0.01 deg/s
	Speed	No Limit Specified	0.05 km/h (0.03 mph)
	Roll and Pitch Angles	-180 to +180 deg	0.03 deg
	Vehicle Heading	0 to 360 deg	0.1 deg
Wheel Speed Encoders WPT/E512	Wheel Speeds	2,000 rpm Maximum	± 0.25 deg

3.3 Constant Radius (50 ft) (Circle) Tests

Constant Radius or Circle tests are used to evaluate vehicle understeer characteristics.[5] A Constant Radius test involves driving a vehicle on a circular path of constant radius (50 ft in this case). The test vehicles were autonomously driven in both the clockwise and counterclockwise directions. The ATV RTD was used to steer the vehicles and control the vehicle throttle (speed) during these tests.

A circular path of 50 ft radius was generated in GPS coordinates and the "path-following" feature of the RTD was used to control the steering input during these tests. The path-following algorithm has a collection of parameters used to model driver look-ahead distance, vehicle steering properties, and other steering-related control gains that were adjusted to provide good path following for each vehicle tested.

For these vehicles with automatic transmissions, the throttle input was increased in piecewise linear steps to generate speed profiles from a very low speed up to a speed where the lateral acceleration exceeded 0.45 g.

Constant Radius tests were used to determine if the vehicles transitioned from understeer to oversteer during the tests. Roll gradients, vehicle roll angle response as a function of lateral acceleration, were also computed from these tests. Detailed results from the Constant Radius tests are contained in Appendix C.

3.4 Dropped Throttle J-Turn (Step Steer) Tests (Initial Speed of 20 mph)

J-Turn tests, often referred to as step steer tests, involve imparting a rapid steering input up to a fixed magnitude while the vehicle is traveling along a straight path. For the dropped throttle J-Turn tests, the RTD drove each vehicle along a straight-line path (defined by GPS coordinates) from low speed up to a speed of 21 mph. Once 21 mph was achieved, the RTD then dropped the throttle and triggered the steering input precisely when the vehicle speed reached 20 mph. The handlebar (motor) steering input rates used were 40 deg/sec, and the steering dwell or hold time used was 6.0 seconds, at which time the steering angle was programmed to return to 0 deg.

The J-Turn test procedure involved initially running tests with steering magnitudes less than the steering required to produce tip-up events, events that have visual two-wheel lift outcomes. The handlebar steering input magnitude was gradually increased in 1.0 degree increments to the point where a test run resulted in a two-wheel lift event. Then another test run using 0.5 degrees less steering input was used to refine the steering required for two-wheel lift. Once the steering input magnitude required for visual two-wheel lift was determined, repeat test runs using this steering input were conducted. For testing on asphalt, typically the repeat runs using this same steering input could be used to produce three runs that resulted in visual two-wheel lift. However, on the groomed dirt surface the steering magnitudes required for two-wheel lift are not as consistent as they are on asphalt. For some ATVs, when testing on the groomed dirt the steering inputs required for two-wheel lift had to be varied up or down by 0.5-1.0 degrees to get runs that resulted in visual two-wheel lifts. Nonetheless, all the two-wheel lift outcome results contained in this report are for runs that had visual two-wheel lift.

[5] SAE Surface Vehicle Recommended Practice - Steady-State Directional Control Test Procedures for Passenger Cars and Light Trucks, SAE J266, 1996.

These tests provided a measure of the minimum peak lateral acceleration (Threshold Ay) required to cause visual two-wheel lifts during the tests. Detailed results from the Dropped Throttle J-Turn tests are contained in Appendix C.

3.5 Constant Steer Tests (Yaw Rate Ratio Tests)

Constant Steer tests are yet another well-established method used to evaluate a vehicle's understeer characteristics.[6] The ROV industry groups ROHVA and OPEI, as well as CPSC, have used Constant Steer tests to evaluate vehicle yaw rate divergence. The industry groups have developed protocols for computing the ratio of yaw rate gain at a high lateral acceleration range (0.4-0.5 g) divided by the yaw rate gain at a low lateral acceleration range (0.1-0.2 g), and this ratio is referred to here as Yaw Rate Ratio. ROHVA[7] and OPEI[8] have industry voluntary standards that describe similar test and data reduction protocols for computing Yaw Rate Ratio for ROVs. The same test and data reduction protocols were used for the current ATV testing. The only significant difference is that for the ATV testing, the high range of lateral accelerations was reduced to a range of 0.3-0.4 g.

The test procedure used for the Yaw Rate Ratio tests was:

1. The test procedure for tests conducted on asphalt was: Follow a 100 ft diameter (50 ft radius) circle at a speed less than 10 mph until the mean steer angle required to maintain the circular path is established (this is referred to as "initial steer" in this report). If a vehicle understeers during portions of a Yaw Rate Ratio test, its path radius can increase, based on the amount of its understeer. If the path of a vehicle becomes large enough to potentially run off the available test surface, a starting diameter of 50 ft may be used. The first constant steer tests conducted using Vehicle M did result in increased radius, so the option to use a 50 ft diameter to establish the initial steer was used for Vehicle M and Vehicle N. The initial steer angle that was established and used for the tests conducted on asphalt was also used for the tests conducted on groomed dirt.
2. The ATV RTD was then used to steer the steering column (handlebars) to the initial steer angle and hold it there for the duration of the test.
3. The vehicle was then steadily accelerated at a rate not to exceed 1 mph/second. Efforts were made to program the RTD throttle to complete each test run in 30-60 seconds.
4. The tests were ended by the RTD program when a lateral acceleration above 0.4 g was achieved.
5. Items 2-4 were repeated until at least five runs in the first steer direction were completed.
6. Item 1 was repeated in the opposite steer direction, and then Items 2-4 were repeated until at least five runs in the opposite steer direction were completed.

These tests provided a measure of the Yaw Rate Ratios (defined in Section 4.2.3). Detailed results from the Constant Steer tests (Yaw Rate Ratio tests) are contained in Appendix C.

---

[6] Ibid

[7] American National Standard for Recreational Off-Highway Vehicles, ANSI/ROHVA 1-2016, May 2016.

[8] American National Standard for Multipurpose Off-Highway Utility Vehicles, ANSI/OPEI B71.9-2016, August 2016.

3.6 Dynamic Tests Involving Braking

One objective of this task order was to evaluate the ability of Anti-lock Brake System (ABS) technology in ATVs to be used by Electronic Stability Control (ESC) technology to improve vehicle stability. Braking tests were conducted on Vehicle M, the vehicle without ABS, and on Vehicle N, the vehicle equipped with ABS, to gain understanding about the performance of the ABS system and how an ABS equipped ATV might perform differently than a similar ATV not equipped with ABS.

The ABS system on Vehicle N is designed to prevent the front or rear wheels from locking up when either the hand brake, foot brake, or both brakes are applied. There are three wheel speed encoders on Vehicle N, one for the front right wheel, one for the front left wheel, and one for the rear wheels. The ABS technology algorithm uses information from these encoders to detect wheel slip and sense pending wheel lock. If pending wheel lock is sensed during braking maneuvers, the ABS system will off-and-on cycle braking commands to provide braking without locking the wheels.

The hand brake only was used for all braking tests conducted using both Vehicles M and N. Both vehicles have hydraulic disc brakes at the front right wheel, the front left wheel, and the rear right wheel. Also, for both vehicles the hand brake activates both the front and rear brakes.

The first vehicle tested in this study was Vehicle M, the vehicle without ABS. A protocol was established to conduct straight-line braking runs at different levels of braking, including maximum braking using the hand brake. The purpose of conducting these tests on Vehicle M was to establish test conditions that would result in locked wheel braking. The straight-line braking runs were dropped throttle maneuvers, with the throttle dropping when the vehicle speed reached 21 mph, and the hand brake being applied when the vehicle speed reached 20 mph. The RTD was in (straight line) path following mode during the entire braking event, all the way until the vehicle speed came to a stop. Hand brake inputs were controlled using the brake actuator feature of the RTD, and inputs needed to generate nominally 0.40 g deceleration, nominally 0.55 g deceleration, and maximum hand brake deceleration were used for the tests.

For Vehicle M, none of the straight-line braking maneuvers resulted in any wheel lockup on asphalt or groomed dirt. Vehicle M was then tested on dry grass, and again none of the straight-line braking maneuvers resulted in any wheel lockup. To promote wheel lockup under braking, the grass was sprayed with water to reduce the coefficient of friction between the tires and surface. When tested on wet grass, the front wheels of Vehicle M locked up during maneuvers using the two most severe braking levels. More will be said about these results in Section 4.3.

After establishing the fact that heavy braking on Vehicle M could result in locked front wheels on wet grass, braking and turning maneuvers were conducted on wet grass using both vehicles. These maneuvers were to show differences in responses resulting from no ABS versus ABS. The braking and steering maneuvers were 20 mph, dropped throttle, J-turns with braking applied either at the onset of steering or delayed by 0.5 sec after the start of the steering input.

To summarize, for both Vehicles M and N, braking maneuvers included varying severity straight-line braking tests on asphalt, groomed dirt, dry grass, and wet grass, as well as braking and turning maneuvers on wet grass. Braking test results are contained in Appendix D.

4. DISCUSSION OF TEST RESULTS

Appendix A (Laboratory Test Results) contains tables with results from the laboratory tests conducted on Vehicle M and Vehicle N. Appendix B (Cumulative Laboratory Test Results) contains bar charts of key laboratory metrics for Vehicles M and N, as well as for the Vehicles A-L (the ATVs tested previously for CPSC).[9] Graphical results from the dynamic tests that did not include braking are contained in Appendix C (Dynamic Test Results) and from dynamic tests that included braking are in Appendix D (Braking Test Results).

4.1 Discussion of Laboratory Test Results

Appendix A contains tabular results of laboratory measurements made by SEA. There are four pages of results, two pages for each vehicle. The first page for each vehicle contains a table of results from the VIMF and Steering Ratio tests, and the second page for each vehicle contains a table of results from the Tilt Table tests.

The first 19 rows of the first page for each vehicle contain measurements related to the mass (weight), track width, wheelbase, center-of-gravity location, and inertia properties, as well as static rollover propensity calculations, based on measurements made using the VIMF. These measurements are shown for all four laboratory loading conditions tested. The final row contains the value for steering ratio, measured in the Autonomous Ballast to Driver Loading condition.

The second page of tabular results for each vehicle lists the tilt table angles and tilt table ratios for the lateral and longitudinal Tilt Table tests conducted. These tables also list which wheel lifted first for each Tilt Table test; either Front or Rear for the lateral tilts and either Right, Left, or Equal (indicating simultaneous right and left wheel lift) for the longitudinal tilts.

Appendix B contains five pages, each containing two bar charts with results from laboratory measurements made on 14 ATVs in the Driver loading condition. The charts are useful for gauging how the two MY 2021 sister vehicles (Vehicle M without ABS and Vehicle N with ABS) compare with the ATVs tested previously (Vehicles A-J are MY 2014 vehicles and Vehicles K and L are MY 2015).

Vehicle M and N are similar in weight and size (i.e., similar wheelbase and trackwidth) to each other. They are heavier than any of the 12 MY 2014-15 vehicles tested, and they are among the vehicles with the largest wheelbases and track widths.

Vehicle N has a lower CG height than Vehicle M. In the Driver loading condition, the OEM-specification tire pressure for Vehicle N (the vehicle equipped with ABS) is lower than the tire pressure for Vehicle M. This accounts for some of the difference in CG height, but not all of it. The chassis of Vehicle N sits closer to the ground than the chassis of Vehicle M, by an amount consistent with their differences in CG height. Since Vehicle N has a lower CG height than Vehicle M, it has higher SSF and KST values than Vehicle M. However, compared to all the vehicles tested, the SSF and KST values for both Vehicles M and N are in the higher range of values, among the other larger vehicles tested previously.

---

[9] *Vehicle Characteristics Measurements of All-Terrain Vehicles – Results from Tests on Twelve 2014-2015 Model Year Vehicles*, HHS Contract HHSP233201400030I, SEA, Ltd. Report to CPSC, November 2016. https://www.cpsc.gov/s3fs-public/SEA_Report_to_CPSC_Vehicle_Characteristics_Measurements_of_All_Terrain_Vehicles.pdf

The TTR, FTTR, and RTTR values for Vehicle N are less than those for Vehicle M, although Vehicle N has a lower CG height. The reason for this is likely because Vehicle N has a lower tire pressure than Vehicle M, and thus there is more tire deflection, which decreases the TTR values. Compared to all the vehicles tested, the TTR, FTTR, and RTTR values for both Vehicles M and N are in the higher range of values, among the other larger vehicles tested previously. Likewise, the steering ratio and measured maximum speed for Vehicles M and N are in the range of values for the other larger vehicles tested previously.

The two MY 2021 ATVs (Vehicles M and N) weighed more than any of the other twelve MY 2014-2015 ATVs test previously. Nevertheless, the laboratory measurements for SSF, KST, and TTR indicate that the rollover resistance of Vehicles M and N are generally like the other larger MY 2014-2015 vehicles tested previously.

4.2 Discussion of Dynamic Test Results

Appendix C contains the graphical and tabular test results for both vehicles tested in the Autonomous Ballast to Driver Loading condition. All test results for each vehicle are presented together, with results for Vehicle M on Pages 1-33 and Vehicle N on Pages 34-66 of Appendix C. For both vehicles there are 16 pages of results from dynamic tests conducted on asphalt followed by 16 pages of results for tests conducted on groomed dirt. The last page for each vehicle contains results from its steering ratio test. The sections of graphical results for each vehicle and test surface are in the following order:

- Constant Radius (50 ft) (Circle) Tests
- Dropped Throttle J-Turn (Step Steer) Tests (Initial Speed of 20 mph)
- Constant Steer Tests (Yaw Rate Ratio Tests)

The discussion in this section will cover each test in the order listed above. A couple of general comments regarding the graphs presented for all test types are:

- The lateral accelerations shown on the graphs are the lateral accelerations parallel to the road plane, not the vehicle body-fixed lateral accelerations.
- The steering angles shown on the graphs are roadwheel steer angles, which are the RTD steer actuator input angles (handlebar angles) divided by the measured steering ratio.

4.2.1 Constant Radius (50 ft) (Circle) Tests

For each vehicle there are four pages showing results from both the clockwise (CW) and counterclockwise (CCW) Circle tests. The first page shows time domain plots of Roadwheel Steer Angle, Lateral Acceleration, Speed, Roll Angle, and Yaw Rate. All the dynamic test data was sampled at 100 Hz. For the Circle test results, the data shown was digitally low-pass filtered to 1.0 Hz using a phaseless, eighth-order, Butterworth filter. The vehicle speed was increased up to the time when lateral acceleration level exceeded 0.45 g, at which time the RTD dropped the throttle and then ended the maneuver and data collection. The time domain data is plotted from about three seconds prior to the time the vehicle starts to move until the time when the RTD routine ends the data collection.

On the first page of Circle test graphs for each vehicle, the thin black lines for the CW and CCW tests show the full range of data collected. The thicker lines (red for CW and blue for CCW) indicate the range of data used to fit the subsequent understeer and roll gradient characteristic curves. These ranges typically start from the time the vehicle attained a speed of 5.5 mph, which is a lateral acceleration of 0.04 g on a 50 ft radius circle. By the time most of the vehicles reached 5.5 mph, the RTD steering had settled to a steady state. However, in a few cases, a speed somewhat greater than 5.5 mph was needed before the RTD steering settled to steady state. The range of data used for the curve fits was ended when the vehicle attained a lateral acceleration of 0.40 g. The speed plots show that the Circle tests were conducted using a very slow rate of increase in speed during the circle tests. Regarding conducting circle tests for passenger vehicles, SAE J266[10] states: "If speed is steadily increased, the rate of increase shall not exceed 1.5 km/h per second (0.93 mph per second), and data shall be recorded continuously, so long as the vehicle remains on radius." The overall rates of speed increase during the Circle tests conducted are less than the J266 recommended maximum allowable rate.

The second page for each vehicle shows graphs of Roadwheel Steer Angle versus Ay (lateral acceleration). The CW test results are in the upper right quadrants of the graphs and the CCW test results are in the lower left quadrants of the graphs. The thin red and blue lines show data in the selected ranges, as described above. For both the CW and CCW data, there is a thicker blue line indicating second-order polynomial curve fits to the range of data selected. The red circles on these graphs are the geometric Ackermann steer angles, the vehicle wheelbase (L) divided by the circle radius (R), given by:

$$\delta_{SW(Geometric\ Ac\,ker\,mann)} = \frac{(180/\pi) \times L}{\mathrm{R}}$$

The geometric Ackermann steer angles are not the same as the actual roadwheel steer angles required to negotiate the circles at very low speed, with Ay close to zero. The actual roadwheel steer angles, which can be referred to as the measured Ackermann steer angles, are greater than the geometric Ackermann steer angles due primarily to compliance and lash in the steering system, and compliance in the suspension systems and tires.

The third page for each vehicle contains a graph of Roadwheel Steer Angle minus (measured) Ackermann Angle versus Ay (lateral acceleration). For these graphs, the signs of the CCW data are reversed so that the CW and CCW results can be directly compared. The thin lines show data in the range of data selected for each vehicle as described above, and the thick lines are the second-order polynomial curve fits to the data. Notice that the measured Ackermann steer angles are the abscissae of the curve fits taken at Ay equal to zero, so the curve fits tend to zero as Ay goes to zero. For a circle test: understeer (US) can be defined as the condition when the steering input required to maintain the circular path increases as the vehicle speed increases, neutral steer can be defined as the condition when the steering input required to maintain the circular path does not change as the vehicle speed increases, and oversteer (OS) can be defined as the condition when the steering input required to maintain the circular path decreases as the vehicle speed increases. The second-order polynomial curve fits do a good job of representing the underlying data whether the vehicle exhibits understeer, neutral steer, or oversteer characteristics during the Circle tests.

[10] SAE Surface Vehicle Recommended Practice - Steady-State Directional Control Test Procedures for Passenger Cars and Light Trucks, SAE J266, 1996.

For circle tests where the vehicles exhibited a transition from understeer to oversteer, the points of transition from understeer to oversteer are indicated on the graphs by black circles, and they are mathematically the points where the slopes of the curve fits change from being positive to negative. The values of the lateral acceleration at the points of transition are also indicated on the graphs

The fourth page for each vehicle contains a graph of Roll Angle versus Ay (lateral acceleration). The CW test results are in the lower right quadrants of the graphs and the CCW test results are in the upper left quadrants of the graphs. The thin lines show data in the range of vehicle speeds selected for each test. The thick lines are linear curve fits to the CW and CCW data over the selected ranges. The average of the CW and CCW curve fit slopes are listed on the graphs as the Roll Gradient.

Both Vehicle M and Vehicle N are close to neutral steer vehicles. When tested on asphalt, both vehicles did transition slightly to oversteer, at a lateral acceleration level of 0.34 g for Vehicle M and 0.30 g for Vehicle N. When tested on groomed dirt, both vehicles remained understeering through the entire range of lateral accelerations tested (i.e., they did not transition to oversteer).

Table 4 is a summary table of the lateral acceleration levels at which the vehicles that transitioned from understeer to oversteer did so during the autonomous asphalt and autonomous groomed dirt Circle tests. Results for Vehicles M and N, as well as the other 12 MY 2014-2015 ATVs tested previously on asphalt[11] and groomed dirt[12] are contained in Table 4. "NA" in the table indicates that no transition to oversteer occurred. As mentioned, both Vehicle M and Vehicle N are close to neutral steer vehicles. They are the only two vehicles that exhibited no transition to oversteer on one test surface (groomed dirt) and a mild transition to oversteer on the other test surface (asphalt).

Figure 1 is a bar chart showing the Roll Gradients for Vehicles A-N measured during the Circle tests conducted on asphalt and groomed dirt. The Roll Gradients measured on the two surfaces are relatively close. Six of the vehicles have higher Roll Gradients on the asphalt surface while the other eight (including Vehicle M and N) have higher Roll Gradients on the groomed dirt surface. The Roll Gradients for Vehicle M and N are in the lower range of the vehicles tested, meaning they have relatively high overall roll stiffness.

[11] *Effects on ATV Vehicle Characteristics of Rider Active Weight Shift – Results from Tests on Twelve 2014-2015 Model Year Vehicles*, HHS Contract HHSP233201400030I, SEA, Ltd. Report to CPSC, January 2018. https://cpsc-d8-media-prod.s3.amazonaws.com/s3fs-public/SEA-Report-to-CPSC-Rider-Active-ATV-Study-December-2017_0.pdf

[12] *Vehicle Characteristics Measurements of ATVs Tested on Groomed Dirt – Results from Tests on Twelve 2014-2015 Model Year Vehicles*, HHS Contract HHSP233201400030I, SEA, Ltd. Report to CPSC, February 2018. https://www.cpsc.gov/s3fs-public/SEA-Report-to-CPSC-Groomed-Dirt-ATV-Study.pdf?eK1E6h7IXBtznyCDatWHofAoHHmwD_nr

Table 4: US to OS Transition Points

Constant Radius (50 ft) Circle Tests Lateral Acceleration Level at Point of Transition from Understeer to Oversteer		
	Autonomous Asphalt (g)	Autonomous Groomed Dirt (g)
Vehicle A	0.17	0.16
Vehicle B	0.18	0.24
Vehicle C	NA	NA
Vehicle D	NA	NA
Vehicle E	NA	NA
Vehicle F	0.13	0.20
Vehicle G	0.17	0.11
Vehicle H	0.15	0.25
Vehicle I	0.18	0.23
Vehicle J	0.17	0.21
Vehicle K	0.25	0.23
Vehicle L	NA	NA
Vehicle M	0.34	NA
Vehicle N	0.30	NA

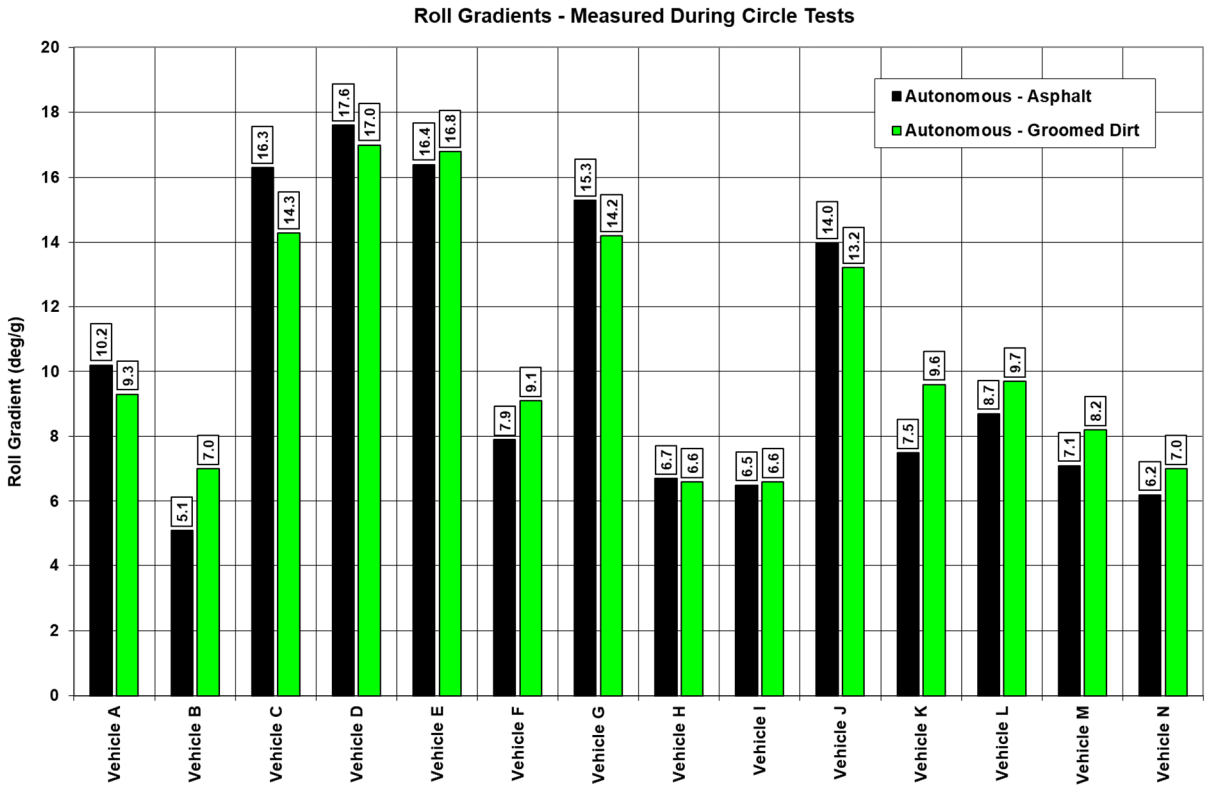

Figure 1: Roll Gradients

4.2.2 Dropped Throttle J-Turn (Step Steer) Tests (Initial Speed of 20 mph)

For each vehicle and for each test surface, there are five pages of results for the Dropped Throttle J-Turn tests. The first four pages show time domain plots for the tests. The first and third pages for each vehicle show plots of Roadwheel Steer Angle, Lateral Acceleration, Speed, Roll Angle, and Yaw Rate; for the six southward and the six northward runs, respectively. The second and forth pages for each vehicle show larger plots of Lateral Acceleration. For the J-Turn test results, the data shown was digitally low-pass filtered to 2.0 Hz using a phaseless, eighth-order, Butterworth filter. The time domain data shown for each vehicle contains data from 0.5 seconds before the ATV RTD steering input was applied until 5.0 seconds after it was applied.

For each vehicle and for each test surface, the plots contain results from three southward right steer J-Turns, three southward left steer J-Turns, three northward right steer J-Turns, and three northward left steer J-Turns. In all cases, the plots contain results from tests that resulted in visually determined two-wheel lift. An SAE standard sign convention is used, with Roadwheel Steer Angle, Lateral Acceleration, and Yaw Rate being positive and Roll Angle being negative for right turns.

The fifth page shown for each vehicle and test surface contains a summary of the peak lateral accelerations measured in each test. These values are the maximum values of lateral acceleration shown on the plots, which contain data that has been filtered to 2.0 Hz. The summary pages show the peak lateral accelerations for the individual runs conducted in the southward and northwards right and left steer directions. The mean values and standard deviations from each of the three sample runs are shown on the summary pages. Also, the average values of the six southward and six northward runs are shown, as is the average of all 12 runs, which is the Threshold Ay value.

A summary of the Threshold Ay values determined from the 20 mph Dropped Throttle J-Turn tests measured on both surfaces is given in Table 5. Values for Vehicles M and N, as well as the other 12 MY 2014-2015 ATVs tested previously, are contained in Table 5. A bar chart with the information contained in Table 5 is provided in Figure 2. Figure 2 is ranked using the asphalt test Threshold Ay values, with the vehicle with the lowest value starting on the left. The five vehicles with the lowest Threshold Ay values on groomed dirt are the same five vehicles with the lowest Threshold Ay values on asphalt. The vehicle with the highest Threshold Ay on groomed dirt (Vehicle H) also has the highest Threshold Ay on asphalt. The Figure 2 bar chart also shows each of the vehicle curb weights.

Threshold Ay values for Vehicle M and Vehicle N are relatively similar for asphalt and groomed dirt, and they are relatively close to each other. The Threshold Ay values for Vehicle M and Vehicle N are in the middle to high value range among the other vehicles tested.

Table 5: Threshold Ay Values

20 mph Dropped Throttle J-Turn Tests Threshold Lateral Acceleration		
	Autonomous Asphalt (g)	Autonomous Groomed Dirt (g)
Vehicle A	0.448	0.406
Vehicle B	0.585	0.547
Vehicle C	0.520	0.505
Vehicle D	0.579	0.528
Vehicle E	0.570	0.562
Vehicle F	0.465	0.426
Vehicle G	0.459	0.445
Vehicle H	0.602	0.598
Vehicle I	0.551	0.527
Vehicle J	0.505	0.505
Vehicle K	0.540	0.554
Vehicle L	0.558	0.563
Vehicle M	0.564	0.555
Vehicle N	0.540	0.556

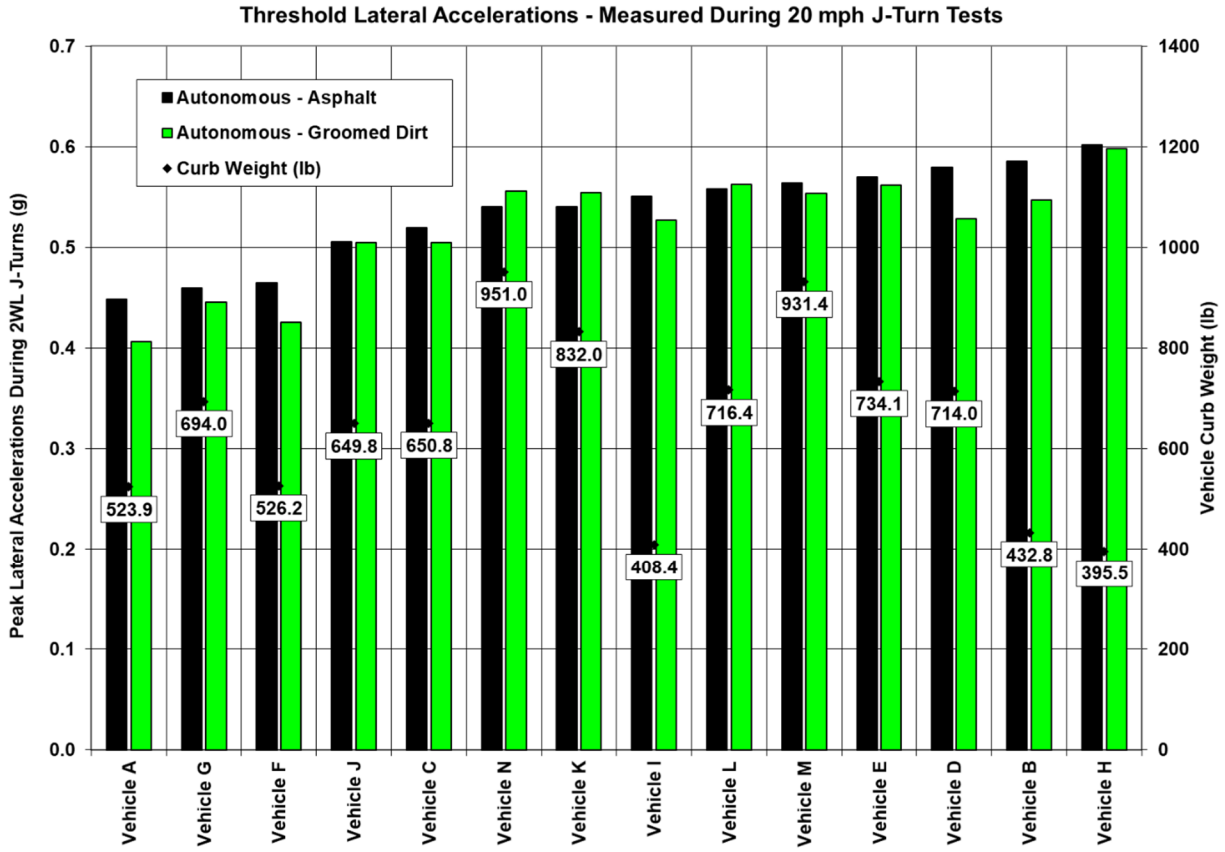

Figure 2: Ranked (by Asphalt Tests) Threshold Ay Values

4.2.3 Constant Steer Tests (Yaw Rate Ratio Tests)

There are seven pages of Constant Steer test results for each vehicle and test surface. The first page shows time domain plots of Roadwheel Steer Angle, Estimated Ay (Estimated Lateral Acceleration), Speed, Roll Angle, and Yaw Rate. There are plots for the five right direction steer tests (CW tests) and for the five left direction steer tests (CCW tests). For all the graphs from the Constant Steer tests, the Roadwheel Steer Angle, Speed, Roll Angle and Yaw Rate data shown is unfiltered. Per the OPEI and ROHVA ANSI protocols, the Estimated Ay data shown is computed by multiplying the Yaw Rate (filtered using a low-pass Butterworth filter with a cut-off frequency of 1.0 Hz) and Speed (filtered using a low-pass Butterworth filter with a cut-off frequency of 1.0 Hz). The thin lines show all the data collected for each run, and the thick lines indicate the data that was selected for post processing, when the Estimated Ay is in the range of 0.1-0.2 g and in the range of 0.3-0.4 g.

The second page of results from the Constant Steer tests contains the plots of Estimated Ay versus Speed for all ten tests. The third page of results contains the plot of Yaw Rate versus Speed for all ten tests, and this is the graph that also shows the slope values for the individual test run initial and final ranges (and their standard deviations), the individual test run CW and CCW slope ratios (and their standard deviations), the average CW and CCW slope ratios (the Yaw Rate Ratios), and the final average of the CW and CCW slope ratios (the Average Ratio). All the linear curve fits in the initial and final ranges are shown, and the thick black lines indicate where combinations of yaw rate and speed equal 0.4 g of lateral acceleration.

The following steps were taken to compute the slopes and Yaw Rate Ratios contained on the third page graphs:

1. For each test run, to determine the data regions for analysis, the yaw rate and speed channels were filtered using a low-pass Butterworth filter with a cut-off frequency of 1 Hz. Then the estimated lateral acceleration in units of "g's" was computed using the following equation:

$$\text{Estimated } A_y = \frac{\pi}{180} \times \frac{\text{Yaw Rate} \times \text{Speed}}{32.2}$$

   where Yaw Rate is in deg/sec and Speed is in ft/sec.

   The protocol used to compute Estimated Ay is the same as the protocols contained in ANSI/ROHVA 1-2016 and ANSI/OPEI B71.9-2016.[13]

2. The estimated lateral acceleration, Estimated Ay, was used to determine the start and stop points for the following regions:

   a. The Initial Region is from 0.1 to 0.2 g.
   b. The Final Region is from 0.3 to 0.4 g.

[13] The equations given in ANSI/ROHVA 1-2016 and ANSI/OPEI B71.9-2016 to compute Estimated Ay differ from the equation listed above because metric dimensions are used in the voluntary standards. However, all the equations compute Estimated Ay in units of "g's", by dividing by the gravitational constant defined as 9.8 m/s^2 or 32.2 ft/s^2.

3. For each test run, in both the initial and final regions, linear slopes of unfiltered yaw rate versus data index and linear slopes of unfiltered speed versus data index were computed.[14] The slopes can be classified as:

   a. Y1 = linear slope of the yaw rate versus index plot for Initial Region
   b. Y2 = linear slope of the yaw rate versus index plot for Final Region
   c. V1 = linear slope of the vehicle speed versus index plot for Initial Region
   d. V2 = linear slope of the vehicle speed versus index plot for Final Region

4. The Yaw Rate Ratio (R) for each run was then computed using the following equation:

$$\text{Yaw Rate Ratio (R)} = \frac{\left(\frac{Y2}{V2}\right)}{\left(\frac{Y1}{V1}\right)}$$

   Note: This value may be negative or positive.

5. Steps 1 through 4 were then repeated for all ten test runs.

6. The following final slope ratios were then computed:

   a. Right Turn Yaw Rate Ratio (CW Average) = Average of the absolute values of the 5 right turn test runs
   b. Left Turn Yaw Rate Ratio (CCW Average) = Average of the absolute values of the 5 left turn test runs
   c. Average Yaw Rate Ratio (Average Ratio) = Average of the Right Turn and Left Turn Yaw Rate Ratios

The fourth and fifth pages for each test condition contain magnified sections of the individual final slope regions for the right turn (CW) and left turn (CCW) runs, respectively. These graphs also contain black lines indicating where combinations of yaw rate and speed equal 0.4 g of lateral acceleration. A vehicle with severe oversteer in the final slope region will have a steep slope (high Final Slope value), and this will produce a high Yaw Rate Ratio. Steep final slopes are indicative of divergent vehicle behavior, a condition when the yaw rate and lateral acceleration gains are high, and the vehicle is prone to yaw and/or tip-up instability.

The sixth and seventh pages show individual path plots for the right turn (CW) and left turn (CCW) runs, respectively. As speed is increased during a Constant Steer test, an understeering vehicle will travel on a path of increasing radius, and an oversteering vehicle will travel on a path of decreasing radius. The path plot graphs have green, red, and black line portions, indicating ranges of lateral acceleration during the runs. The initial regions are shown with the green lines and the final regions are shown with the red lines.

Table 6 contains results comparing the Yaw Rate Ratios determined from Constant Steer tests conducted on groomed dirt and asphalt, for Vehicles M and N as well as the other 12 MY 2014-2015 ATVs tested previously. A bar chart with the information contained in Table 6 is provided

[14] The ANSI/ROHVA 1-2016 and ANSI/OPEI B71.9-2016 protocols specify computing slopes as versus *time*. Given the form of the final computation for Yaw Rate Ratio, computing the slopes versus *time* or versus *data index* result in the same answer for Yaw Rate Ratio.

in Figure 3. Figure 3 is ranked using the asphalt test Yaw Rate Ratio values, with the vehicle with the lowest value starting on the left.

Vehicles C, D, E and L did not transition to oversteer during the Circle tests on asphalt or groomed dirt; and these four vehicles have Yaw Rate Ratios below or close to 1.0 on both surfaces. The two MY 2021 vehicles tested in this study, Vehicles M and N, have the next lowest Yaw Rate Ratios. They have values close to 1.0, consistent with the finding from the Circle tests that these two vehicles are very close to neutral steer vehicles. Also consistent with the finding from the Circle tests, both Vehicle M and Vehicle N are somewhat more understeering on groomed dirt than on asphalt.

The ANSI/ROHVA 1-2016 and ANSI/OPEI B71.9-2016 criteria for passing their constant steer handling test using an ROV is that neither the right turn Yaw Rate Ratio nor the left turn Yaw Rate Ratio exceeds 4.5.

Table 6: Comparison of Yaw Rate Ratio Values

Constant Steer Tests Yaw Rate Ratios		
	Autonomous Asphalt Ratio	Autonomous Groomed Dirt Ratio
Vehicle A	9.70	21.1
Vehicle B	3.36	79.5
Vehicle C	0.53	0.96
Vehicle D	0.25	0.52
Vehicle E	0.14	0.41
Vehicle F	4.65	4.67
Vehicle G	8.40	6.46
Vehicle H	9.89	14.7
Vehicle I	7.22	2.73
Vehicle J	18.1	3.22
Vehicle K	2.24	0.94
Vehicle L	1.27	1.14
Vehicle M	1.39	0.80
Vehicle N	1.87	1.64

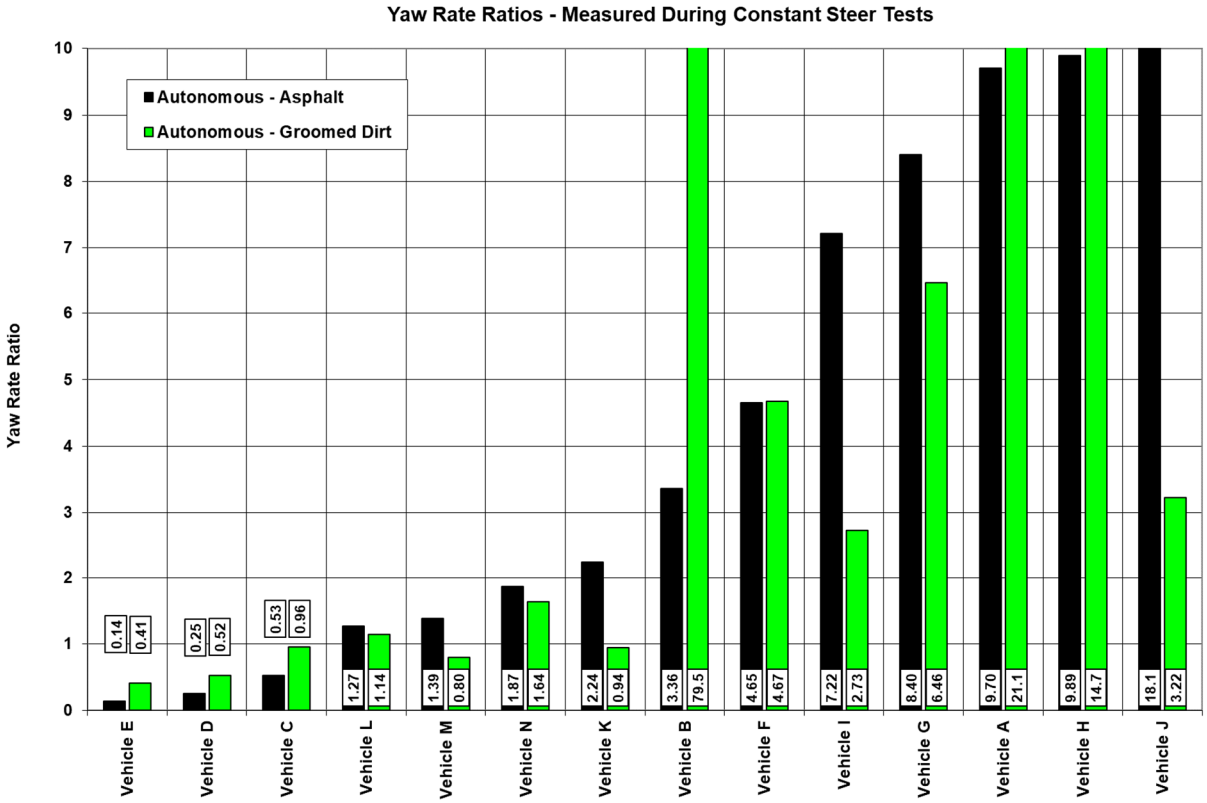

Figure 3: Ranked (by Asphalt Tests) Yaw Rate Ratio Values

4.3 Discussion of Braking Test Results

Appendix D contains six pages of graphical results from the braking tests. The left column of graphs on each page contains results for Vehicle M, the non-ABS equipped vehicle, and the right column of graphs contain results for Vehicle N, the vehicle equipped with ABS. Pages 1-4 of Appendix D contain results from varying severity straight-line braking tests conducted on asphalt, groomed dirt, dry grass, and wet grass, respectively. Page 5 contains results from runs with maximum braking at the onset of J-turn steering and Page 6 results from runs with maximum braking delayed by 0.5 sec after the onset of J-turn steering. These braking and turning runs were conducted on wet grass.

Pages 1-4 results for both vehicles each contain graphs from straight-line braking runs at three different levels of braking severity: nominal 0.40 g deceleration, nominal 0.55 g deceleration, and maximum hand brake deceleration. There are two graphs for each run. The top graph shows vehicle speed and the four individual wheel speeds, and the bottom graphs shows the deceleration (Ax) during each run. The wheel speeds plotted are in mph, and they are computed from the rotational wheel speed times the tire rolling radius. When the vehicle is traveling at a constant speed, the wheel speeds are close to the vehicle speed. Stopping time and stopping distance are shown for each straight-line braking run. The time and distance are from when the vehicle speed falls to 20 mph, when the hand brake is rapidly applied, until the vehicle speed goes to zero.

The results on Page 1 of Appendix D show that on asphalt, both vehicles have similar responses. There was no wheel lockup for either vehicle and no ABS activity on Vehicle N. Each vehicle had more than 0.6 g of deceleration during the maximum braking runs, indicating that their front to rear brake proportioning was well tuned to give good braking performance without wheel lockup. Page 2 shows that results on groomed dirt where like those on asphalt, except on groomed dirt there is the presence of Vehicle N ABS activity during the maximum braking run. Starting about 0.25 sec after the brakes are applied and lasting through the duration of the run, the front wheel speeds drop and then recover as the ABS cycles the front brakes on-and-off. The wheel speeds but do not go to zero (i.e., the wheels do not lockup) until near the end of the run.

The results on dry grass (Page 3) are like those on groomed dirt, again with Vehicle N ABS activity during the maximum braking run. On dry grass, the stopping distance for Vehicle N under maximum braking was slightly greater than the stopping distance during the nominal 0.55 g braking run. In general, ABS cycling the brakes off to prevent wheel lockup can diminish stopping distance compared to less severe braking conditions that do not trigger ABS activity.

On asphalt, groomed dirt, and dry grass, the coefficient of friction between the tires and test surface was high enough to provide the grip needed to support the commanded braking forces (torques) during all braking runs conducted, and Vehicle M exhibited no wheel lockup during any tests on these test surfaces. To promote wheel lockup under braking, the grass was sprayed with water to reduce the coefficient of friction between the tires and surface. When tested on wet grass, the front wheels of Vehicle M locked up during maneuvers using the two most severe braking levels, as shown on Page 4 of Appendix D. In both the nominal 0.55 g braking and maximum braking runs, both front wheels locked within 0.75 sec of the hand brake application, and they remained locked throughout the remainder of the runs. The coefficient of friction between the tires and wet grass surface was not high enough to support the commanded braking forces (torques) on these runs of Vehicle M that exhibited front wheel lockup.

On wet grass, Vehicle M stopping distances for both the runs with locked front wheels are longer than the stopping distances on the other test surfaces. Also, the deceleration did not exceed 0.6 g during the maximum braking run on wet grass, like it did during runs on the other test surfaces. These results indicate that the sliding coefficient of friction on the wet grass is less than the rolling non-sliding friction on the other tests surfaces.

For Vehicle N, the results on wet grass (Page 4) are like those on groomed dirt and dry grass, with ABS activity during the maximum braking run. For all maximum braking runs conducted using Vehicle N, the deceleration did exceed 0.6 g, even in the runs with ABS activity.

The braking and steering maneuvers were conducted to show differences in ATV responses resulting from no ABS versus ABS. The maneuvers were 20 mph, dropped throttle, J-turns with braking applied either at the onset of steering (Page 5 of Appendix D) or delayed by 0.5 sec after the onset of steering (Page 6). These runs were conducted on wet grass and the results shown are for right turn maneuvers.

The top plot for each run is a co-plot of Roadwheel Steer angle and Brake Stroke versus time. The steering magnitude used for each vehicle in these runs is 90 percent of the average steering magnitude used in the J-turns on asphalt and groomed dirt that resulted in two-wheel lift test outcomes for each vehicle. The intention was to have severe steering input, but not severe enough to have the vehicle tip up onto its safety outriggers. The Brake Stroke shown is the amount of RTD hand brake actuator displacement in mm. The brake actuator to brake lever displacements were adjusted so that 30 mm of Brake Stroke represents maximum hand braking. These co-plots show that the braking and steering inputs occurred at the same time during the Page 5 runs, and the braking was delayed by 0.5 sec during the Page 6 runs.

The other time domain plots on Pages 5 and 6 include: the vehicle speed (Vx) and four wheel speeds, longitudinal acceleration (Ax) and lateral acceleration (Ay), Roll Angle, Yaw Angle, and Heading Change. The bottom plot for each run shows the vehicle path, with vehicle positions plotted at the origin (the reference position at the start of steering), every 0.25 sec after the start of steering, and at the position when the vehicle stopped. The width of each rectangle indicating vehicle position is the average vehicle track width and the length of each rectangle is the vehicle wheelbase. The circles inside rectangles are the vehicle center-of-gravity (CG) locations. The CG positions and heading are measurements from the GPS/IMU, and they show the actual initial heading direction of the runs in the south-southeast direction.

For both braking and steering maneuvers, soon after the brakes are applied the front wheels of Vehicle M lockup and the front wheels of Vehicle N exhibit ABS cycling. The front wheels of Vehicle N do not lockup until the near the end of the maneuvers, when the vehicle speed is close to zero. With its front wheels locked a vehicle generally loses directional control. The front wheels of Vehicle M lockup near 0.5 sec on the Page 5 maneuver and near 1.0 sec on the Page 6 maneuver. There is little change in heading direction after the front wheels lockup, and the path plots show that Vehicle M travels on a nearly straight path after the front wheels lockup. Vehicle N continues to turn after the brakes are applied, because the front wheels are not locked. The change in heading for Vehicle N is greater than for Vehicle M, and the path plots shown on Pages 5 and 6 show that Vehicle N continues along a curved path to the end of each maneuver. For both maneuvers, the stopping time and stopping distance is greater for Vehicle M, because the overall vehicle deceleration was less with the locked front wheels.

4.4 Summary

Vehicle M (the MY 2021 vehicle without ABS) and Vehicle N (the MY 2021 vehicle equipped with ABS) are similar in weight and size (i.e., similar wheelbase and trackwidth) to each other. They are heavier than any of the 12 MY 2014-15 vehicles tested previously, and they are among the vehicles with the largest wheelbases and track widths.

Vehicle N has a lower CG height and higher SSF and KST values than Vehicle M. Compared to all the vehicles tested previously, the CG height, SSF and KST for both Vehicles M and N are in the higher range of values, among the other larger MY 2014-2015 vehicles tested previously.

The TTR, FTTR, and RTTR values for Vehicle N are less than those for Vehicle M, although Vehicle N has a lower CG height. The reason for this is likely because Vehicle N has a lower tire pressure than Vehicle M. Compared to the vehicles tested previously, the TTR, FTTR, and RTTR values for both Vehicles M and N are again in the higher range of values, among the other larger vehicles tested previously. The steering ratio and maximum speed vehicle for Vehicles M and N are in the range of values for the other larger vehicles tested previously.

The dynamic Circle tests and Constant Steer tests indicate that both Vehicle M and N are near neutral steer vehicles. Both vehicles had no transition to oversteer in the Circle Tests conducted on groomed dirt and only a mild transition to oversteer on asphalt. Both vehicles have yaw rate ratios close to 1.0, consistent with the finding from the Circle tests that these two vehicles are very close to neutral steer vehicles. Also consistent with the finding from the Circle tests, both Vehicle M and Vehicle N are somewhat more understeering on groomed dirt than on asphalt. Both MY 2021 ATVs tested had good directional stability in these dynamic maneuvers that did not involve braking. Metrics from Circle and Constant Steer tests on Vehicles M and N were found to be in the range of other vehicles tested previously that also exhibited good lateral stability.

J-turn testing revealed that the threshold Ay values of Vehicle M and Vehicle N are relatively similar for asphalt and groomed dirt, and relatively like each other. The Threshold Ay values for Vehicle M and Vehicle N are in the middle to high value range among the MY 2014-2015 vehicles tested previously.

Applying the hand brake on Vehicles M and N activates braking at all four wheels. Both vehicles exhibited a good balance of front and rear brake proportioning during straight-line braking runs. Vehicle M did not have any wheel lockup on asphalt, groomed dirt, or dry grass test surfaces. Vehicle N also did not have any wheel lockup on these surfaces, but it did exhibit front wheel ABS activity during maximum braking runs on groomed dirt and dry grass. When the grass was watered to reproduce the coefficient of friction between the tires and test surface, Vehicle M had front wheel lockup during the two most severe straight-line braking runs. Vehicle N had no wheel lockup during straight-line braking runs on wet grass, as ABS activity prevented front wheel lockup.

Wet grass braking and turning tests conducted on Vehicle N demonstrated that ABS improved directional control and stopping distance compared to similar tests conducted on Vehicle M, the sister vehicle without ABS. Conducting braking tests on different vehicles that are more prone to wheel lockup and/or conducting tests on surfaces with lower coefficient of friction could reveal additional advantages of ATV ABS. Nonetheless, the tests conducted in this study demonstrated that the benefits of ABS technology in ATVs provide a foundation for using ABS as part of a

comprehensive package for ATV Electronic Stability Control (ESC). For passenger vehicles and other on-road vehicles, ESC technologies have been shown to further improve vehicle stability beyond basic ABS technologies. Likewise, ATV ESC technology has potential to improve ATV stability beyond the improvements provided by ABS alone.

Vehicle M

	Curb	Driver	Autonomous Ballast to Driver Loading	Gross Vehicle Weight (GVW)
VIMF Test Number	7725	7726	7728	7786
Total Vehicle Weight (lb)	931.4	1144.3	1144.6	1444.4
Left Front Weight (lb)	237.7	269.8	269.1	293.3
Right Front Weight (lb)	230.3	258.8	259.9	296.5
Left Rear Weight (lb)	220.2	295.9	296.1	417.8
Right Rear Weight (lb)	243.2	319.8	319.5	436.8
Front Track Width (in)	39.90	39.68	39.90	40.45
Rear Track Width (in)	38.10	38.20	38.10	38.18
Average Track Width (in)	39.00	38.94	39.00	39.32
Wheelbase (in)	50.80	51.00	50.80	51.50
CG Longitudinal (in)	25.27	27.44	27.32	30.47
CG Lateral (in)	0.31	0.21	0.23	0.30
CG Height (in)	20.87	23.80	22.91	24.99
Roll Inertia - I_{XX} (ft-lb-s^2)	43	83	75	120
Pitch Inertia - I_{YY} (ft-lb-s^2)	116	146	174	260
Yaw Inertia - I_{ZZ} (ft-lb-s^2)	122	134	169	236
Roll/Yaw - I_{XZ} (ft-lb-s^2)	2	9	9	32
SSF	0.934	0.818	0.851	0.787
KST	0.934	0.819	0.853	0.791
Steering Ratio (deg/deg)			1.54	

Vehicle M

		Curb	Driver	Autonomous Ballast to Driver Loading	Gross Vehicle Weight (GVW)
Lateral Right Tilt	**Right Tilt First Wheel Lift**	Rear	Rear	Rear	Rear
	Right Tilt Angle (TTA) (deg)	40.3	33.4	34.9	30.1
	Right Tilt Ratio (TTR)	0.848	0.659	0.698	0.581
Lateral Left Tilt	**Left Tilt First Wheel Lift**	Rear	Rear	Rear	Rear
	Left Tilt Angle (TTA) (deg)	41.7	35.2	35.4	31.3
	Left Tilt Ratio (TTR)	0.891	0.705	0.710	0.608
	Average Lateral TTA (deg)	**41.0**	**34.3**	**35.2**	**30.7**
	Average Lateral TTR	**0.869**	**0.682**	**0.704**	**0.594**
Longitudinal Front Tilt	**Front Tilt First Wheel Lift**	Right	Right	Equal	Right
	Front Tilt TTA (FTTA) (deg)	53.3	51.8	51.1	49.0
	Front Tilt TTR (FTTR)	1.342	1.271	1.241	1.149
Longitudinal Rear Tilt	**Rear Tilt First Wheel Lift**	Left	Equal	Left	Equal
	Rear Tilt TTA (RTTA) (deg)	53.9	48.1	46.0	39.7
	Rear Tilt TTR (RTTR)	1.372	1.115	1.037	0.831

Vehicle N

	Curb	Driver	Autonomous Ballast to Driver Loading	Gross Vehicle Weight (GVW)
VIMF Test Number	7821	7822	7919	7823
Total Vehicle Weight (lb)	951.0	1164.9	1164.2	1463.5
Left Front Weight (lb)	240.3	274.2	273.0	309.1
Right Front Weight (lb)	235.8	271.8	266.9	300.9
Left Rear Weight (lb)	228.4	300.7	299.0	420.2
Right Rear Weight (lb)	246.5	318.2	325.3	433.3
Front Track Width (in)	39.80	39.90	39.90	40.10
Rear Track Width (in)	38.20	38.28	38.28	38.28
Average Track Width (in)	39.00	39.09	39.09	39.19
Wheelbase (in)	50.80	51.10	51.00	51.35
CG Longitudinal (in)	25.37	27.15	27.35	29.95
CG Lateral (in)	0.27	0.25	0.33	0.06
CG Height (in)	20.32	23.12	22.55	25.10
Roll Inertia - I_{XX} (ft-lb-s^2)	41	76	75	100
Pitch Inertia - I_{YY} (ft-lb-s^2)	118	144	181	232
Yaw Inertia - I_{ZZ} (ft-lb-s^2)	123	130	171	206
Roll/Yaw - I_{XZ} (ft-lb-s^2)	2	9	9	21
SSF	0.960	0.845	0.867	0.781
KST	0.960	0.846	0.868	0.784
Steering Ratio (deg/deg)			1.50	

Vehicle N

		Curb	Driver	Autonomous Ballast to Driver Loading	Gross Vehicle Weight (GVW)
Lateral Right Tilt	**Right Tilt First Wheel Lift**	Rear	Rear	Rear	Rear
	Right Tilt Angle (TTA) (deg)	38.6	31.7	33.7	26.5
	Right Tilt Ratio (TTR)	0.797	0.618	0.667	0.498
Lateral Left Tilt	**Left Tilt First Wheel Lift**	Rear	Rear	Rear	Rear
	Left Tilt Angle (TTA) (deg)	39.2	32.9	35.2	27.6
	Left Tilt Ratio (TTR)	0.817	0.647	0.706	0.522
	Average Lateral TTA (deg)	**38.9**	**32.3**	**34.5**	**27.0**
	Average Lateral TTR	**0.807**	**0.632**	**0.687**	**0.510**
Longitudinal Front Tilt	**Front Tilt First Wheel Lift**	Left	Left	Right	Left
	Front Tilt TTA (FTTA) (deg)	52.0	48.1	50.6	45.6
	Front Tilt TTR (FTTR)	1.279	1.113	1.219	1.020
Longitudinal Rear Tilt	**Rear Tilt First Wheel Lift**	Right	Right	Equal	Right
	Rear Tilt TTA (RTTA) (deg)	52.6	44.4	43.3	35.8
	Rear Tilt TTR (RTTR)	1.306	0.979	0.944	0.722

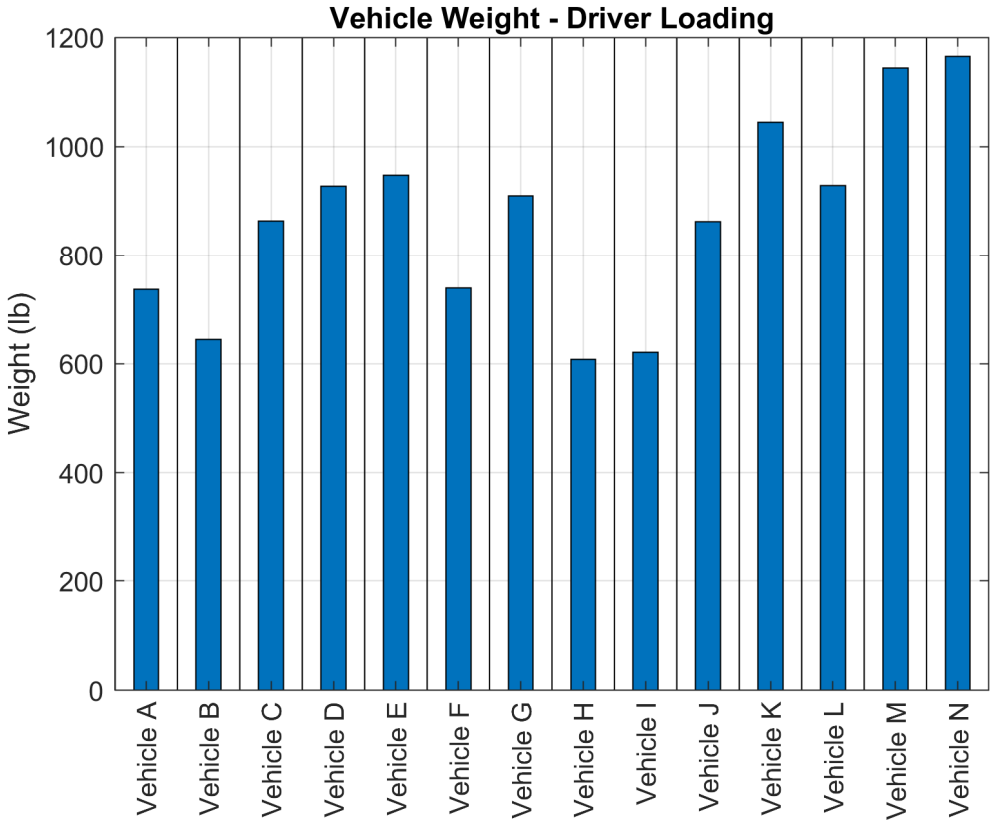

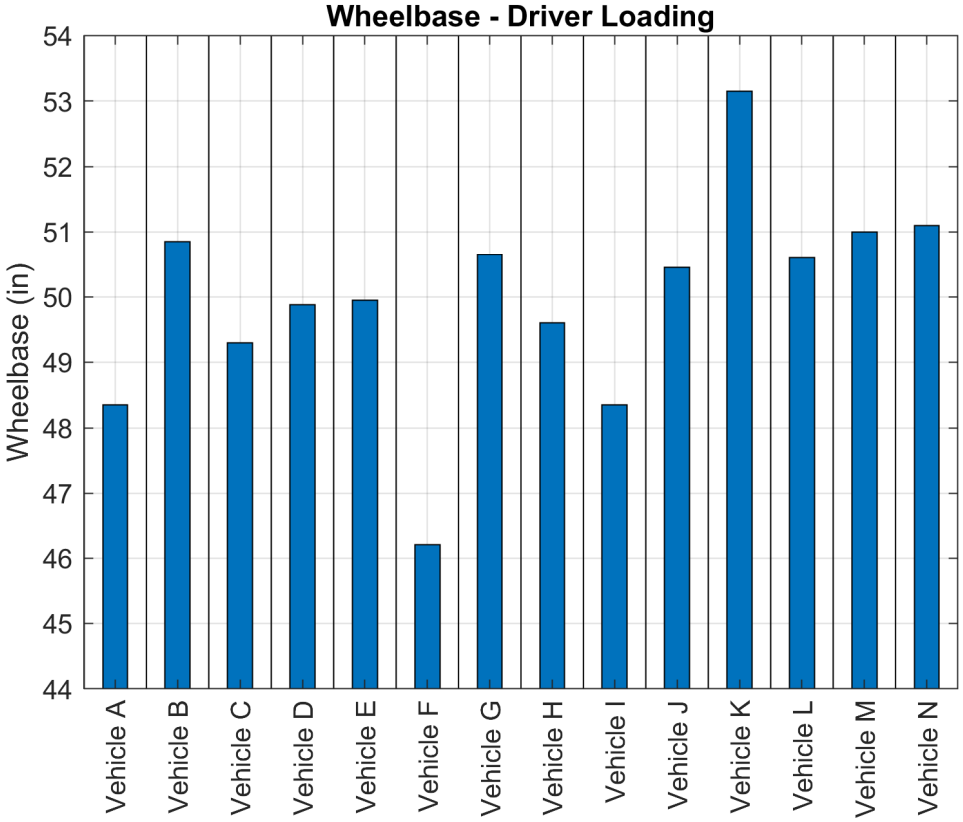

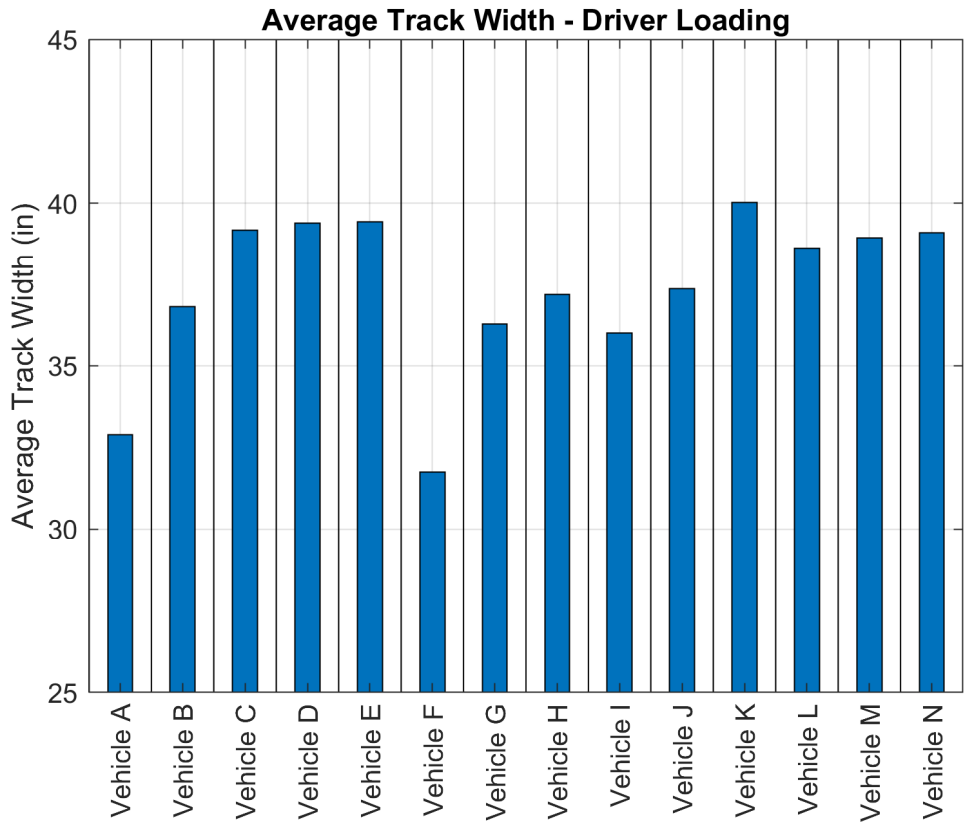

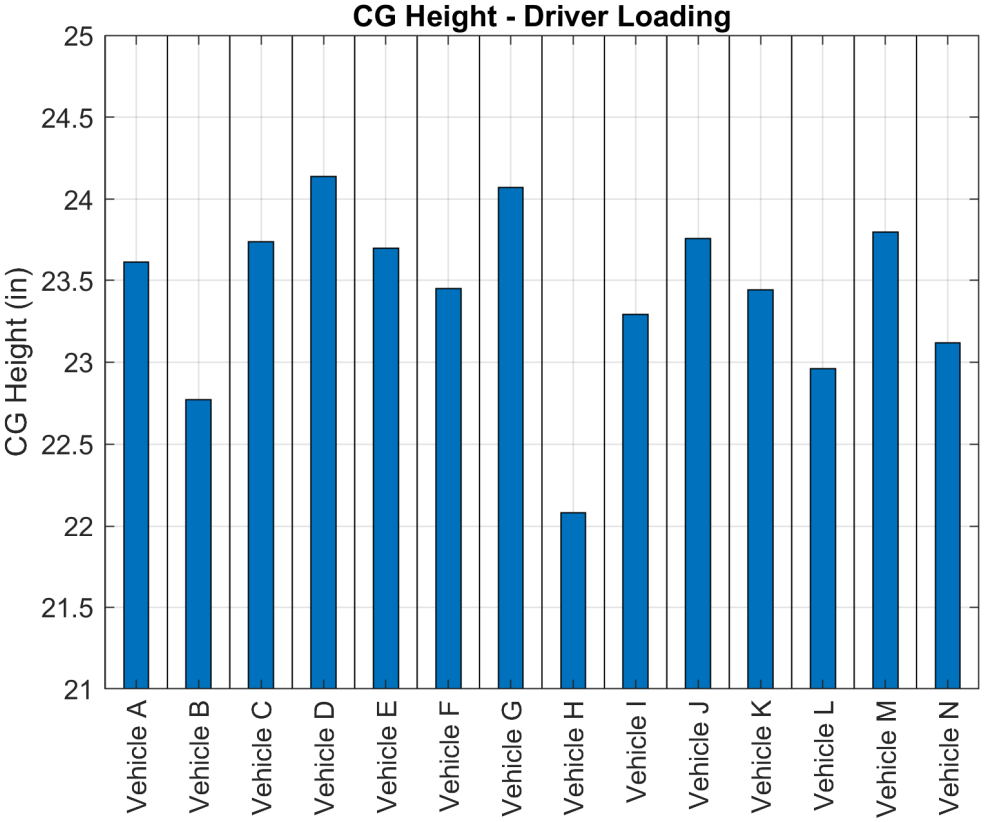

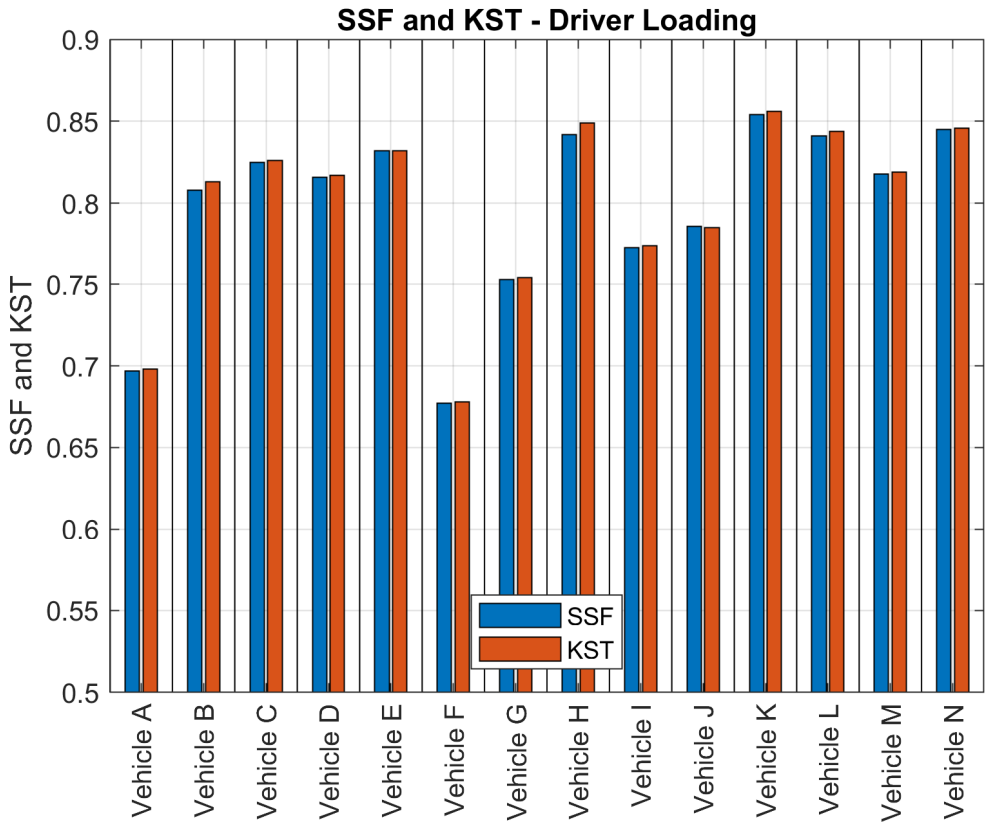

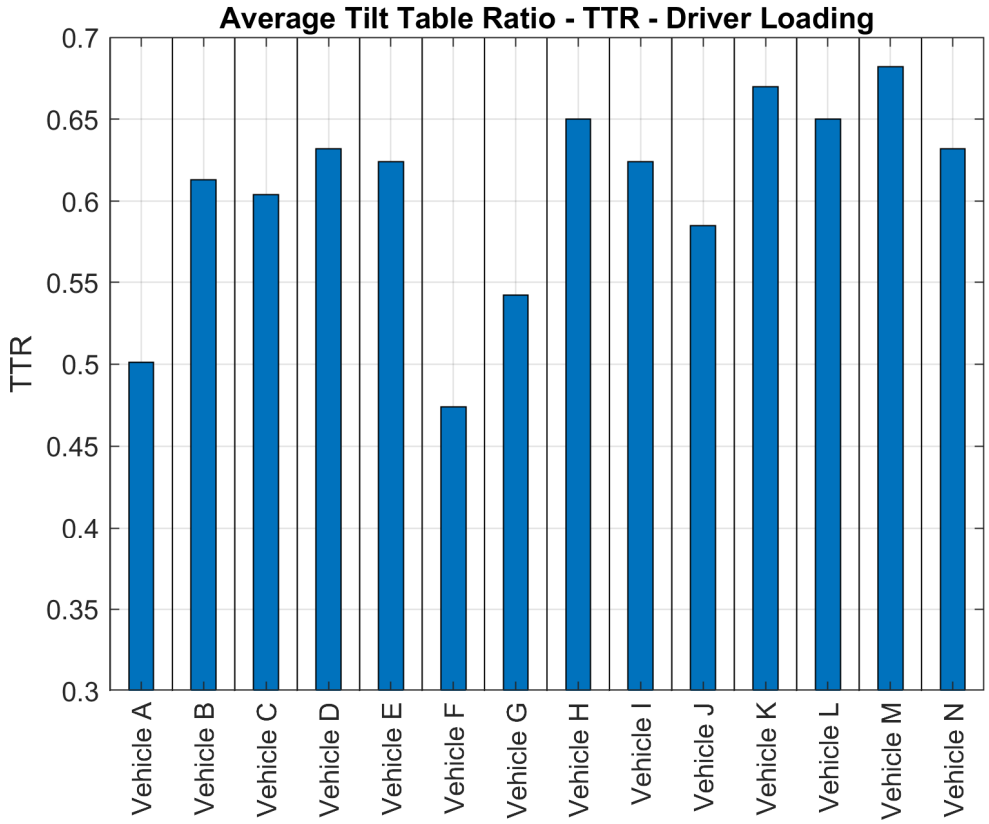

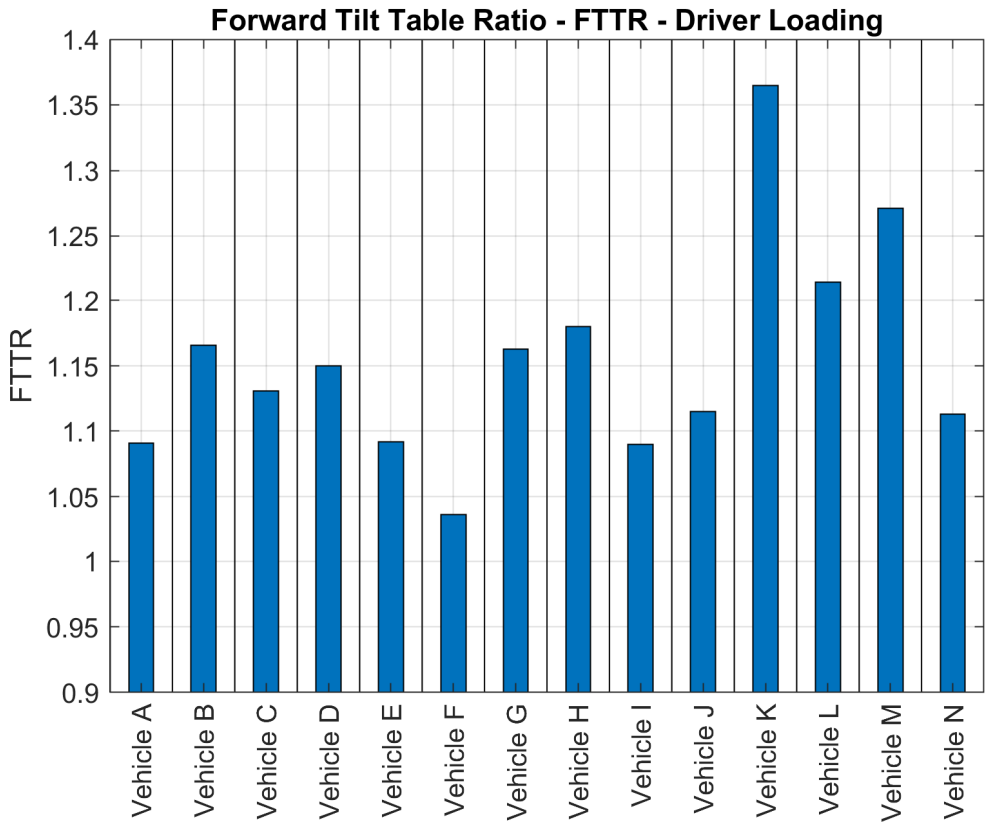

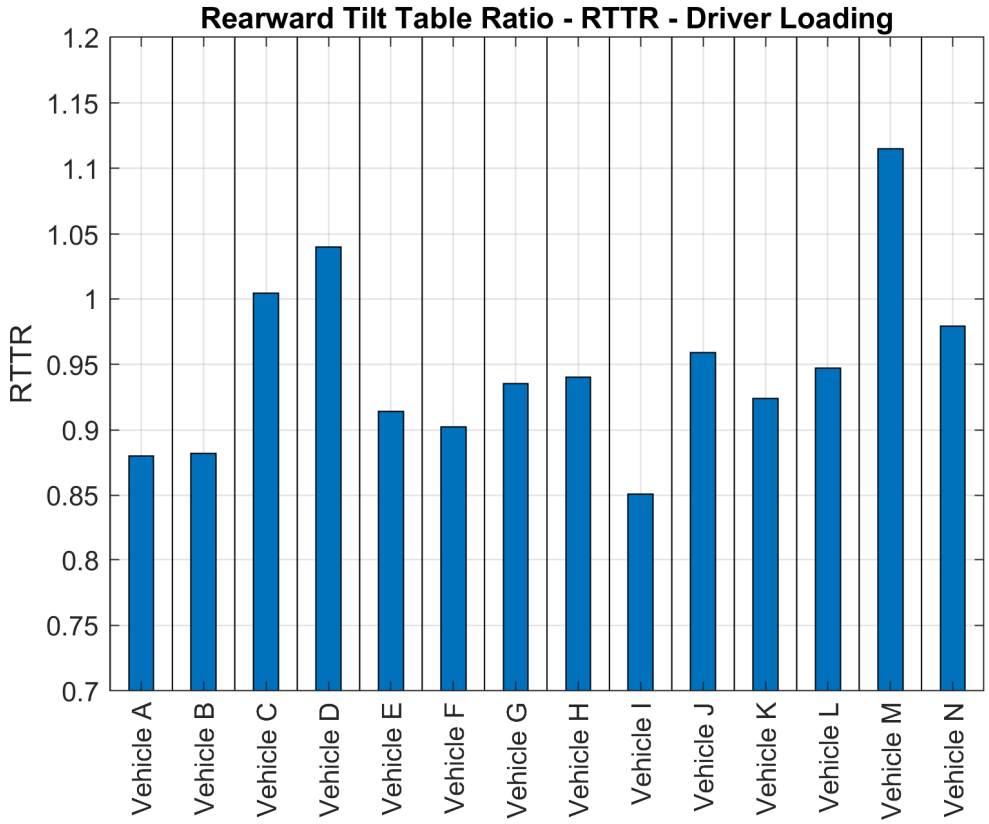

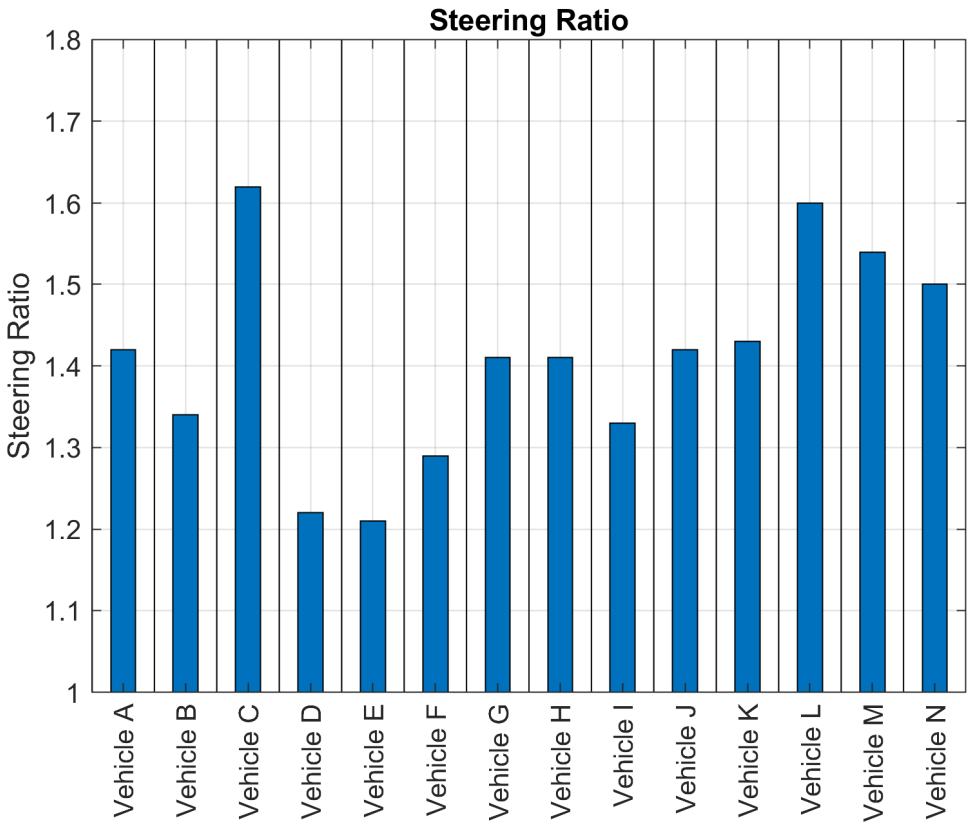

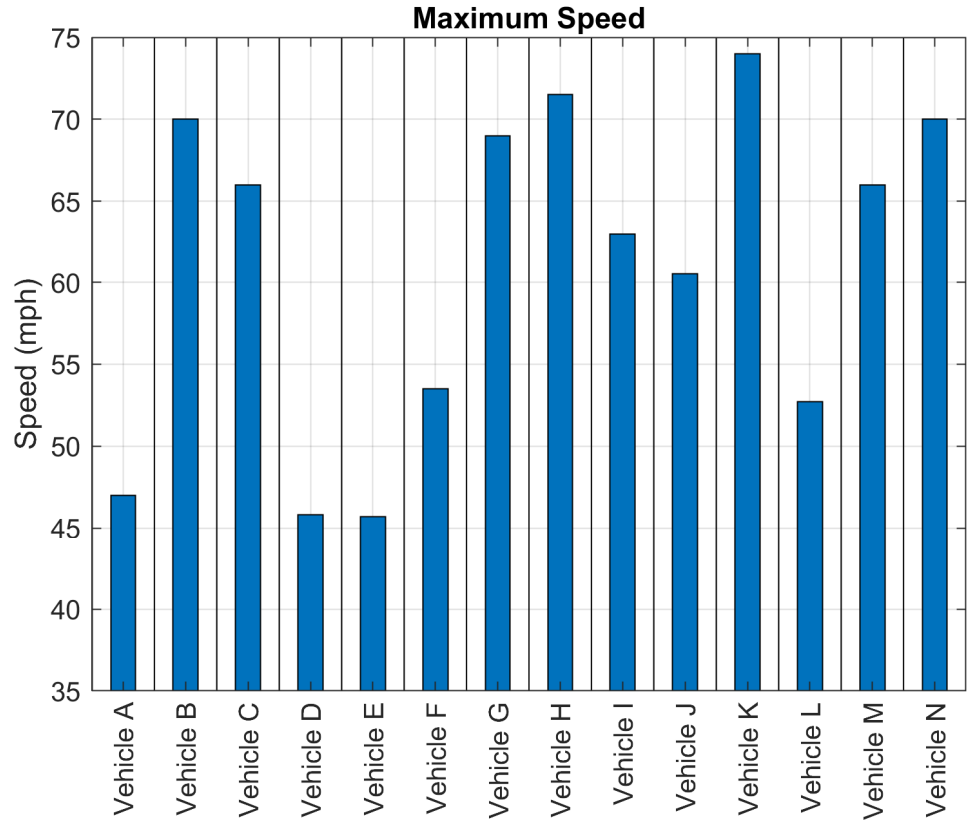

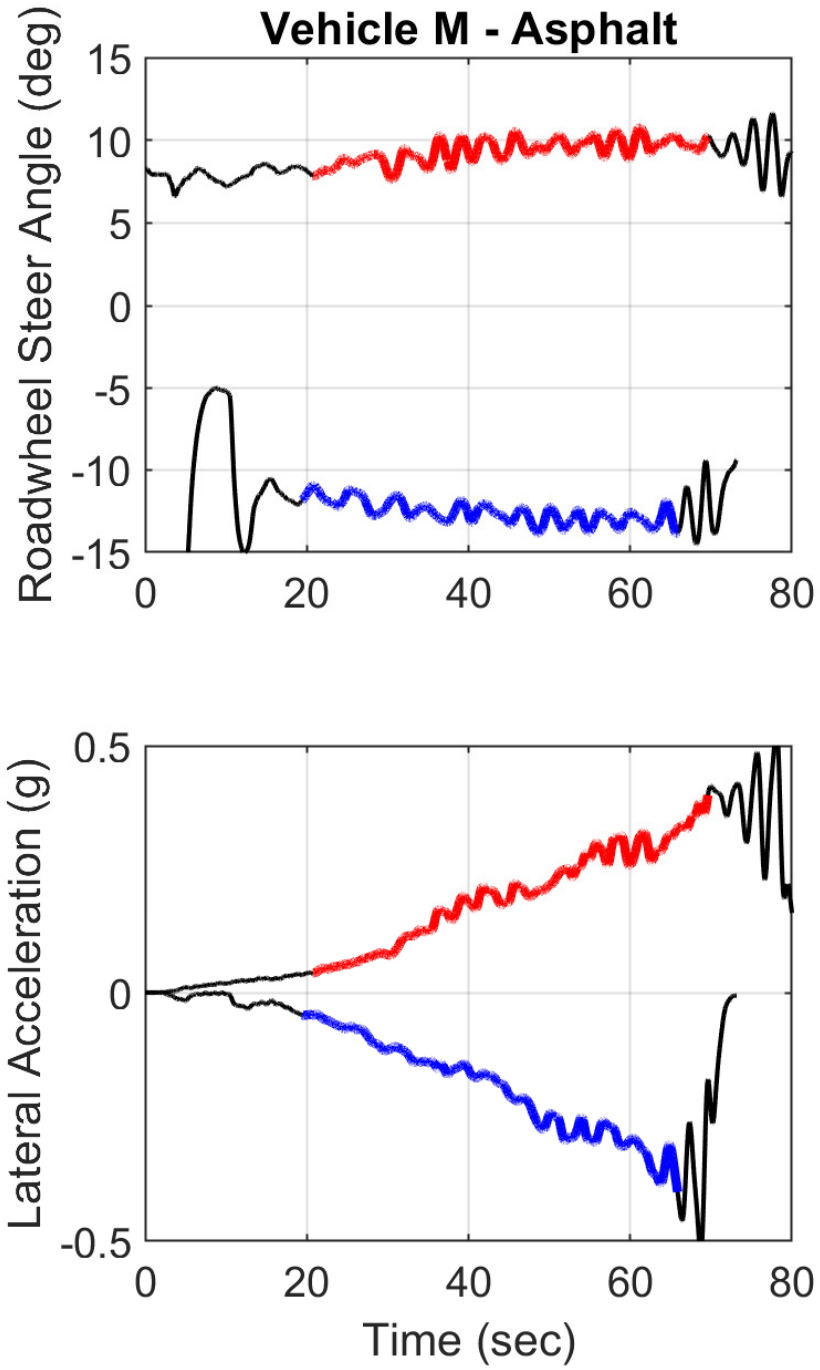

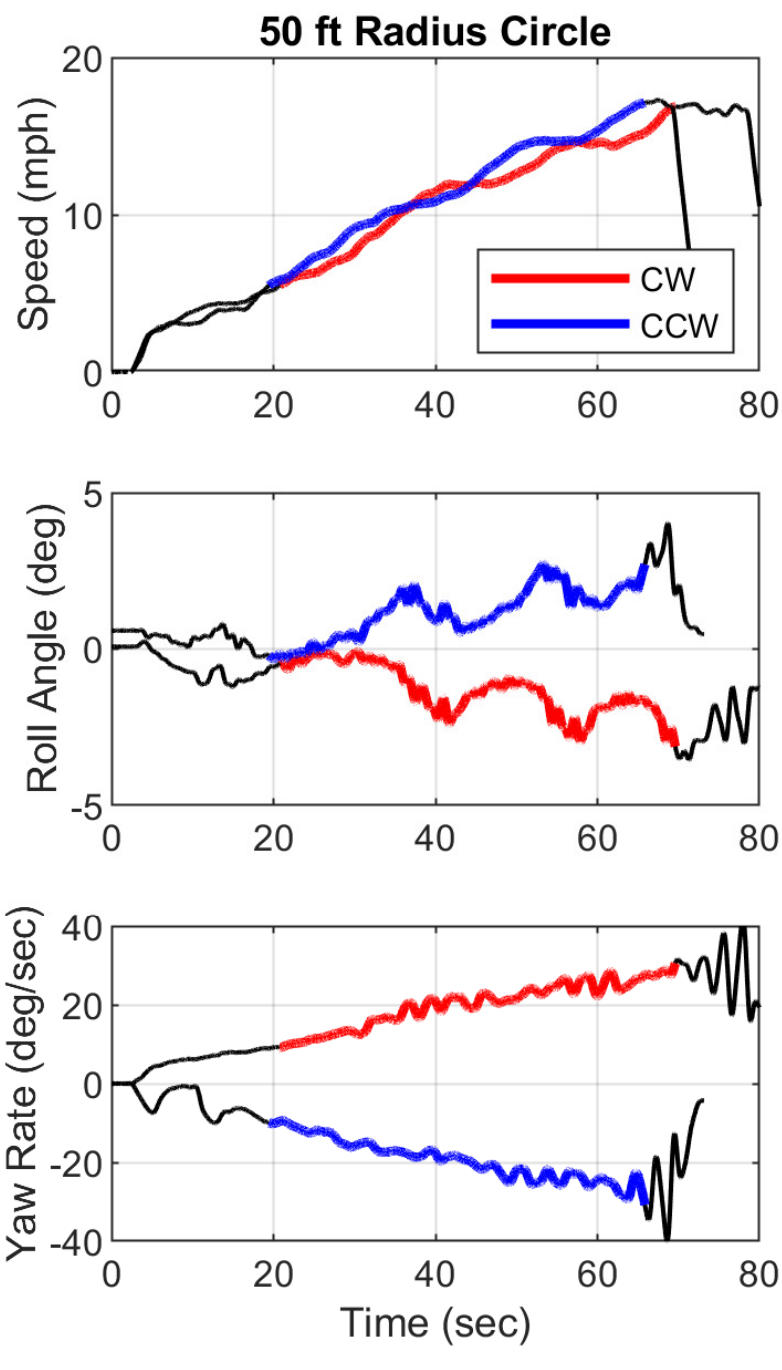

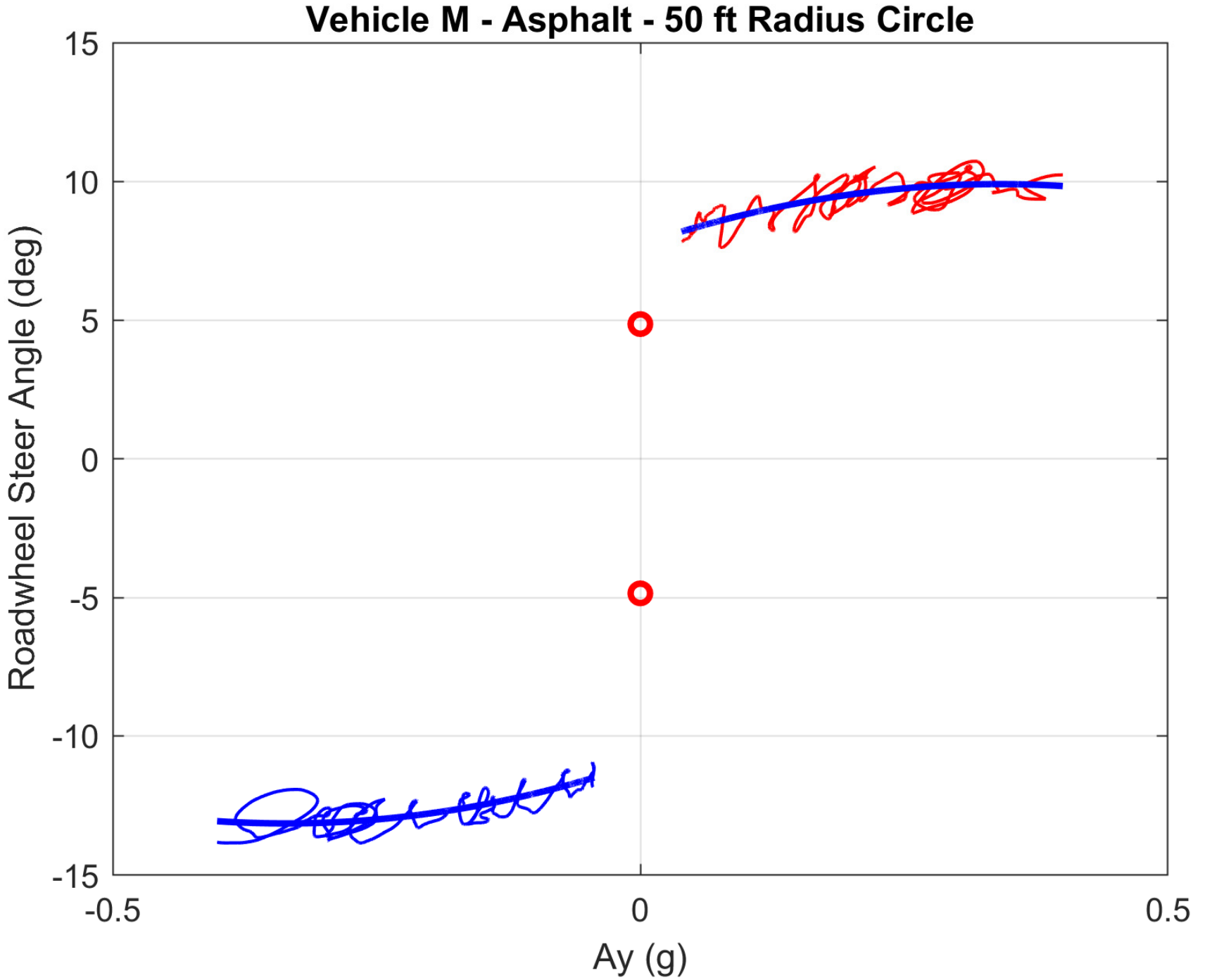

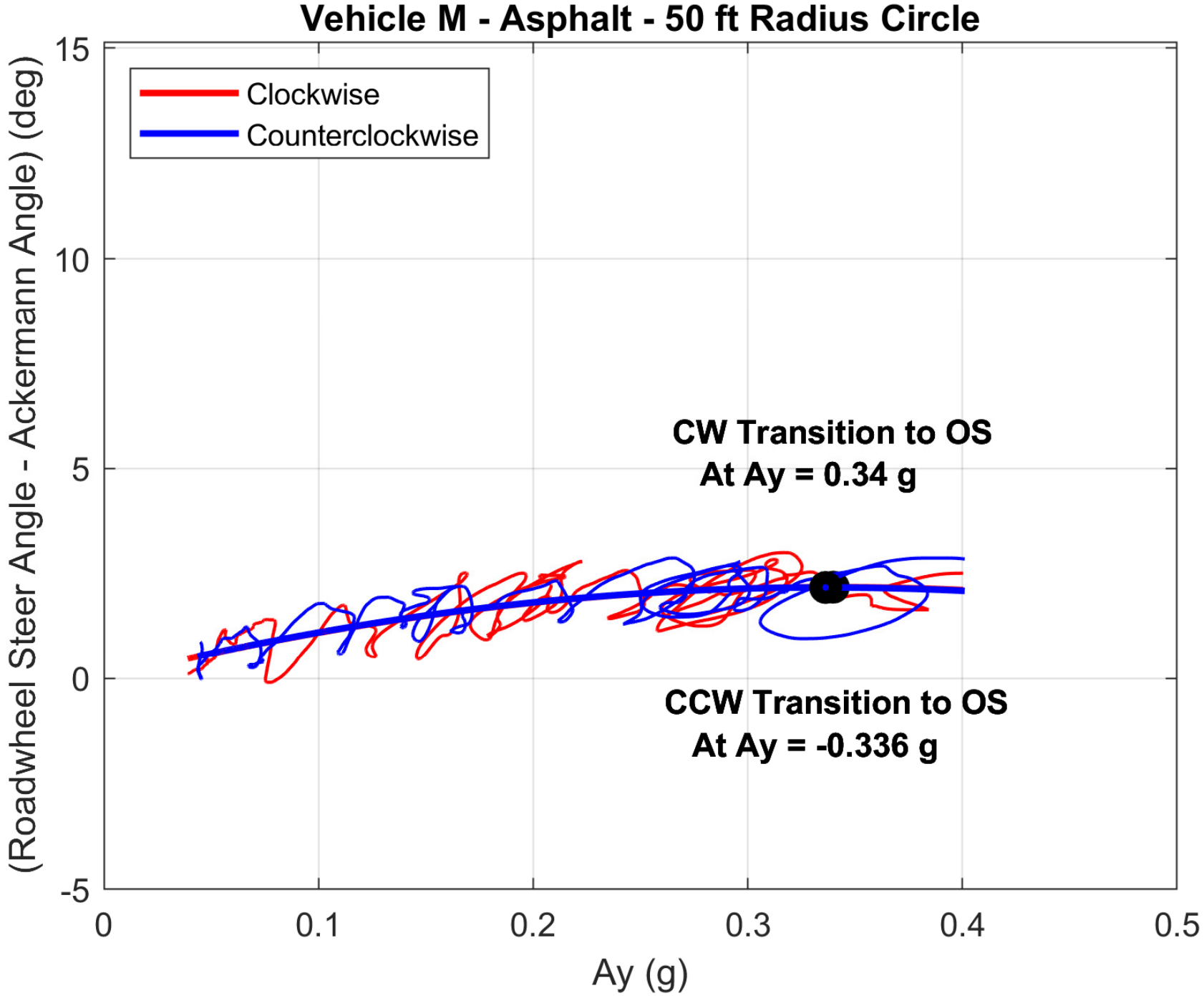

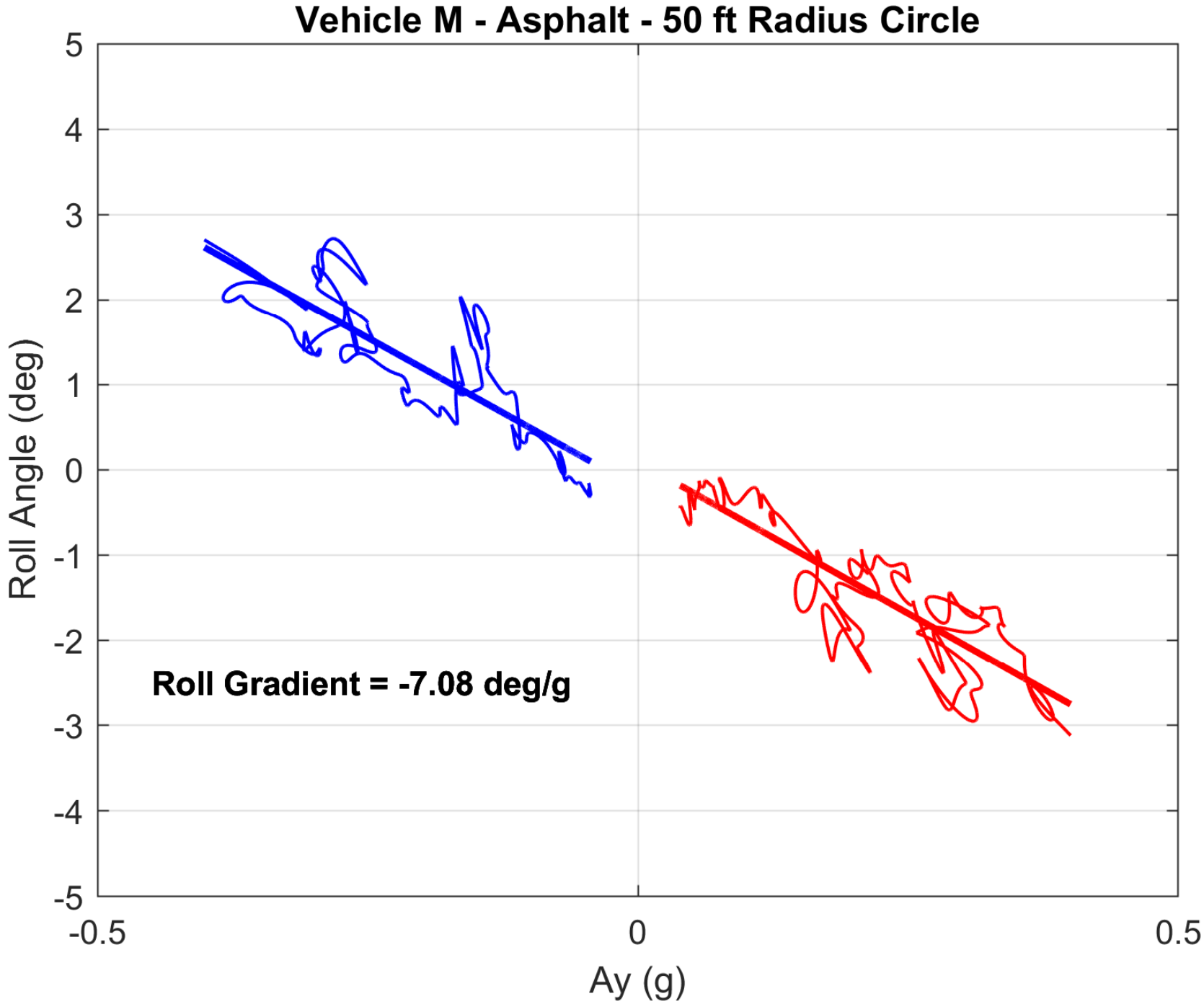

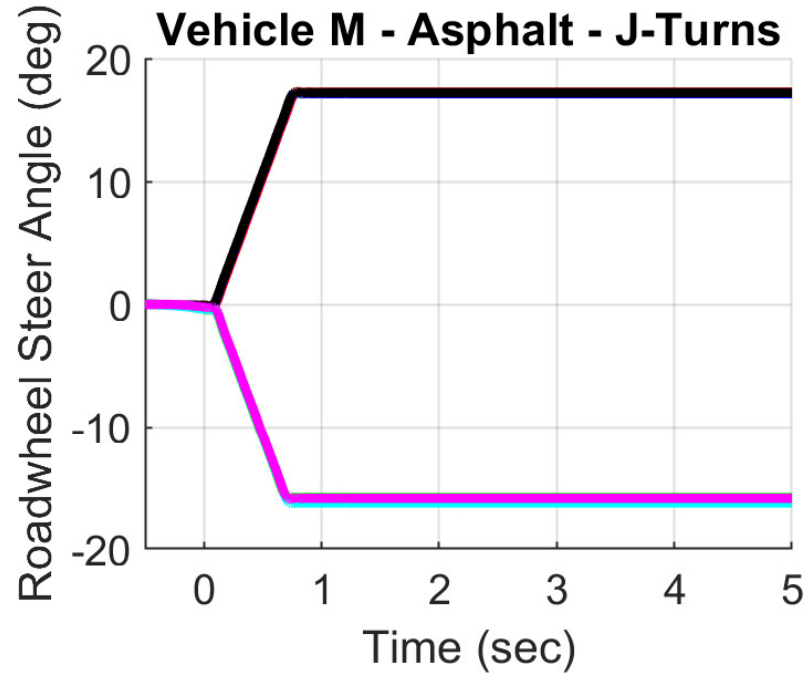

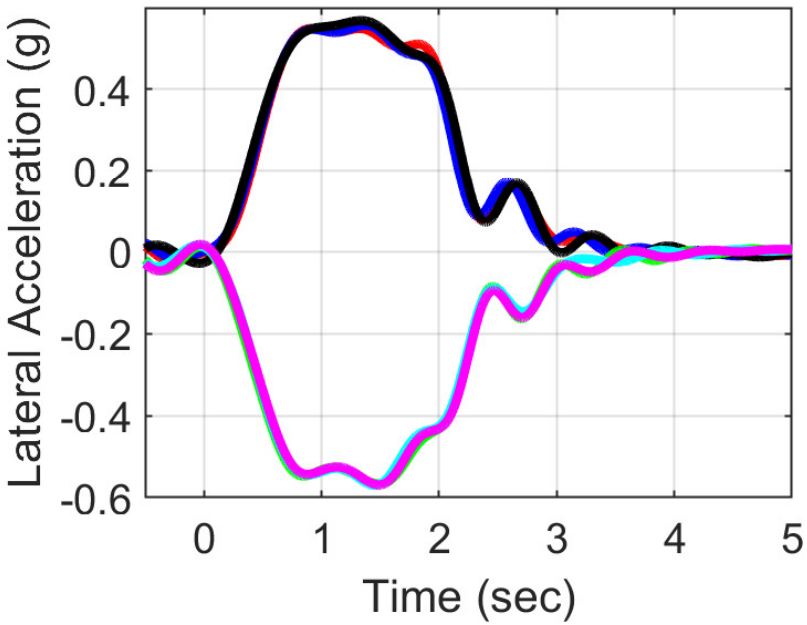

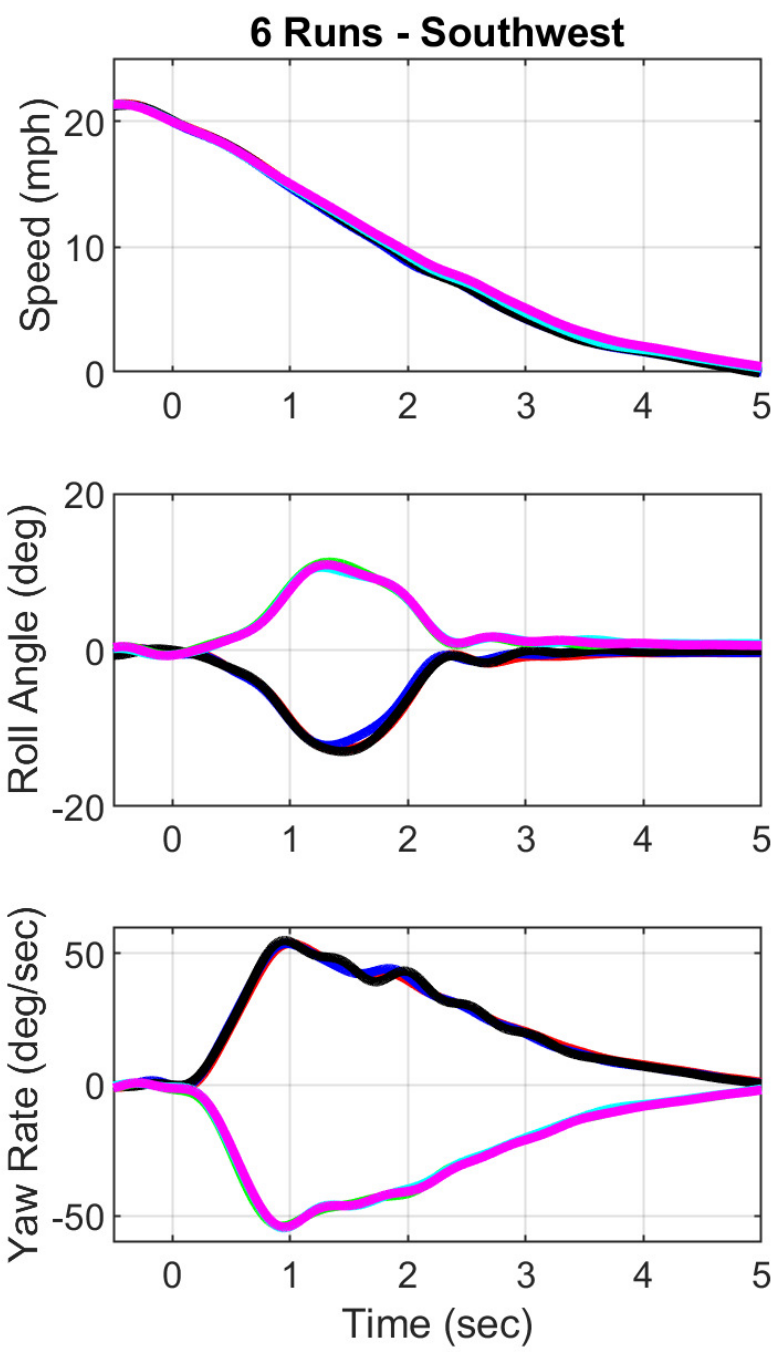

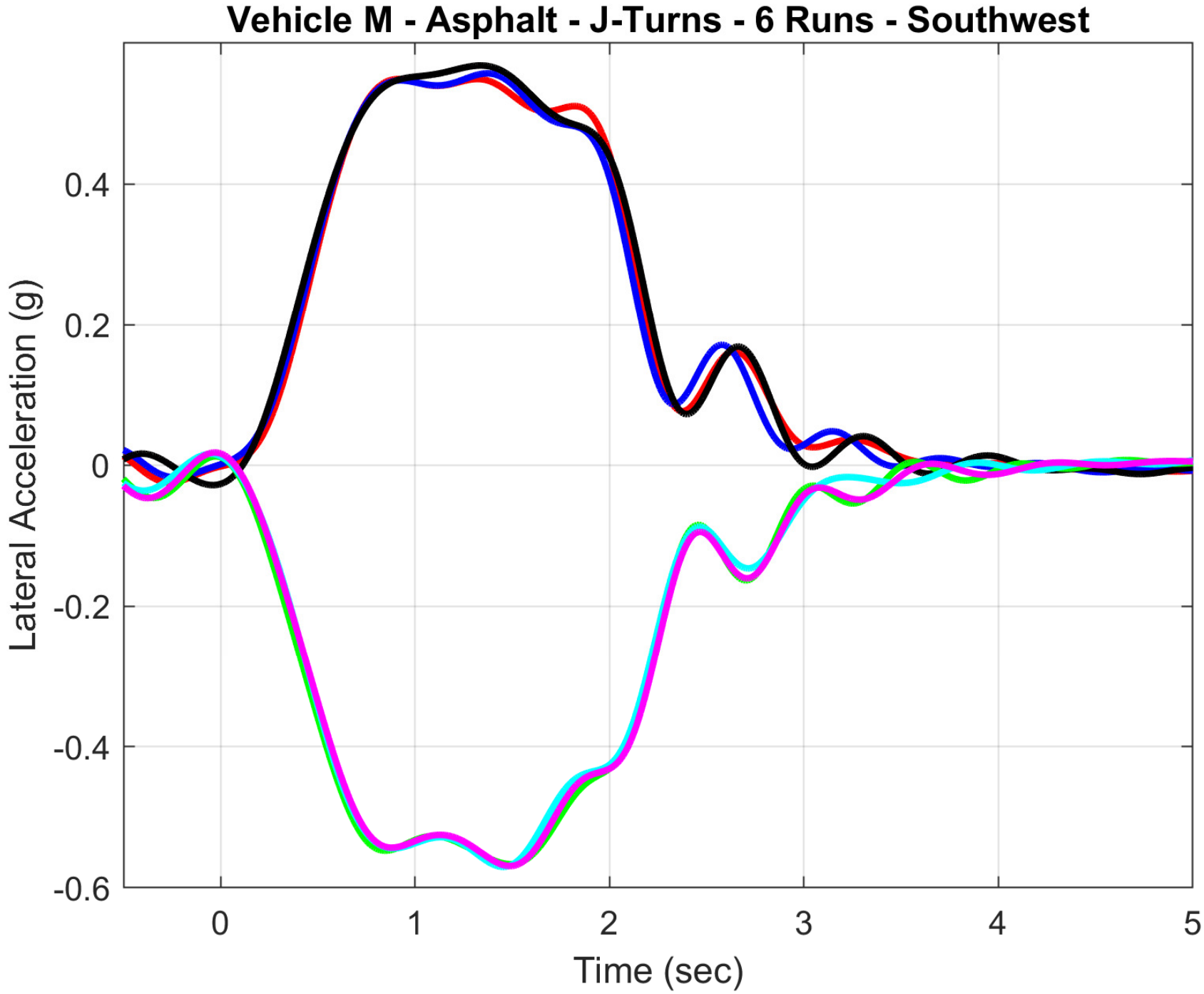

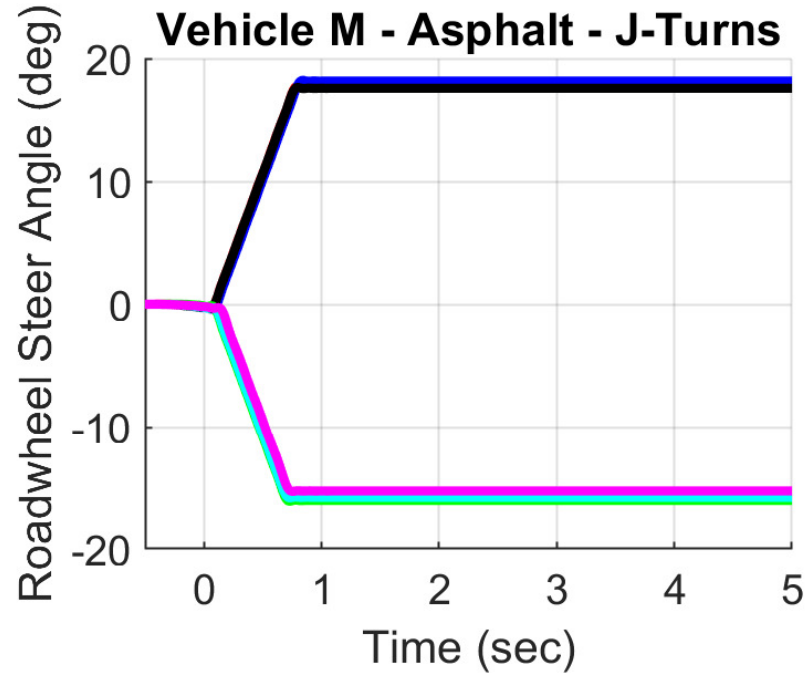

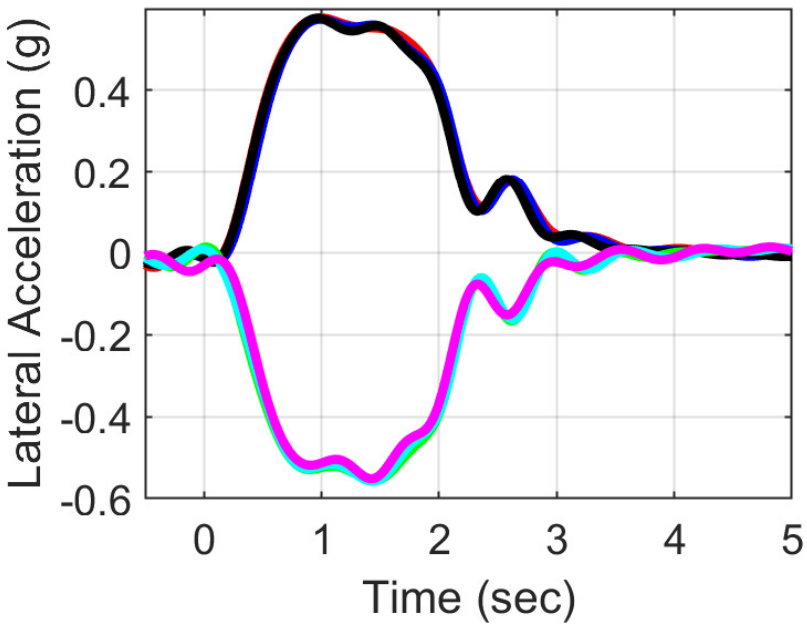

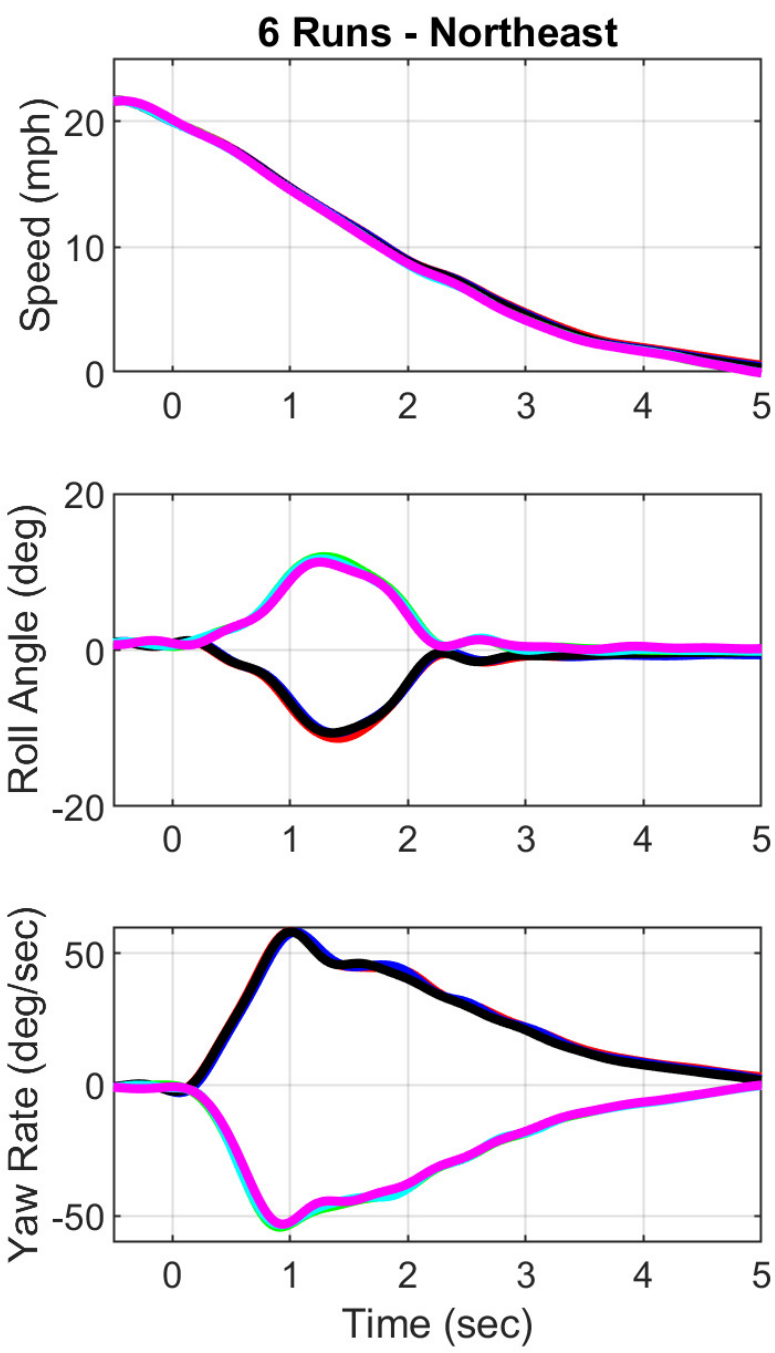

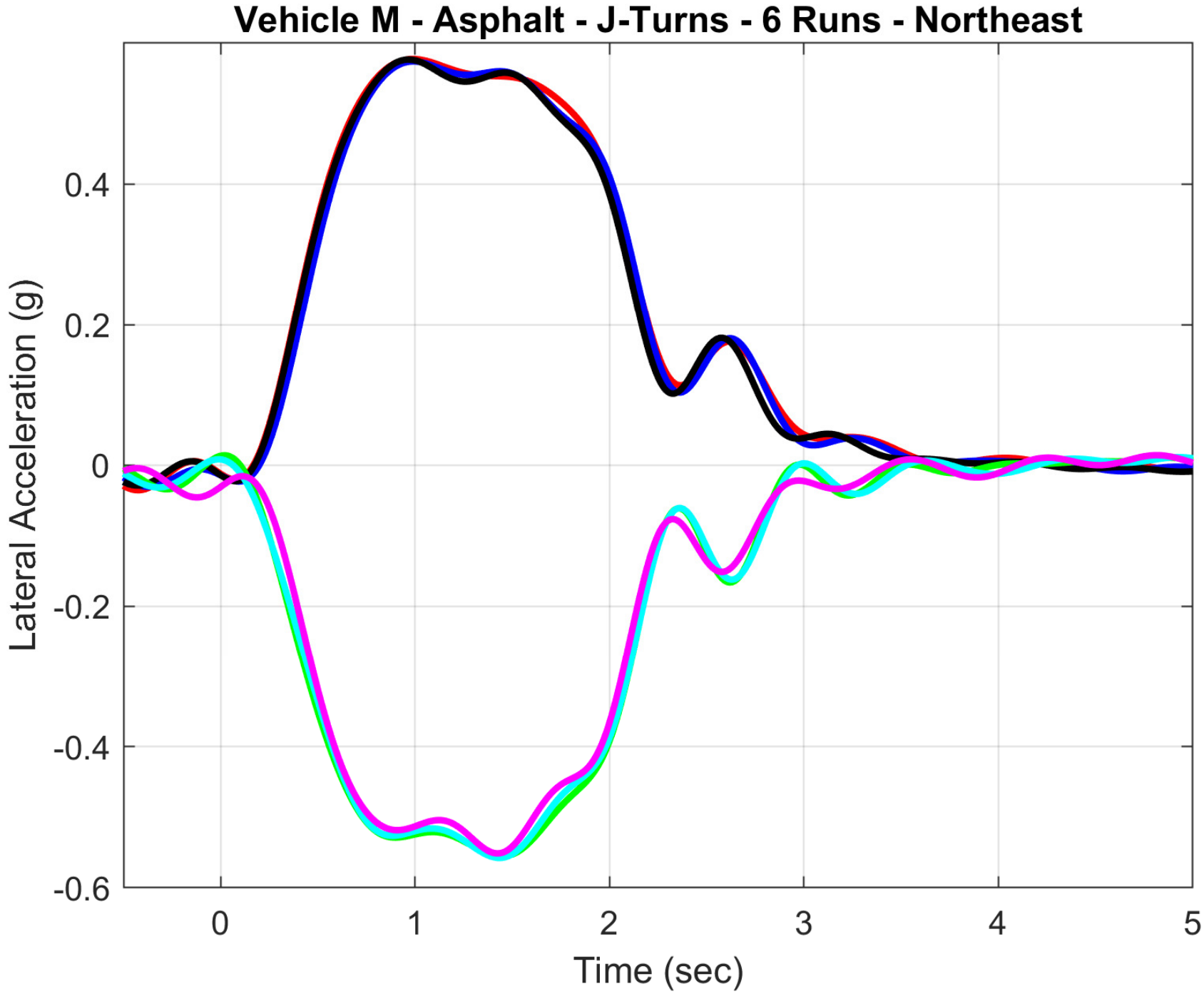

Vehicle M - Asphalt Results

Peak Lateral Accelerations During 2WL J-Turns - All Values in "g's"

Run Number	Northeast Right Turns	Northeast Left Turns
1	0.578	-0.556
2	0.574	-0.558
3	0.577	-0.551
Mean Value of 3 Runs	0.576	-0.555
Standard Deviation of 3 Runs	0.002	0.003

Average of 6 Northeast Runs

0.566

Run Number	Southwest Right Turns	Southwest Left Turns
1	0.549	-0.567
2	0.557	-0.570
3	0.568	-0.569
Mean Value of 3 Runs	0.558	-0.569
Standard Deviation of 3 Runs	0.010	0.002

Average of 6 Southwest Runs

0.563

Average of All 12 Runs

0.564

Threshold Ay

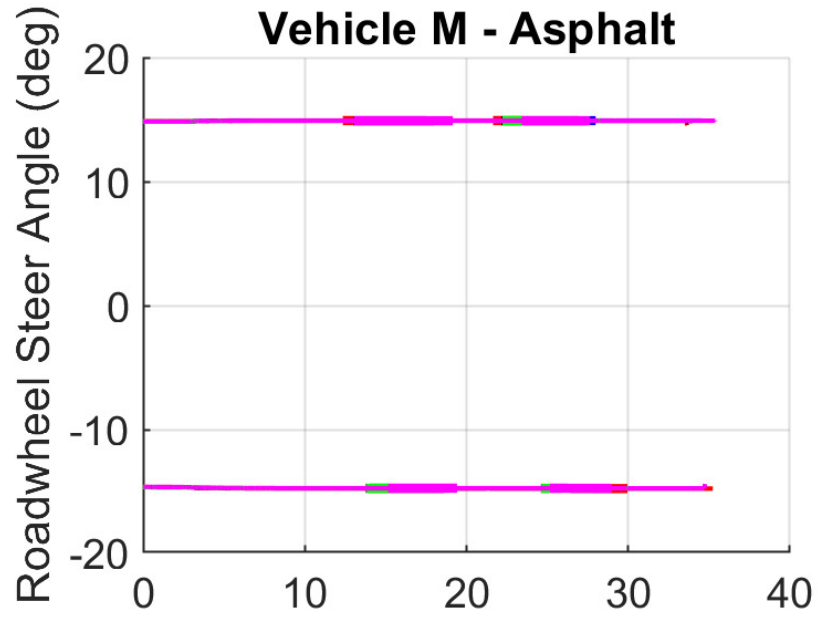

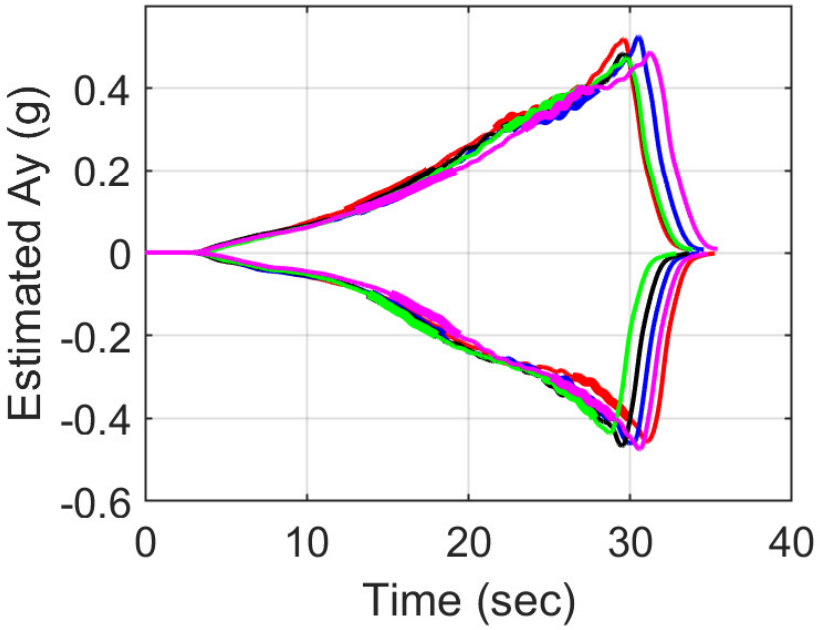

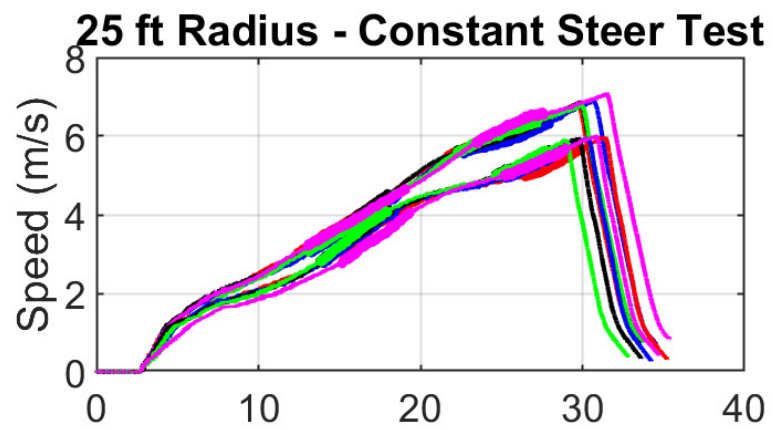

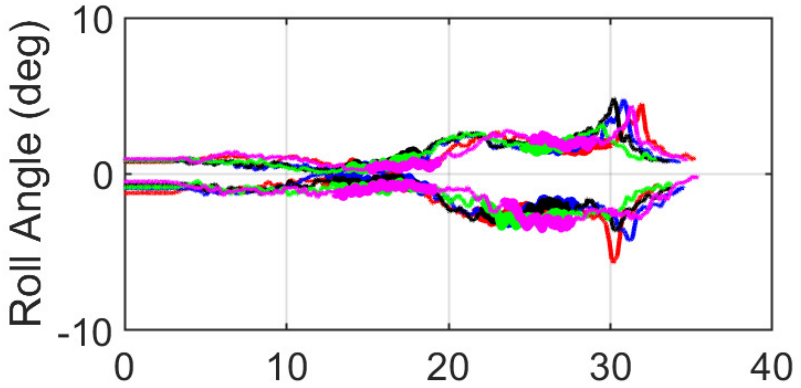

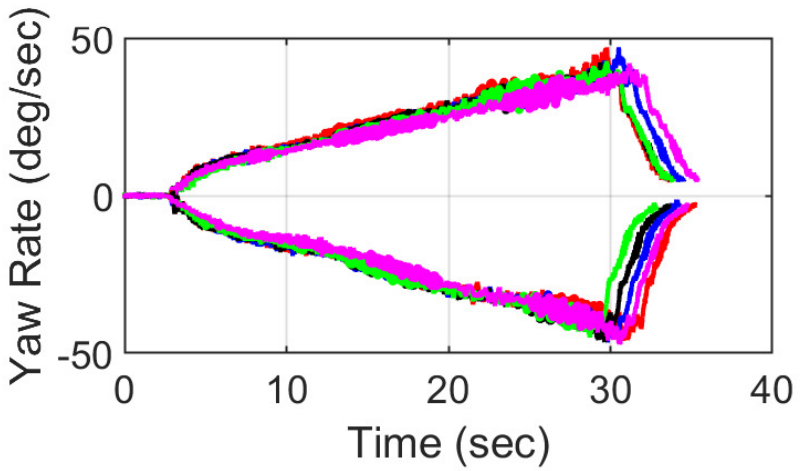

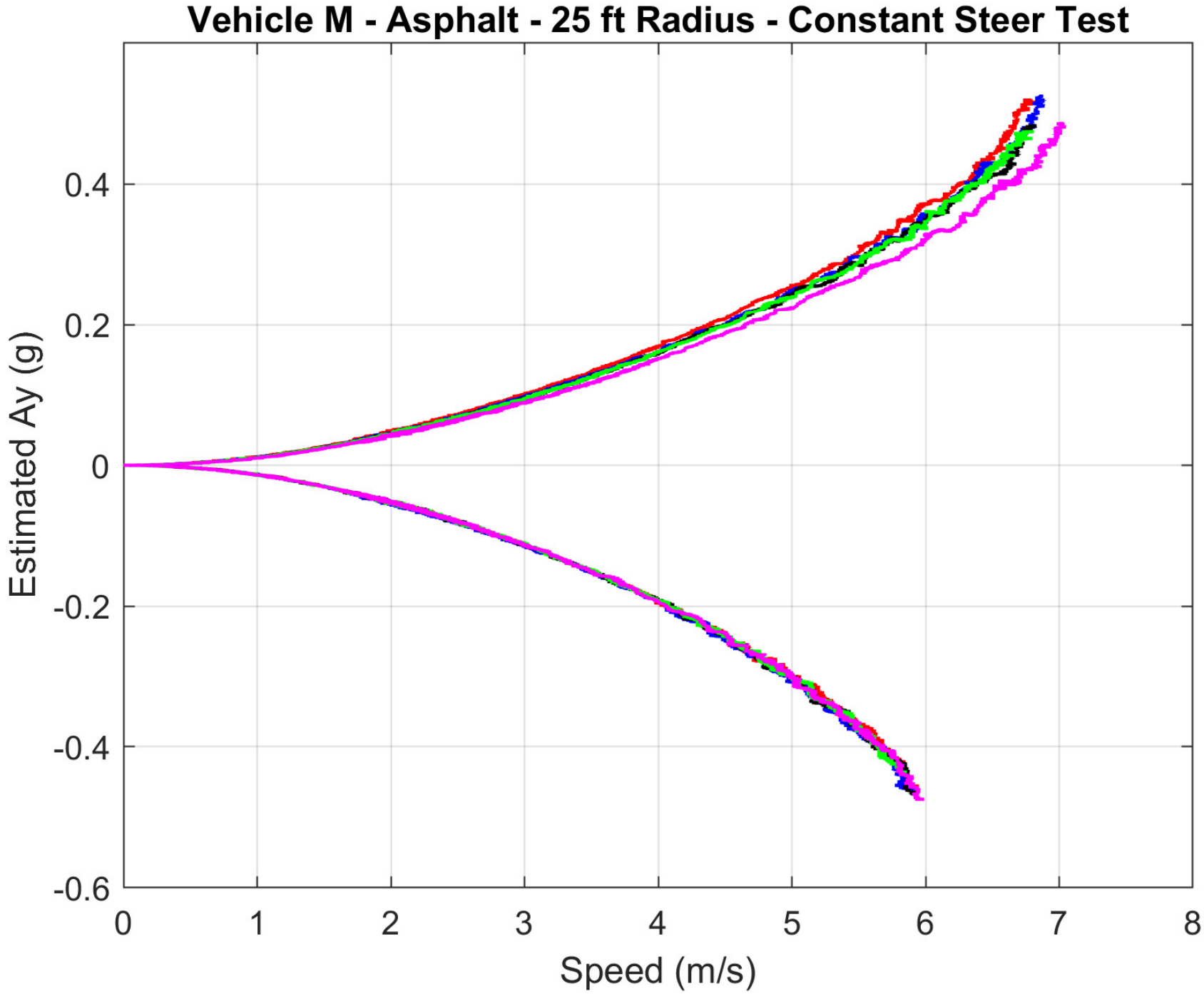

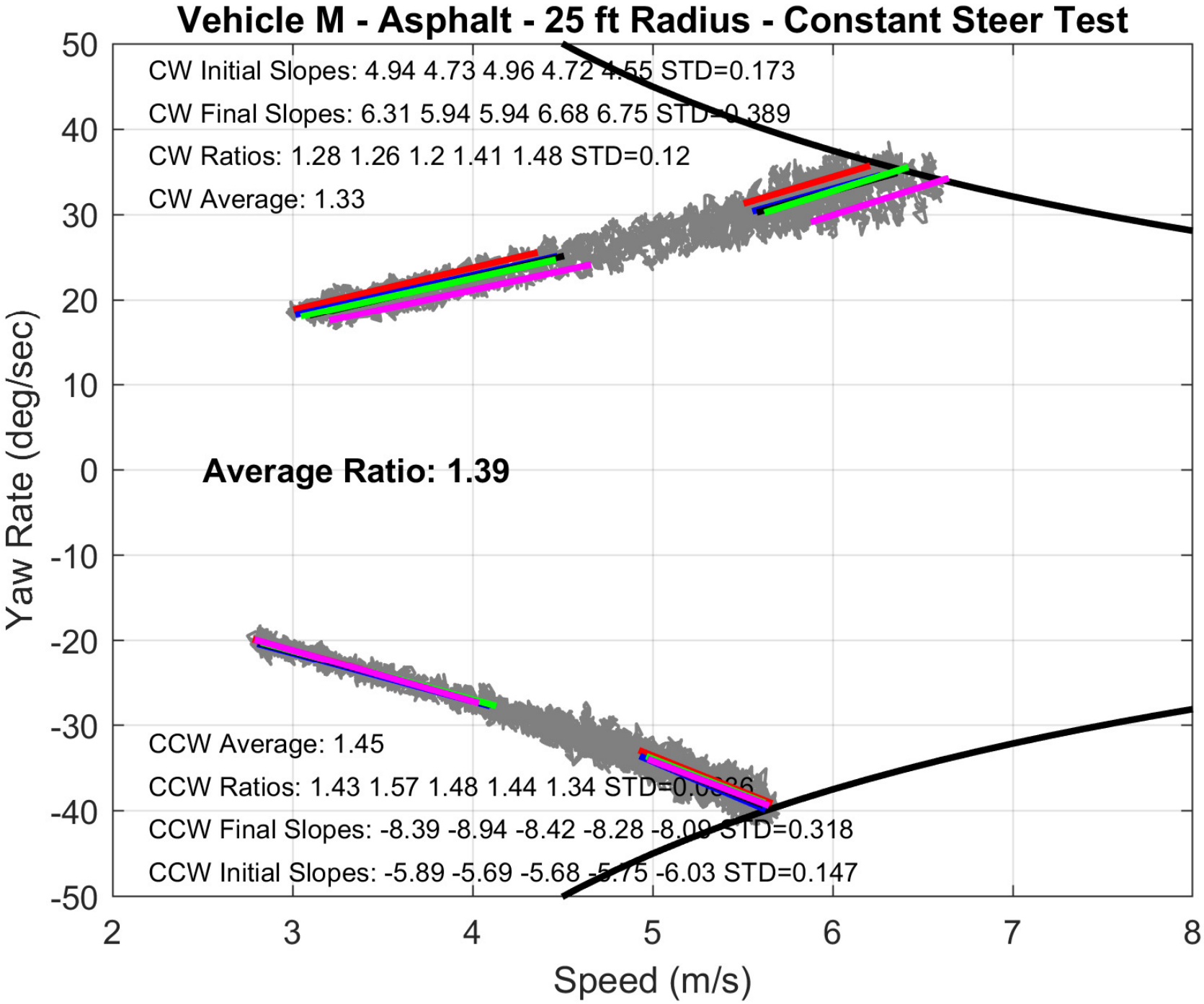

Vehicle M - Asphalt - 25 ft Radius - Constant Steer Test - CW Runs

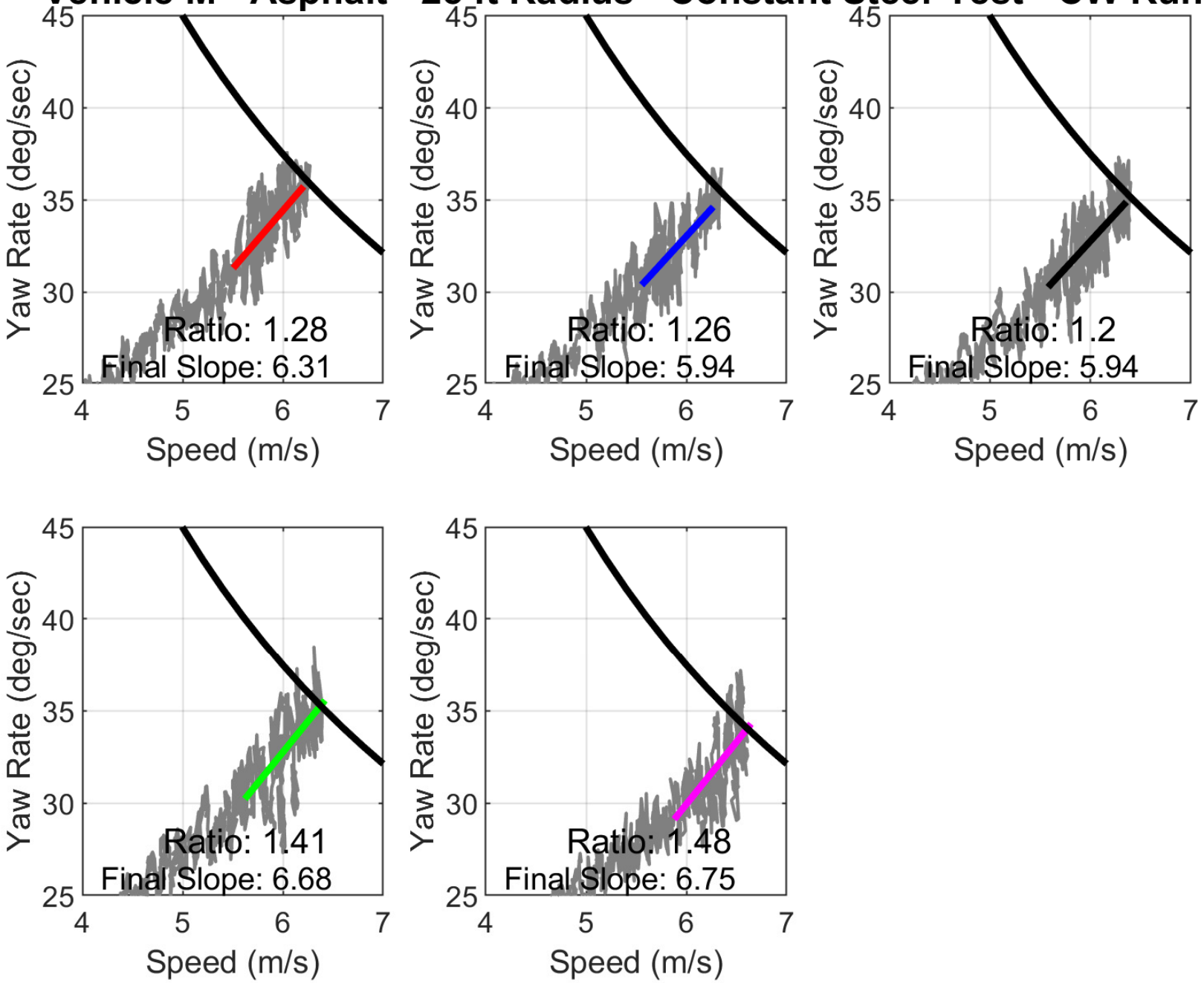

Vehicle M - Asphalt - 25 ft Radius - Constant Steer Test - CCW Runs

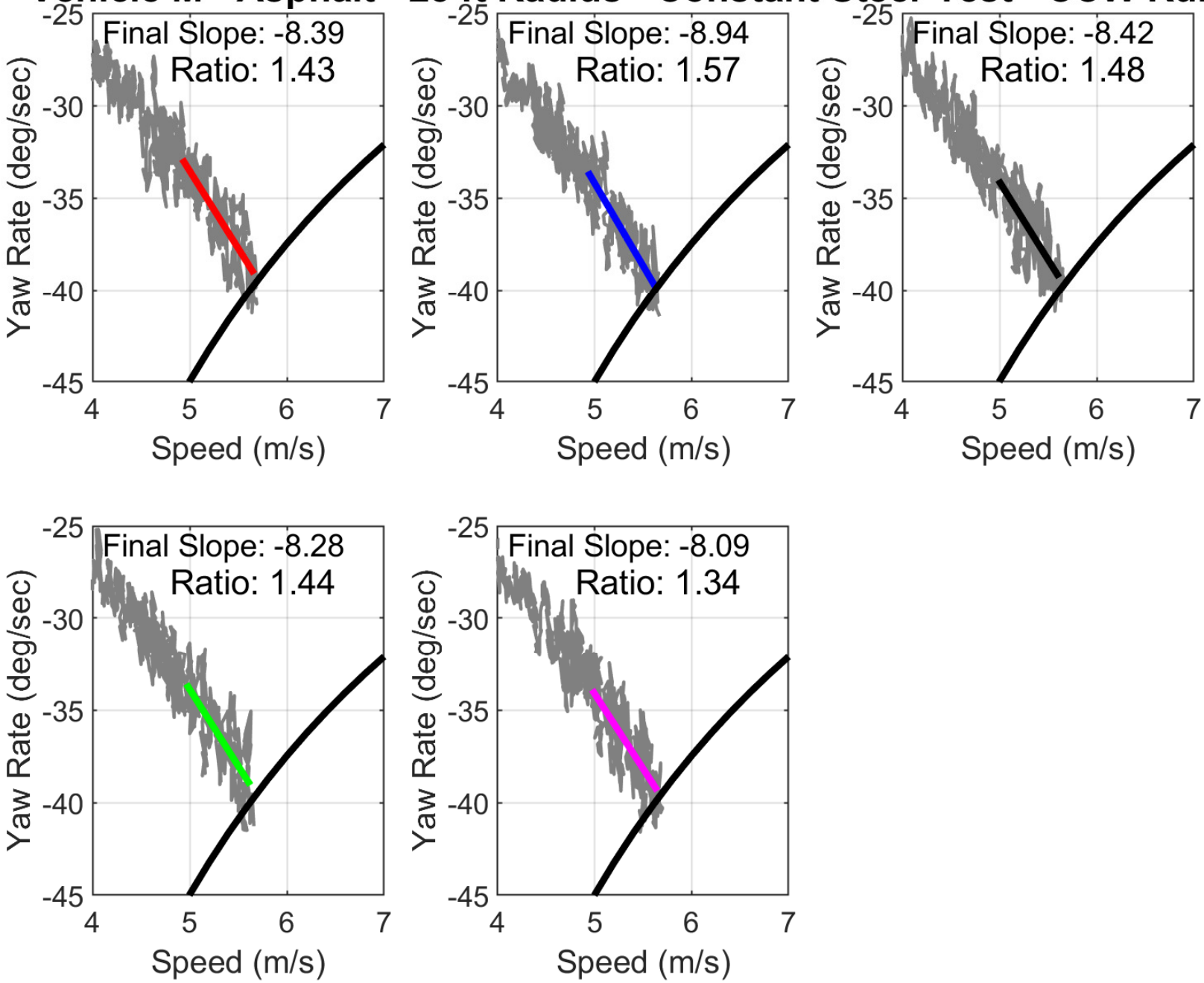

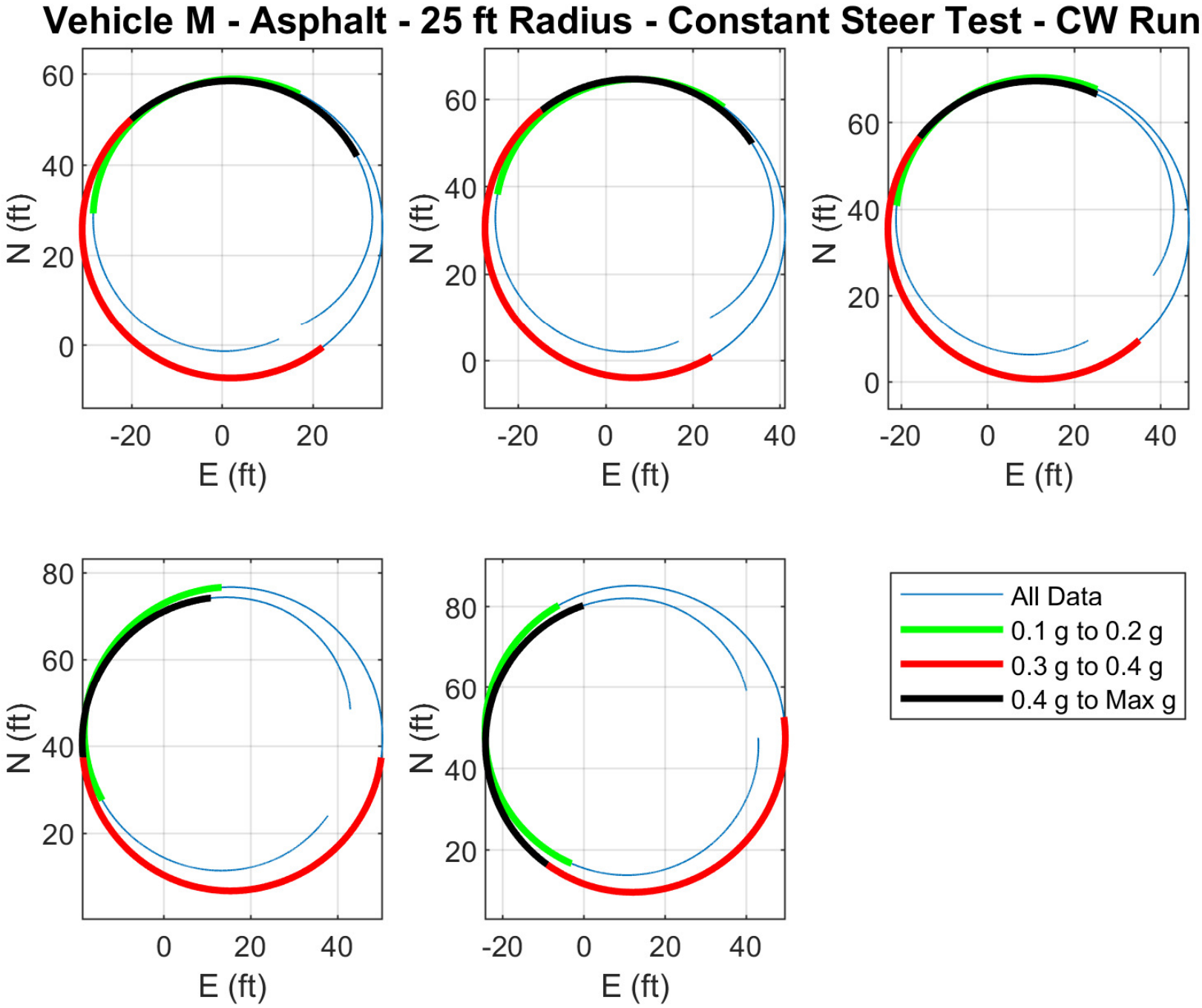

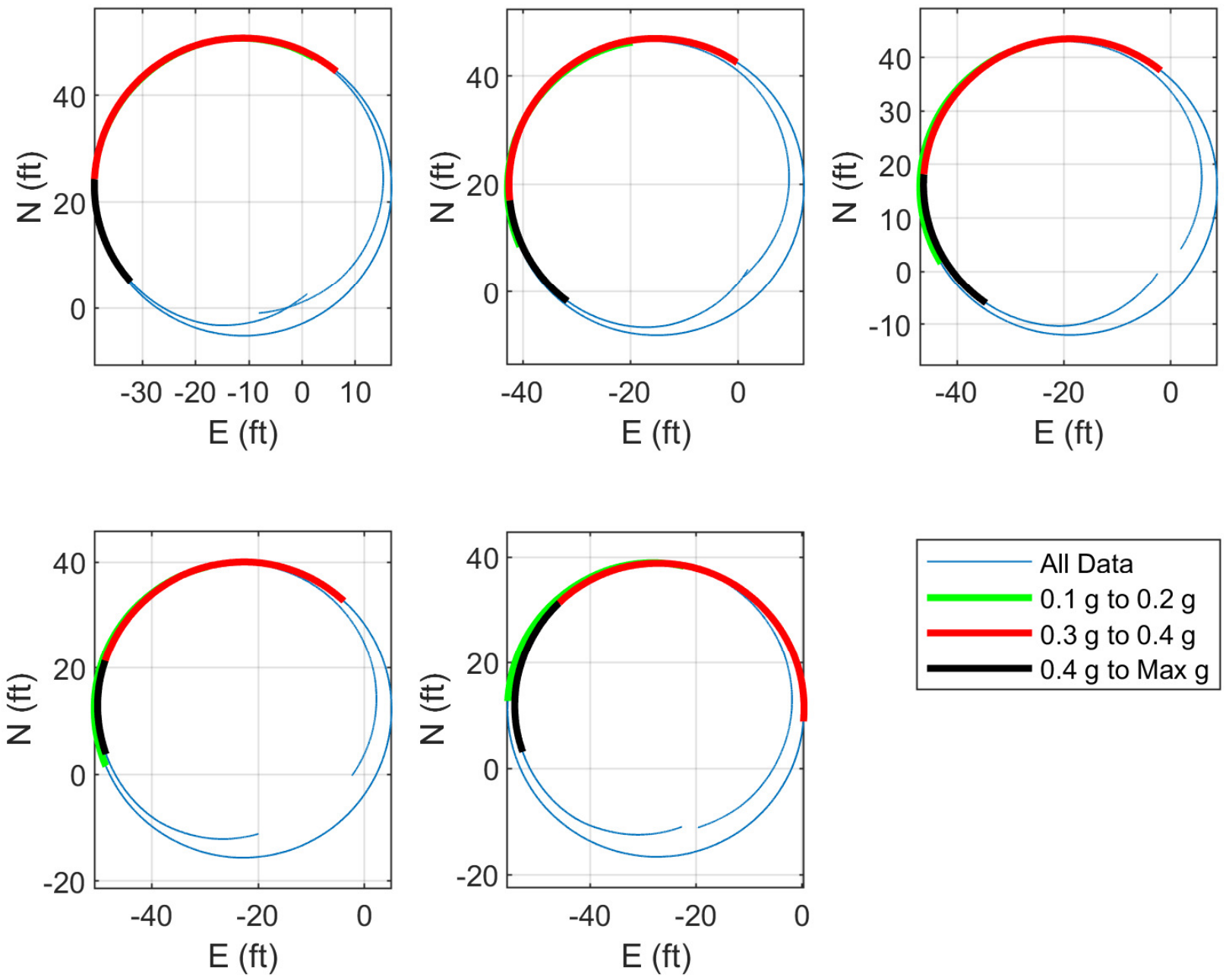

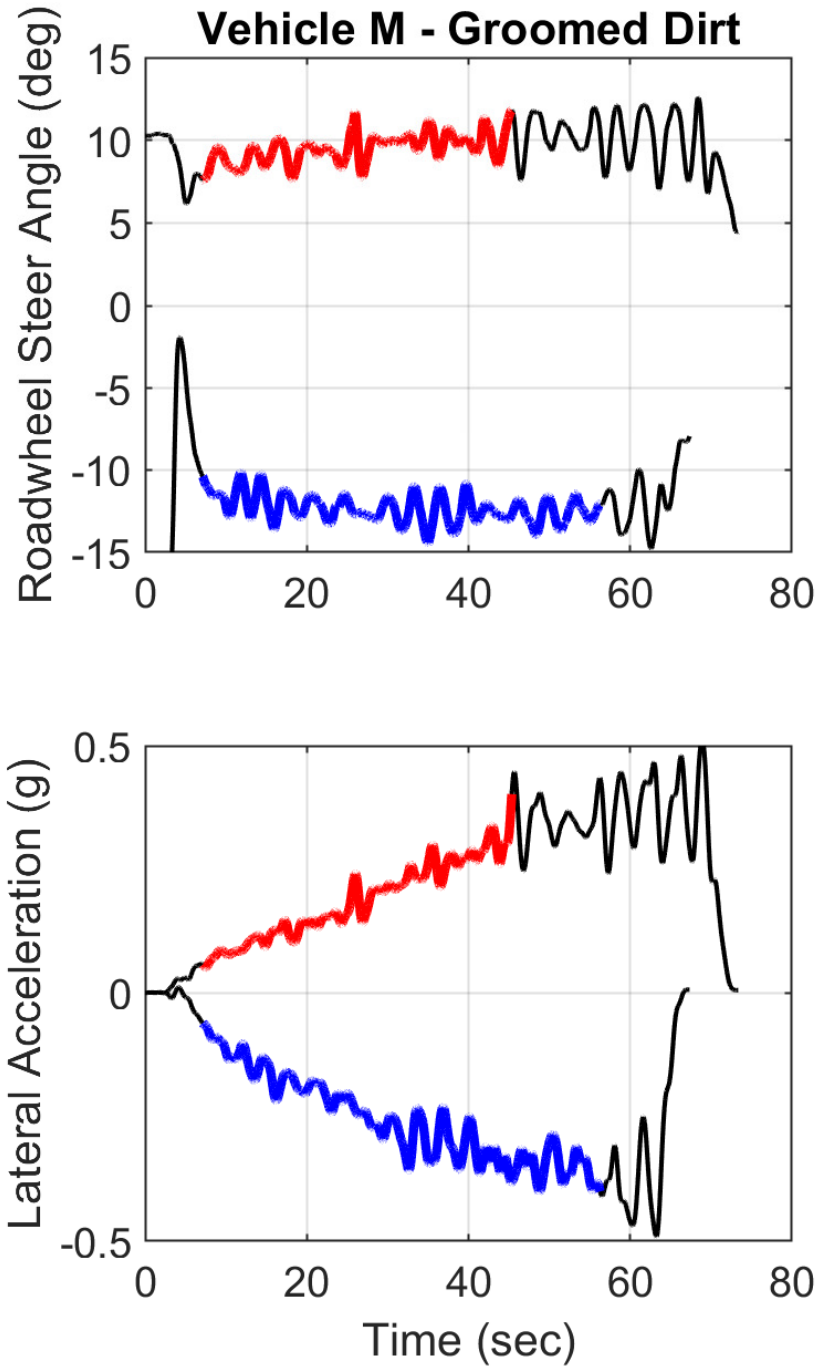

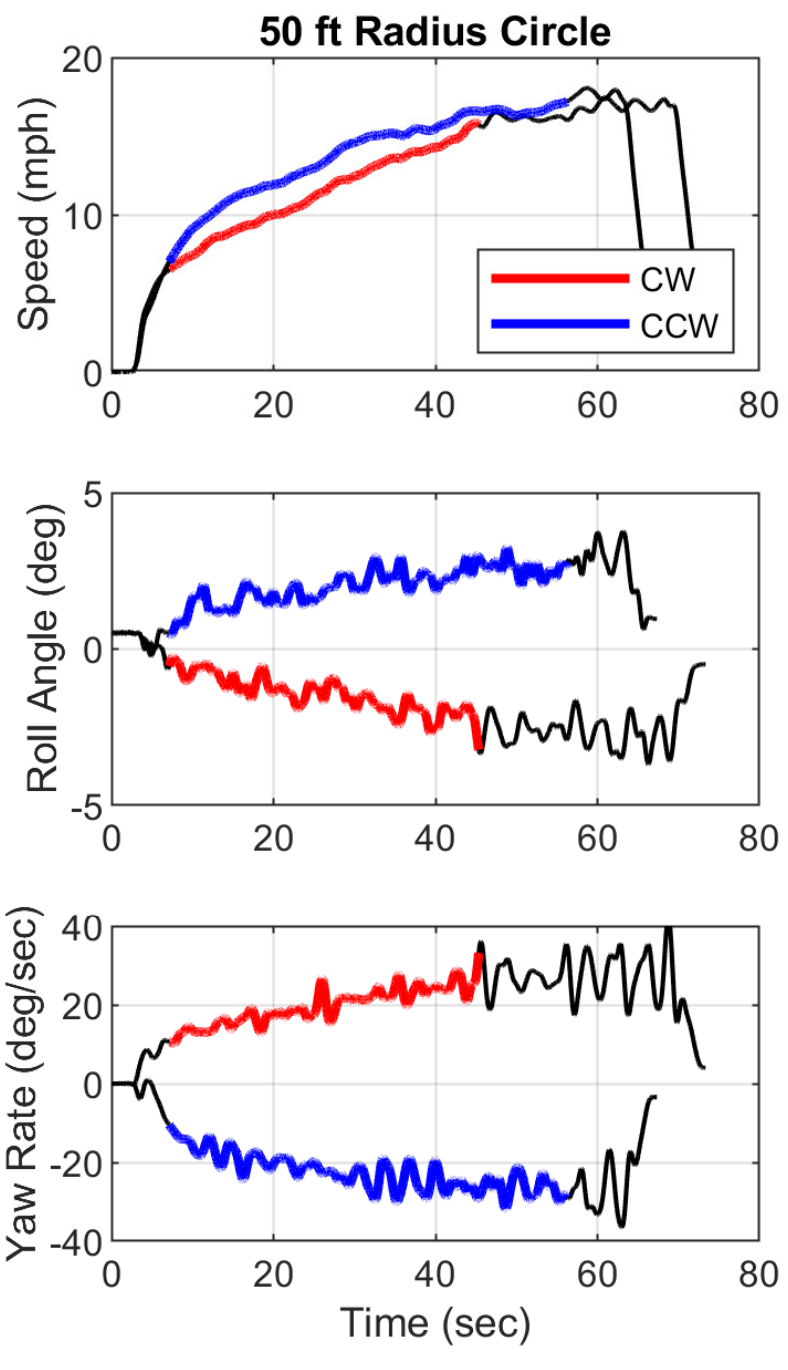

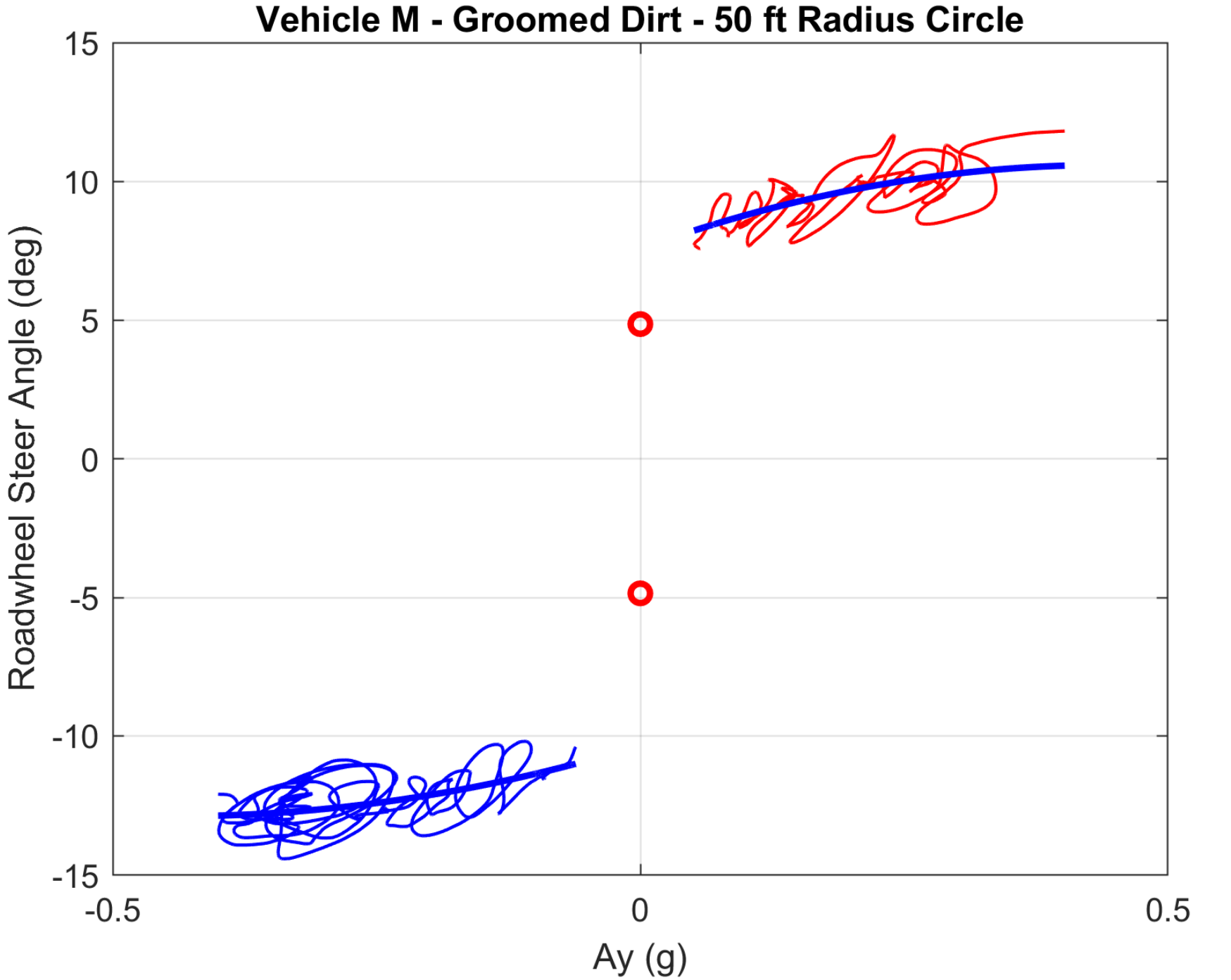

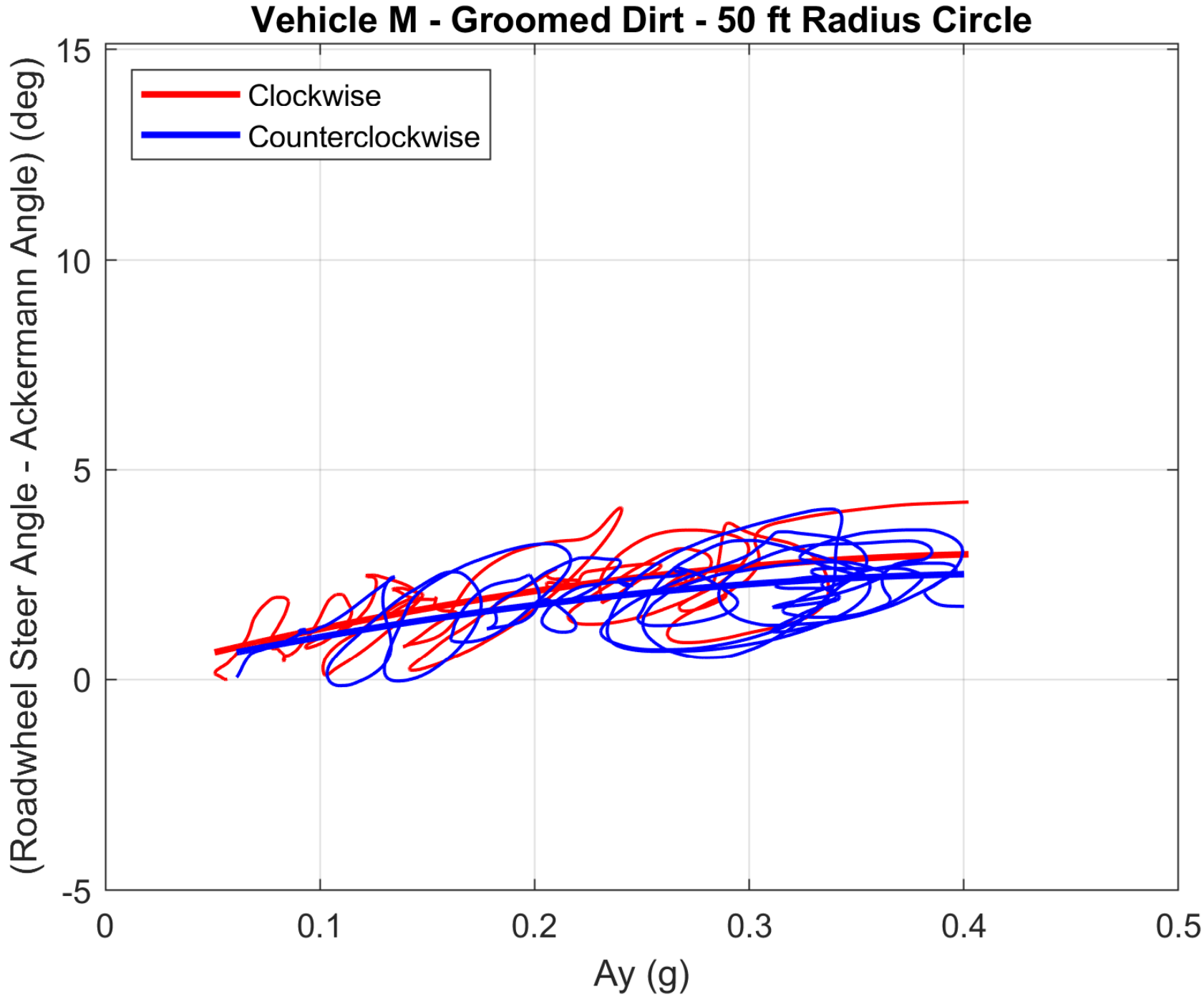

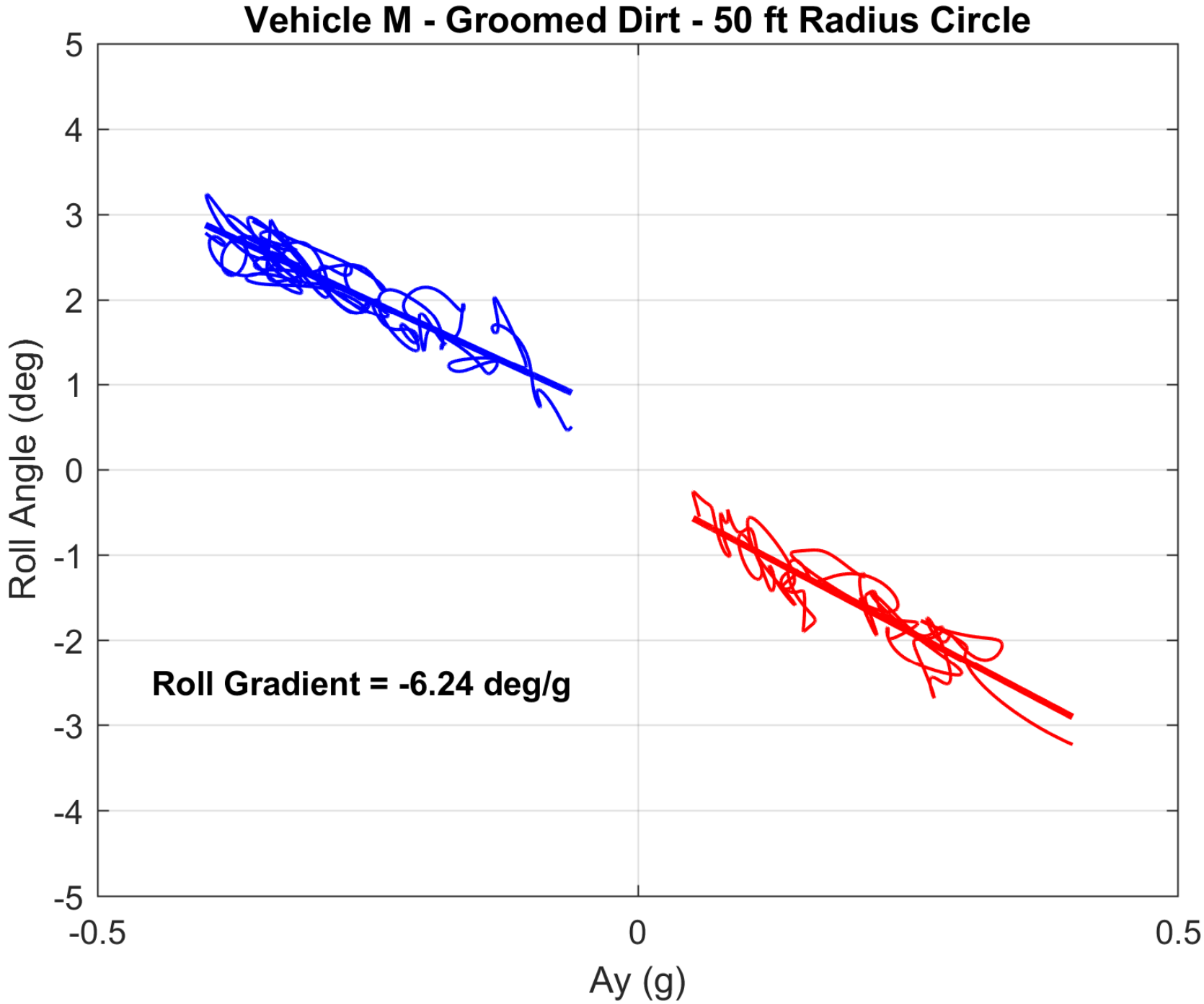

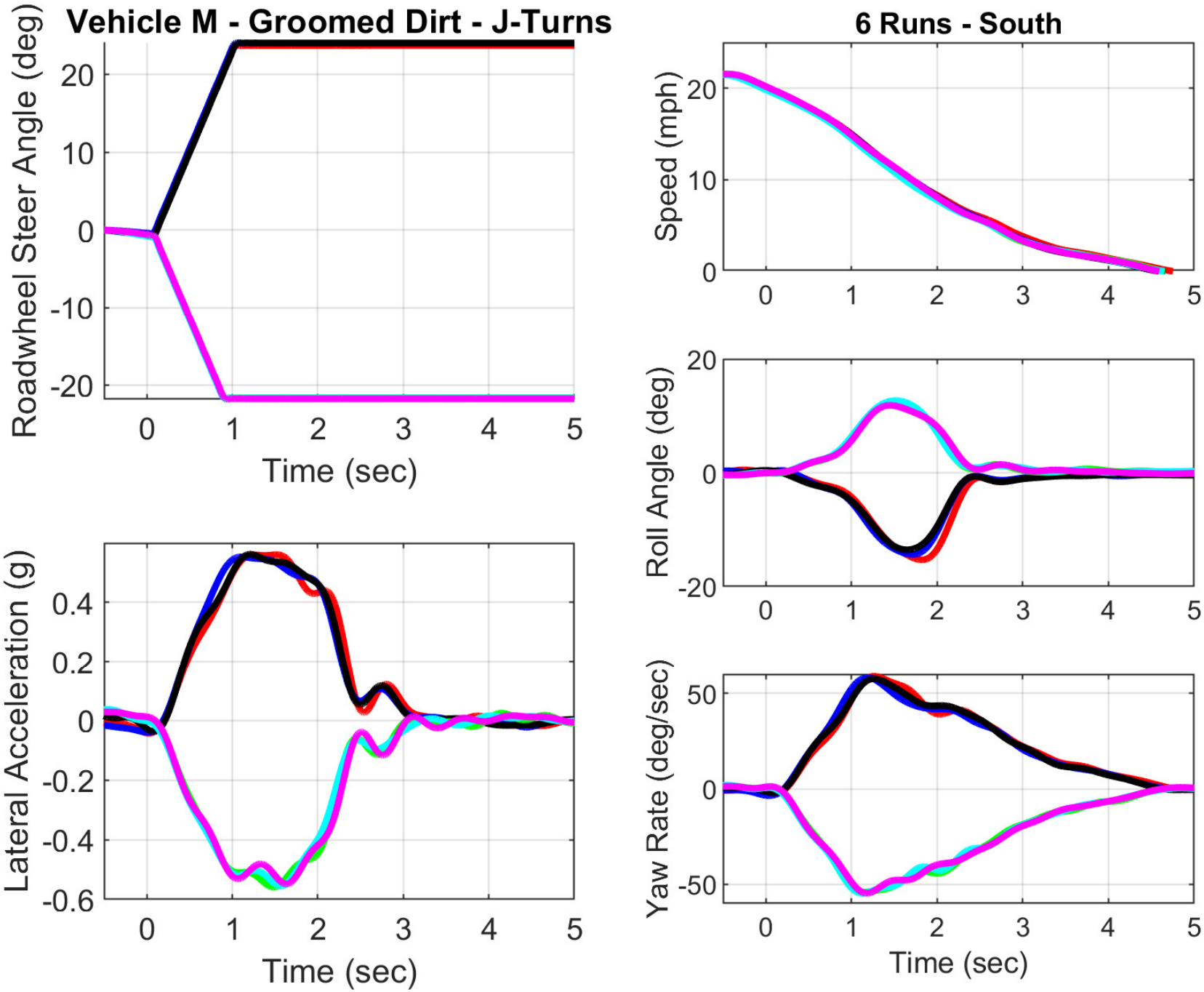

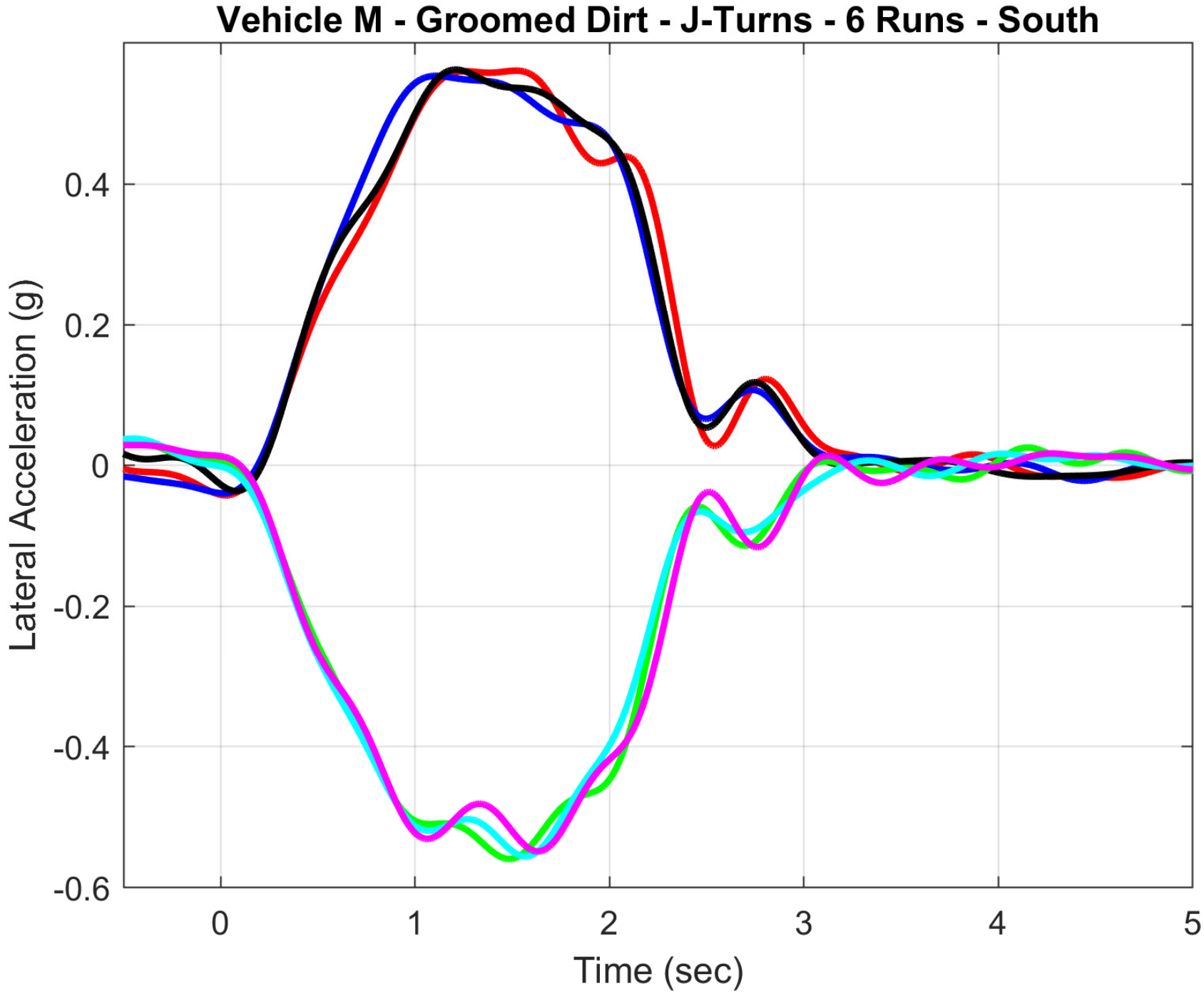

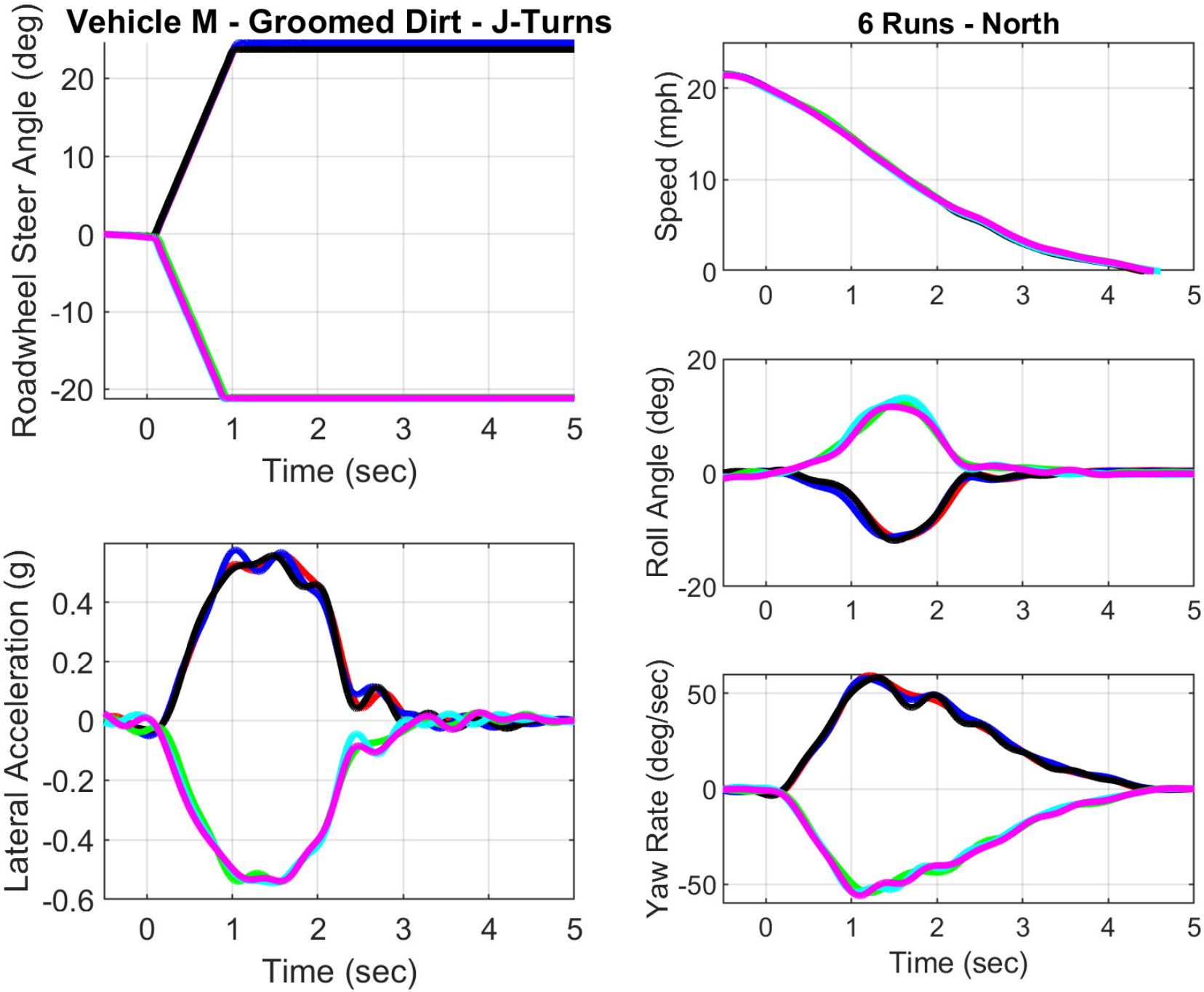

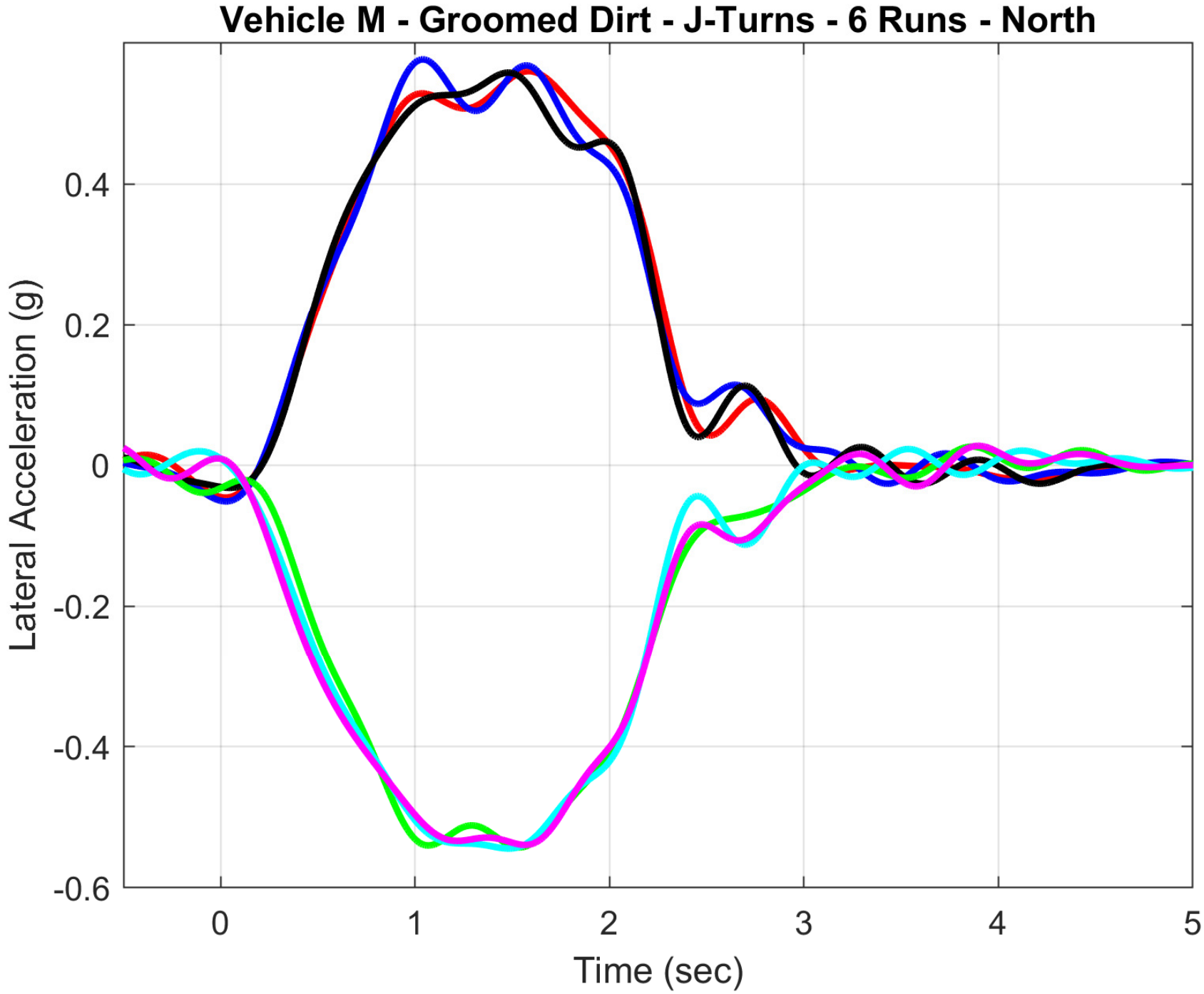

Vehicle M - Groomed Dirt Results

Peak Lateral Accelerations During 2WL J-Turns - All Values in "g's"

Run Number	North Right Turns	North Left Turns
1	0.560	-0.543
2	0.577	-0.544
3	0.558	-0.539
Mean Value of 3 Runs	0.565	-0.542
Standard Deviation of 3 Runs	0.010	0.003

Average of 6 North Runs

0.554

Average of All 12 Runs

0.555

Threshold Ay

Run Number	South Right Turns	South Left Turns
1	0.561	-0.559
2	0.554	-0.556
3	0.563	-0.549
Mean Value of 3 Runs	0.559	-0.554
Standard Deviation of 3 Runs	0.005	0.005

Average of 6 South Runs

0.557

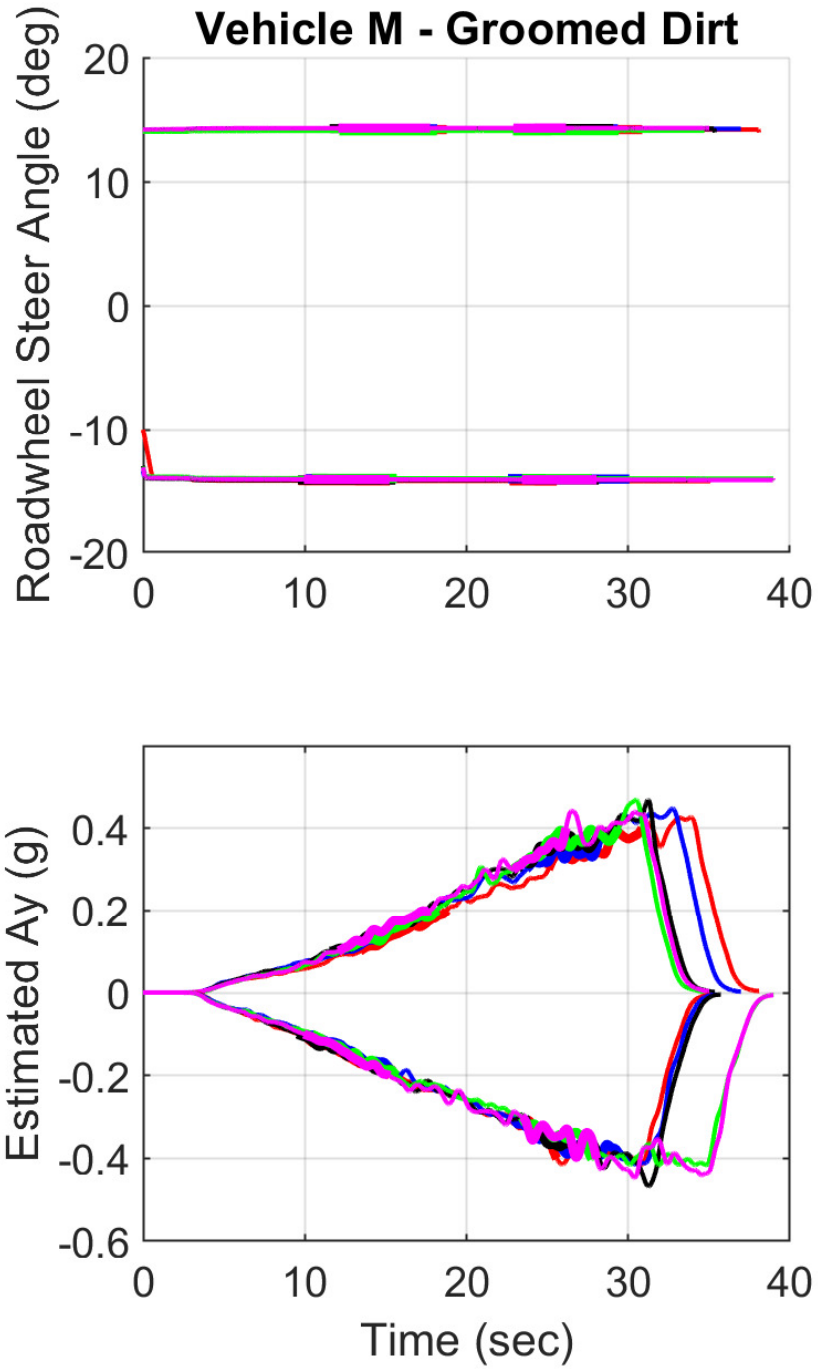

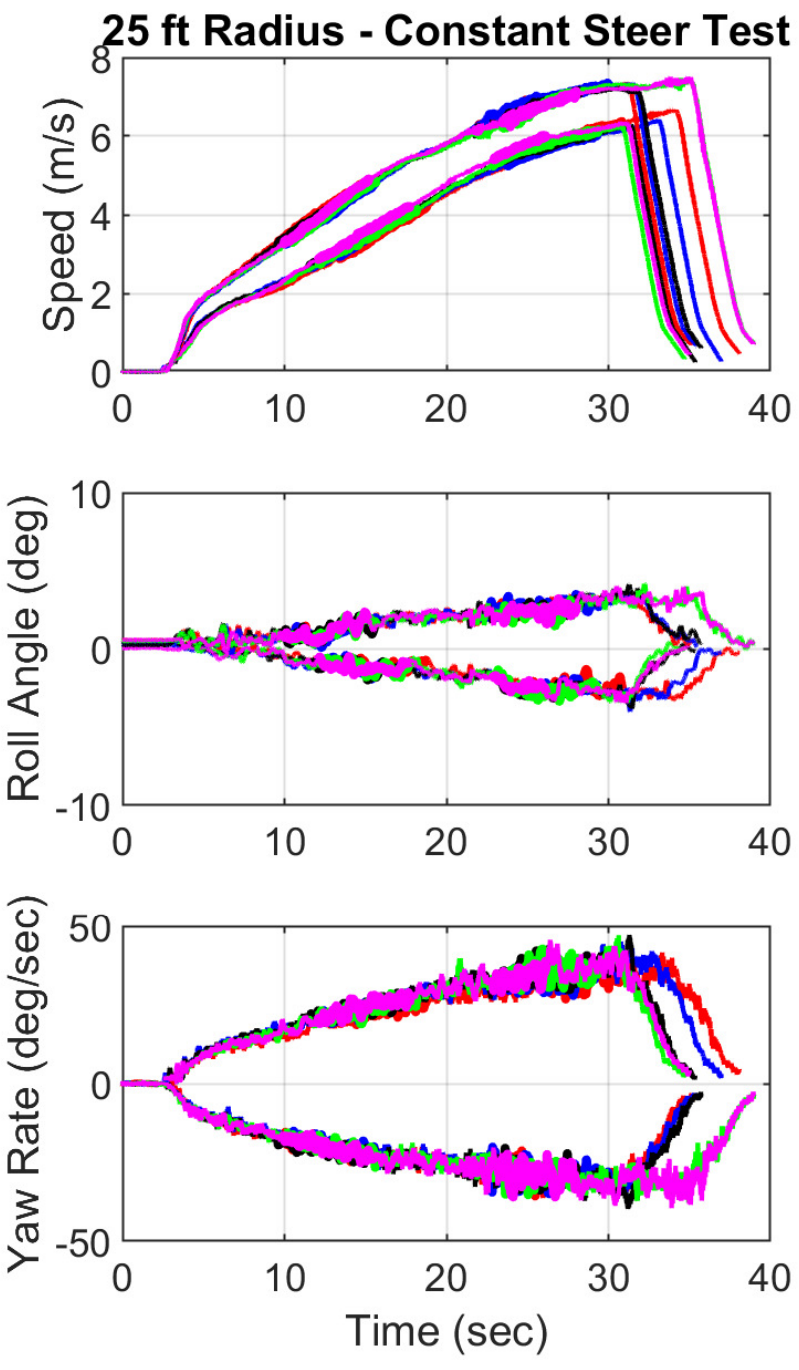

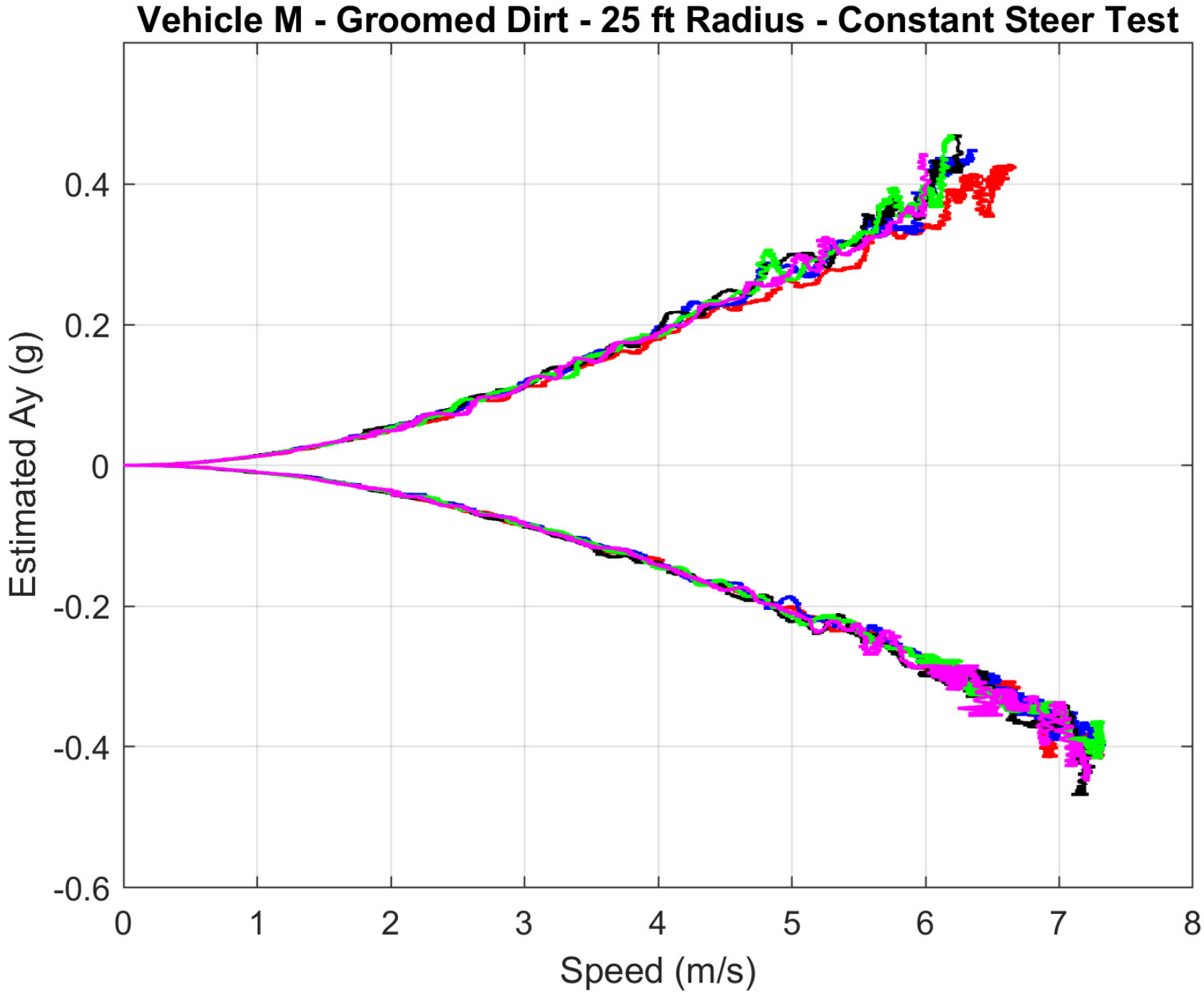

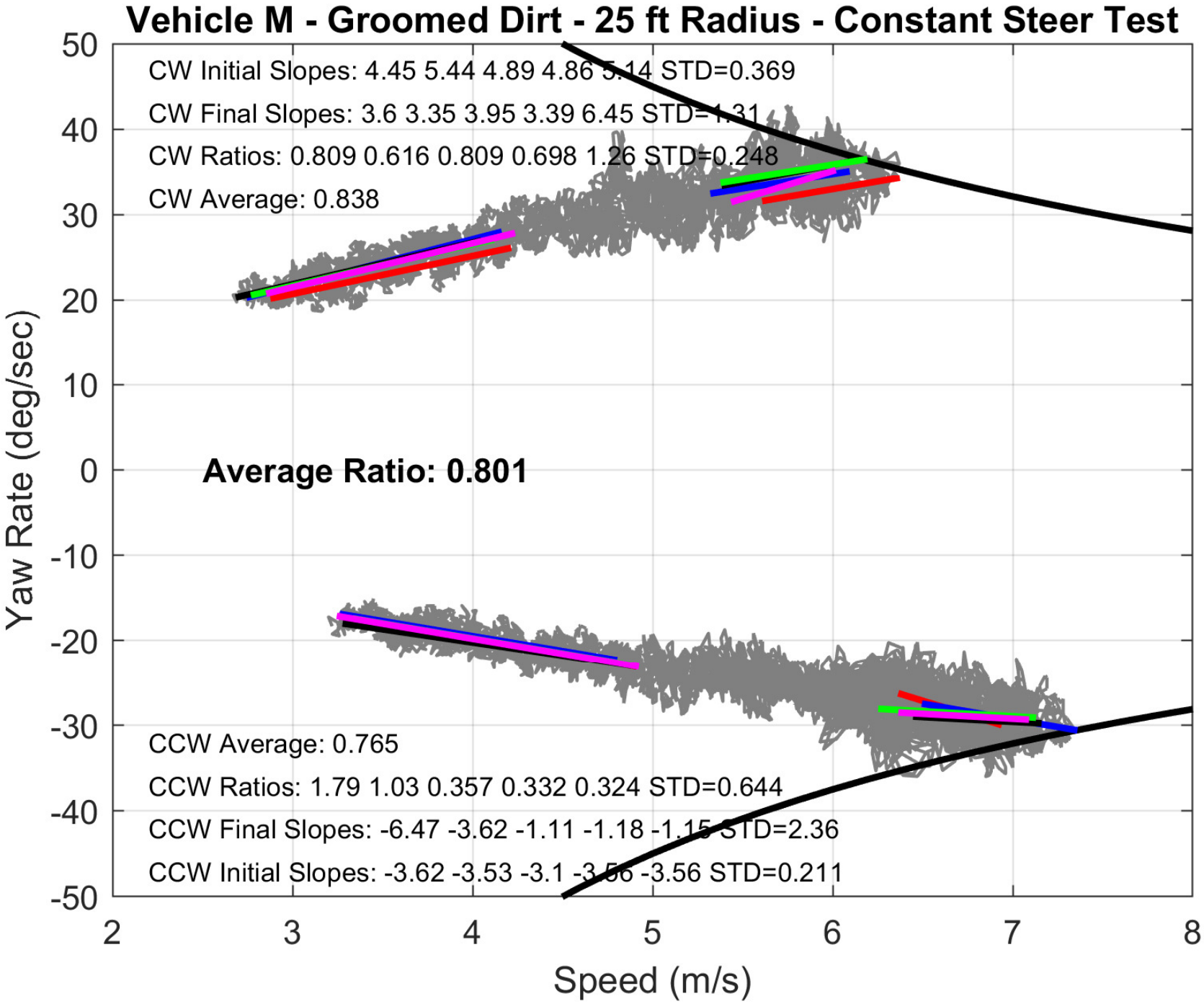

Vehicle M - Groomed Dirt - 25 ft Radius - Constant Steer Test - CW Runs

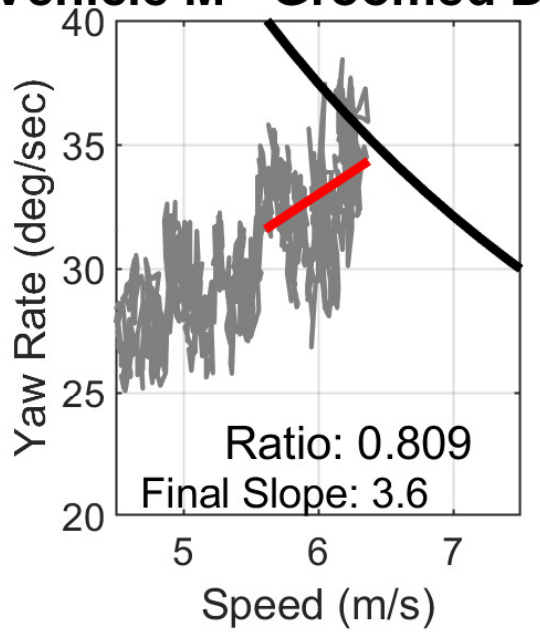

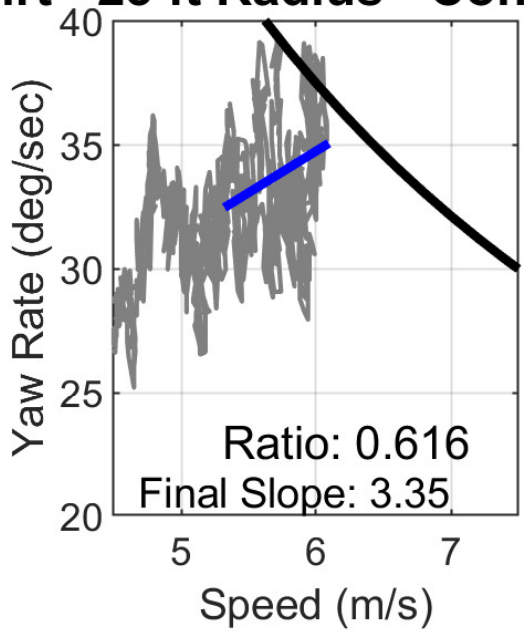

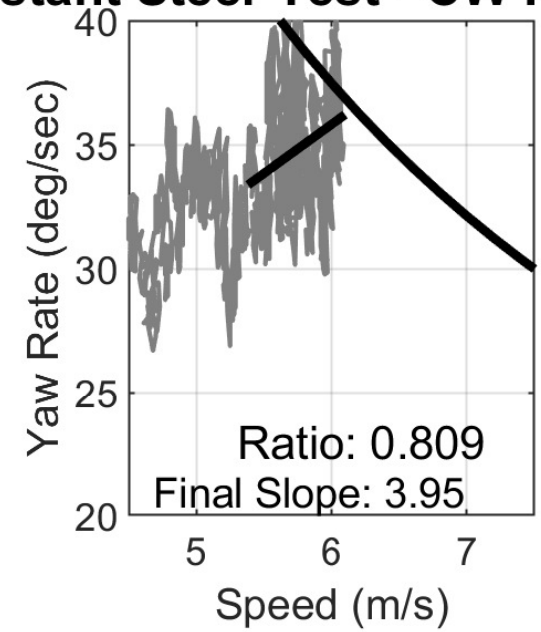

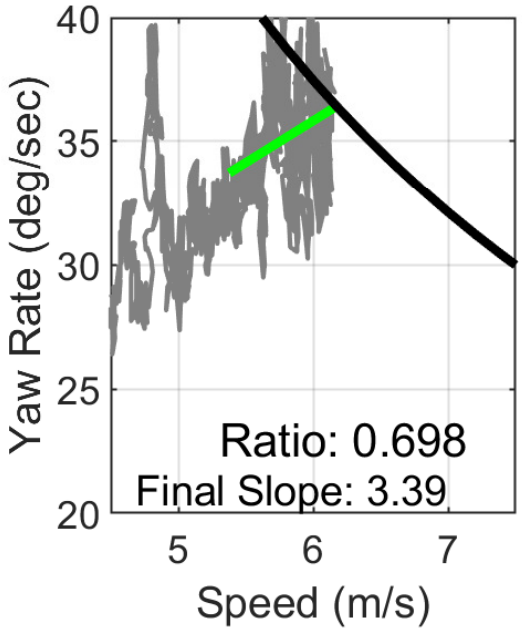

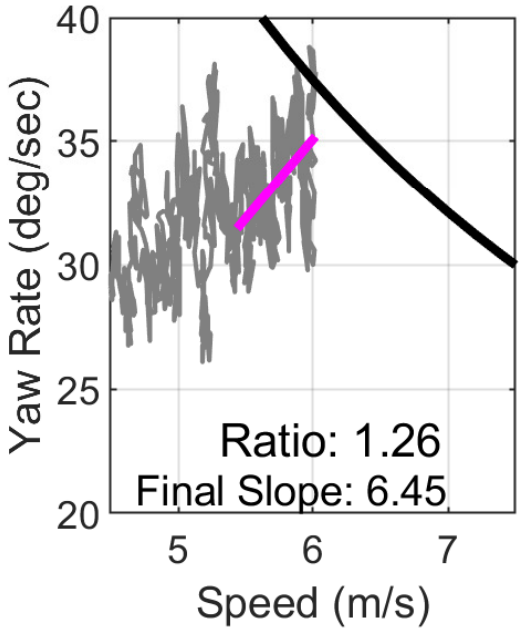

Vehicle M - Groomed Dirt - 25 ft Radius - Constant Steer Test - CCW Runs

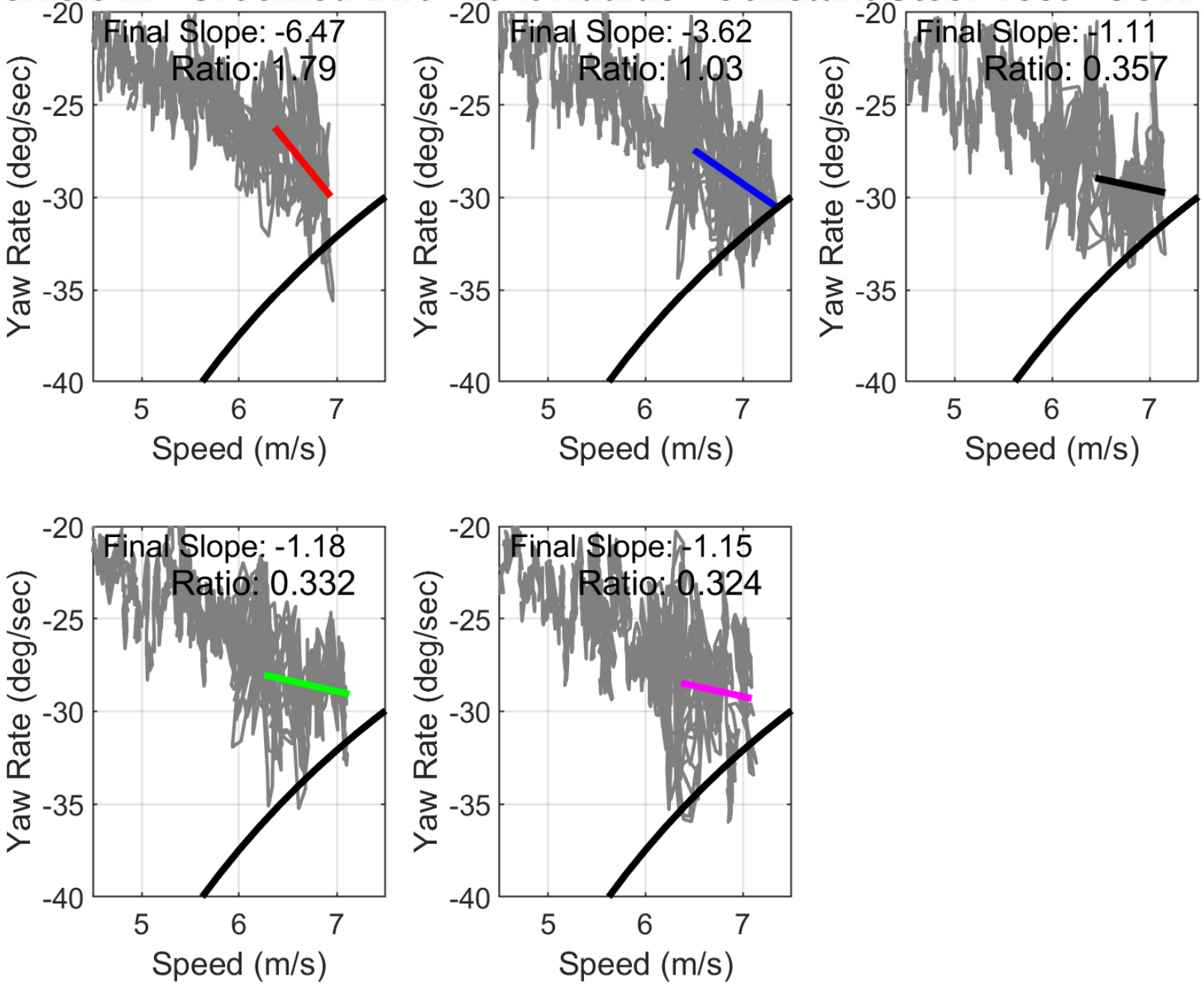

Vehicle M - Groomed Dirt - 25 ft Radius - Constant Steer Test - CW Runs

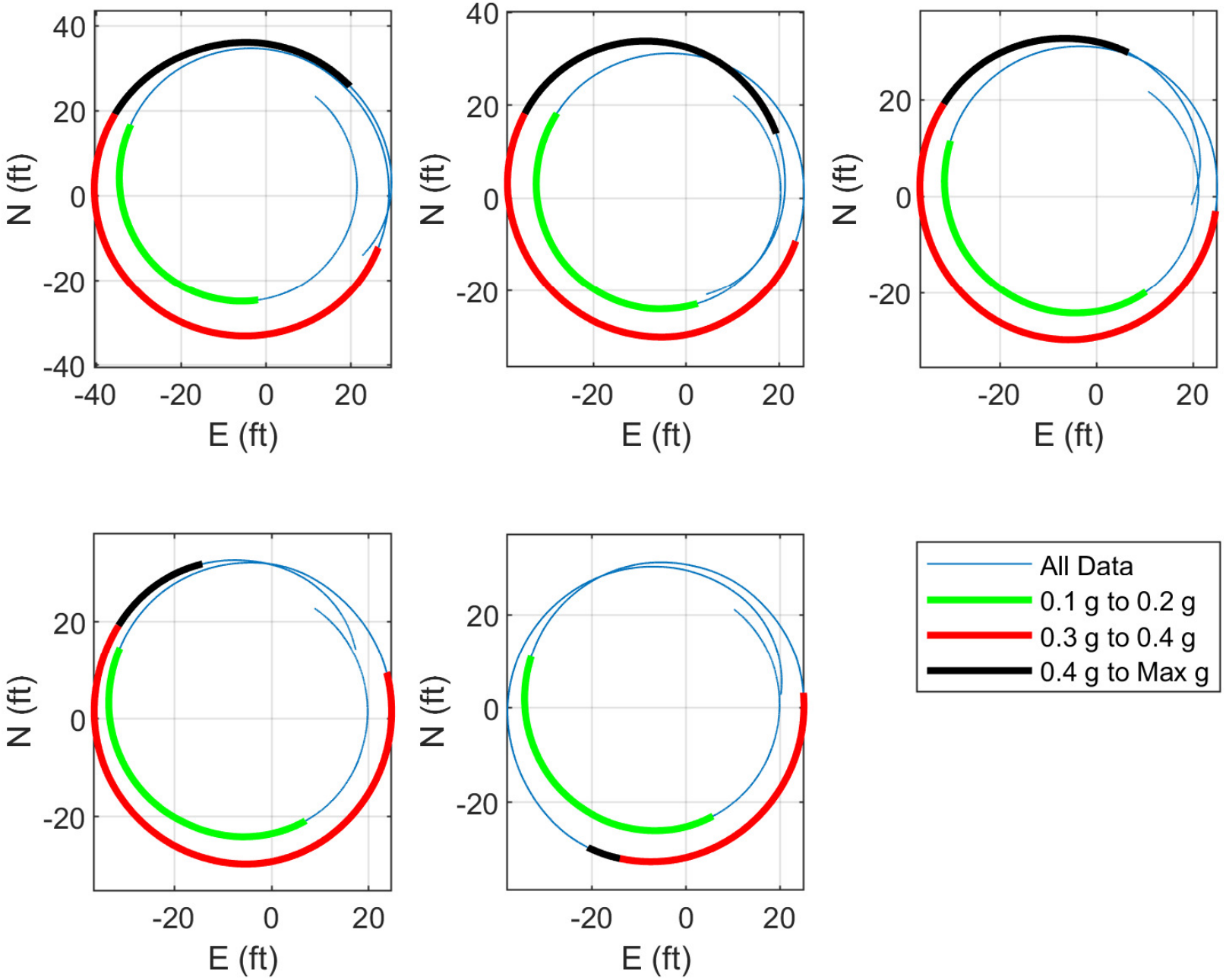

Vehicle M - Groomed Dirt - 25 ft Radius - Constant Steer Test - CCW Runs

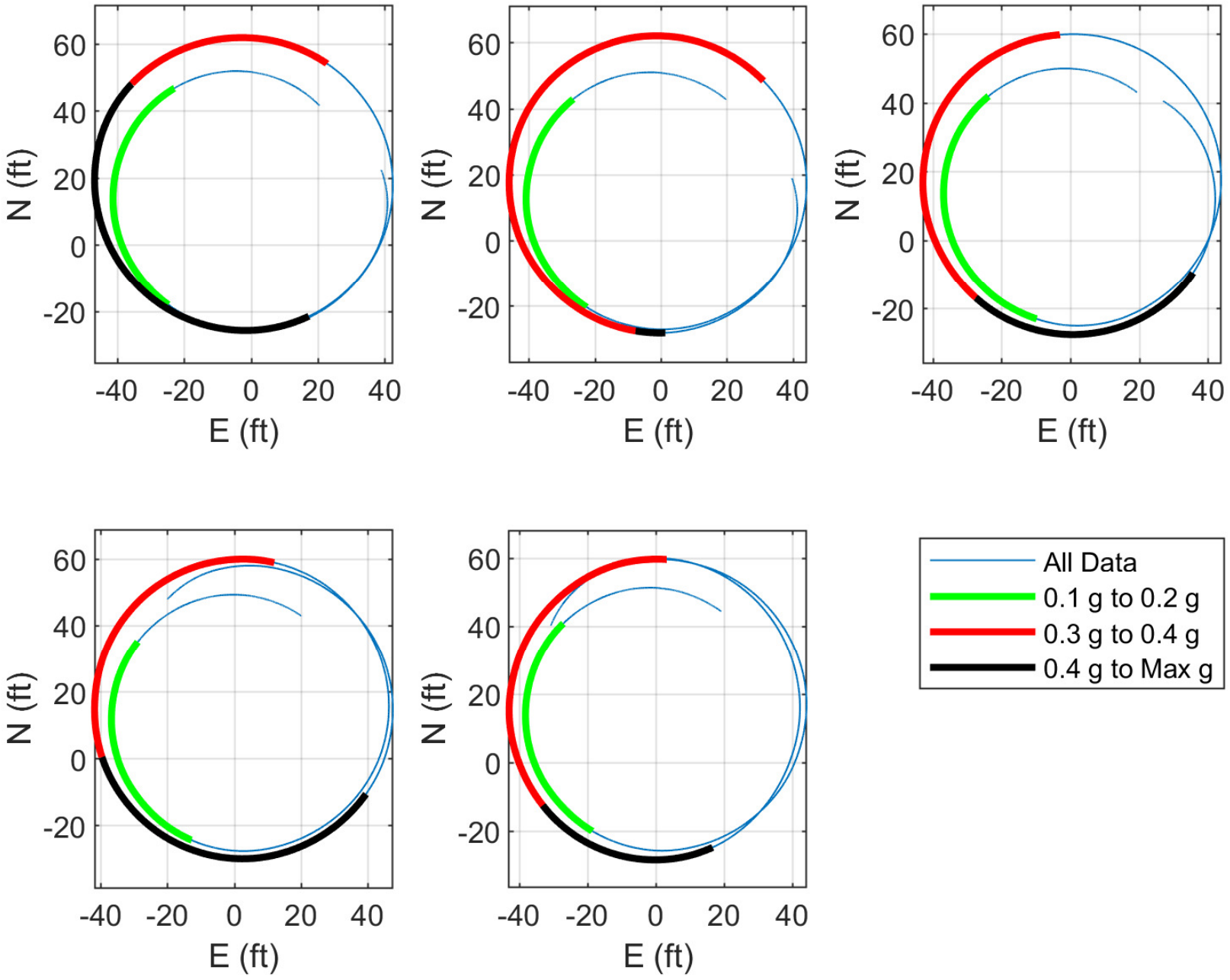

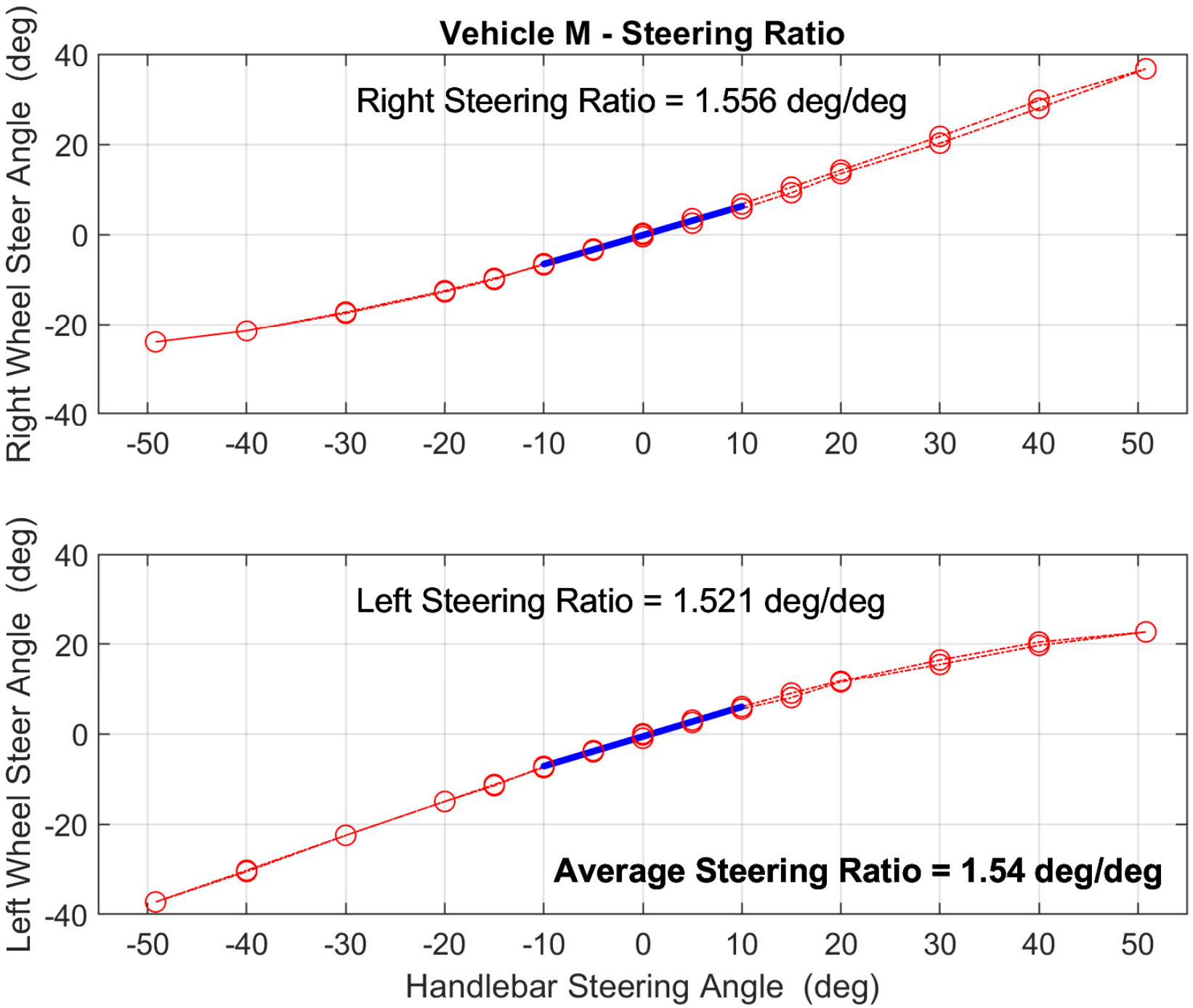

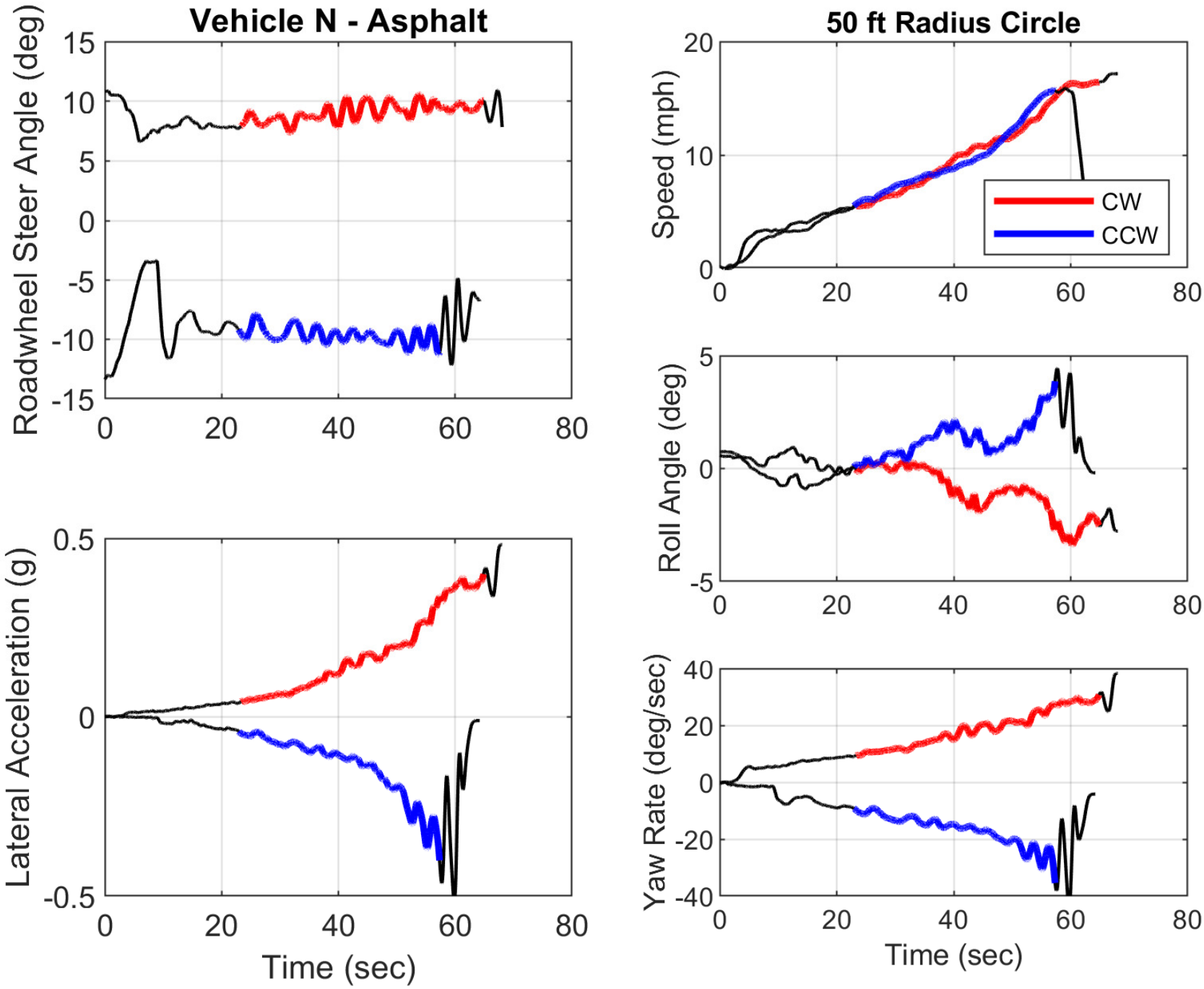

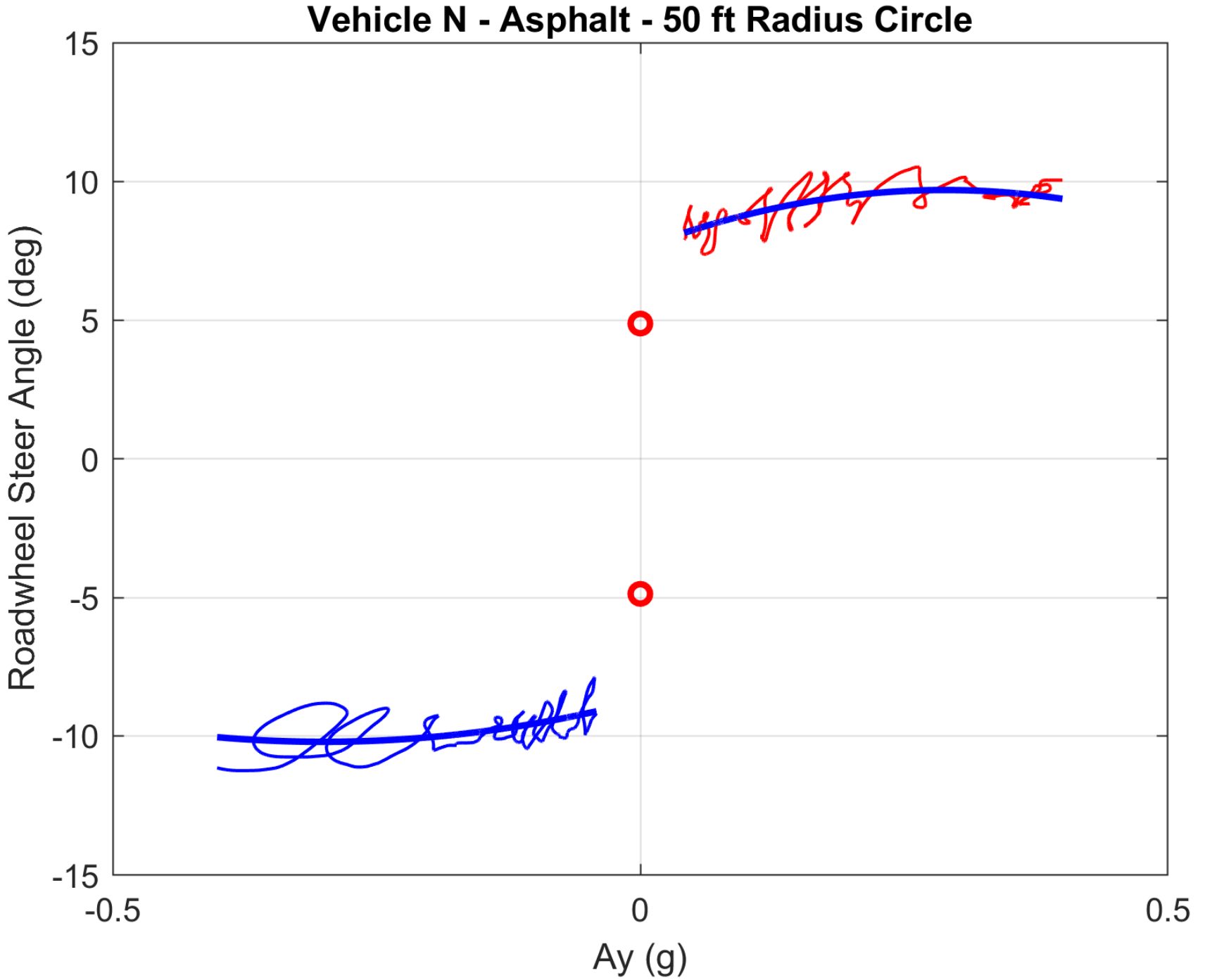

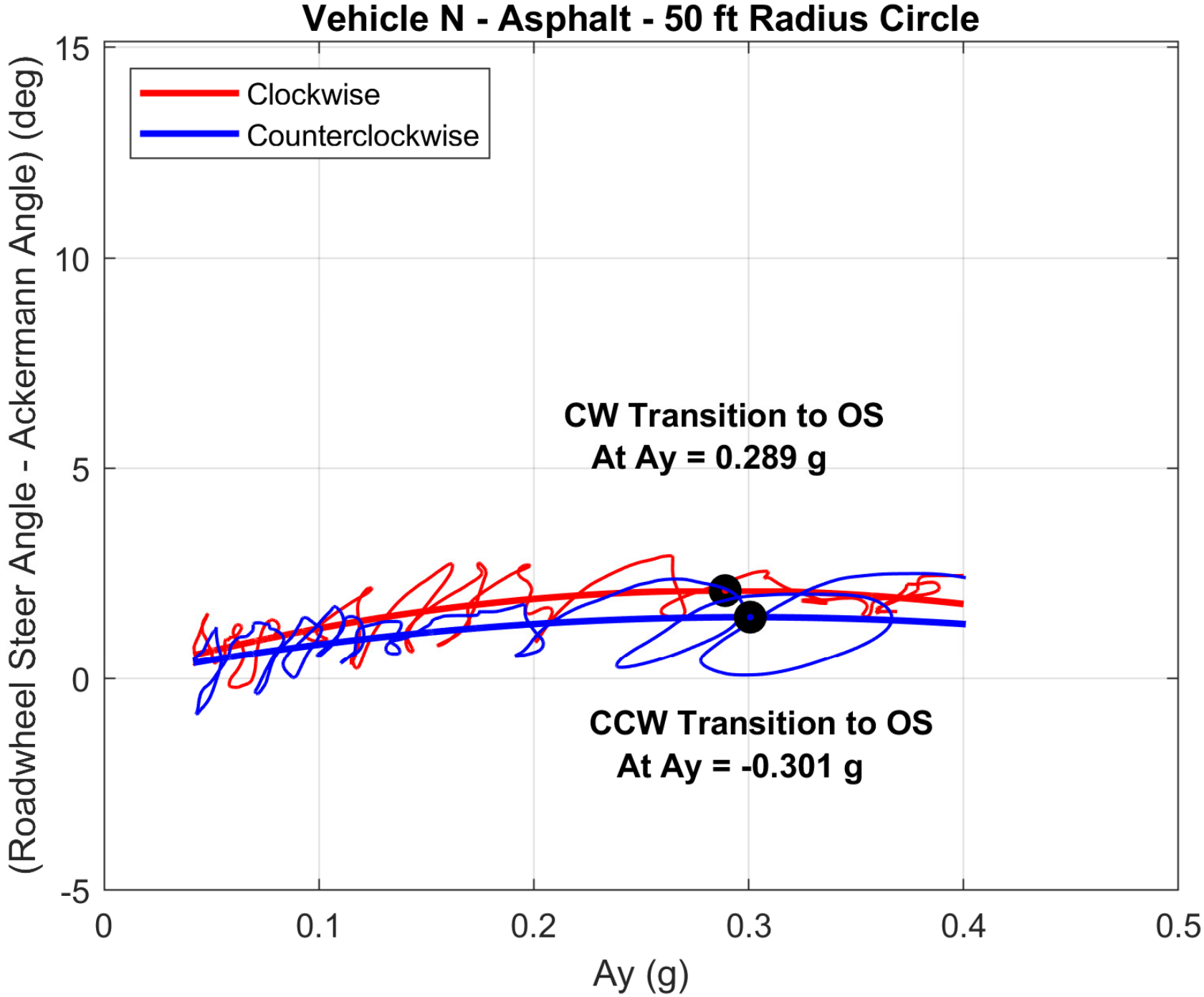

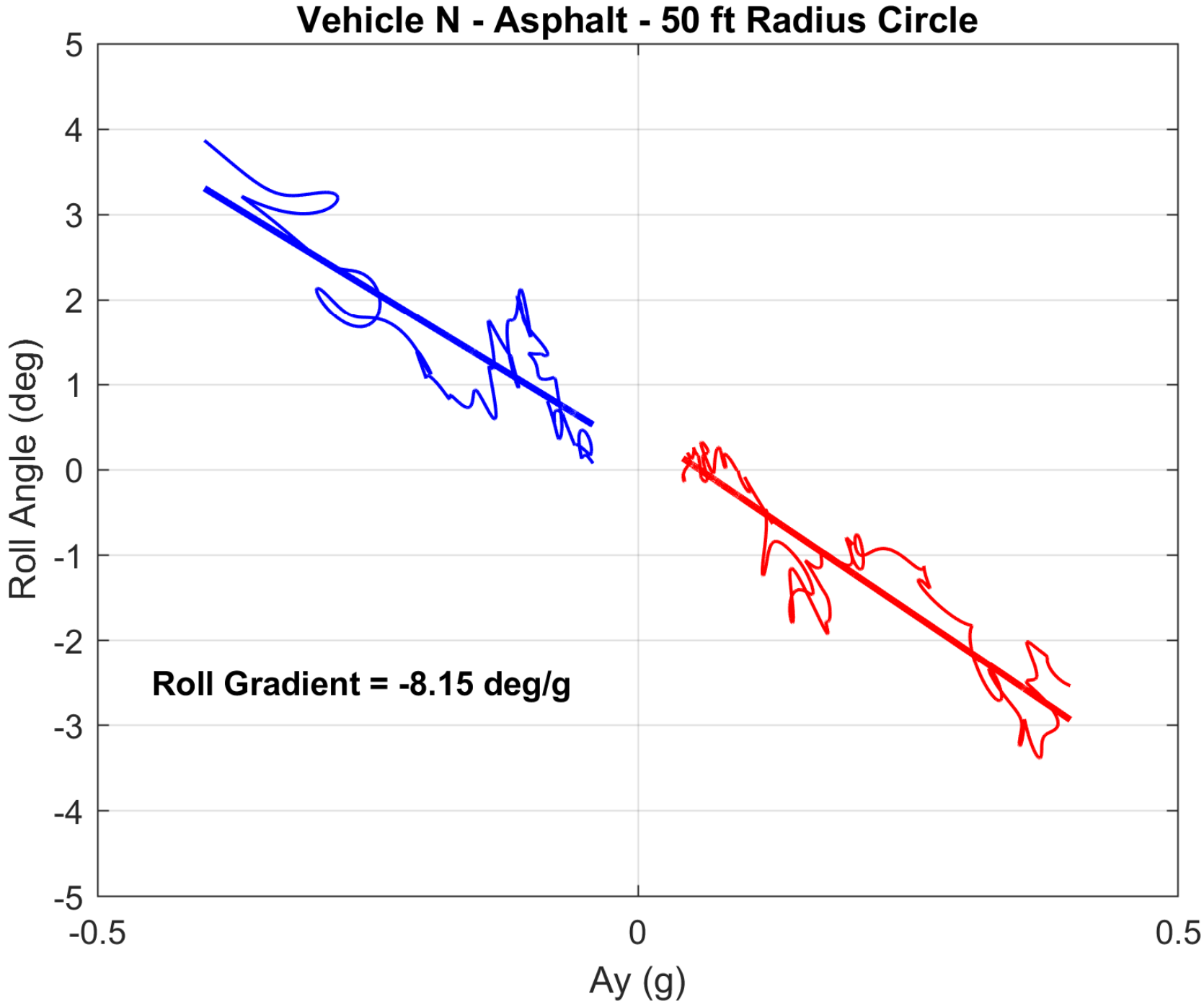

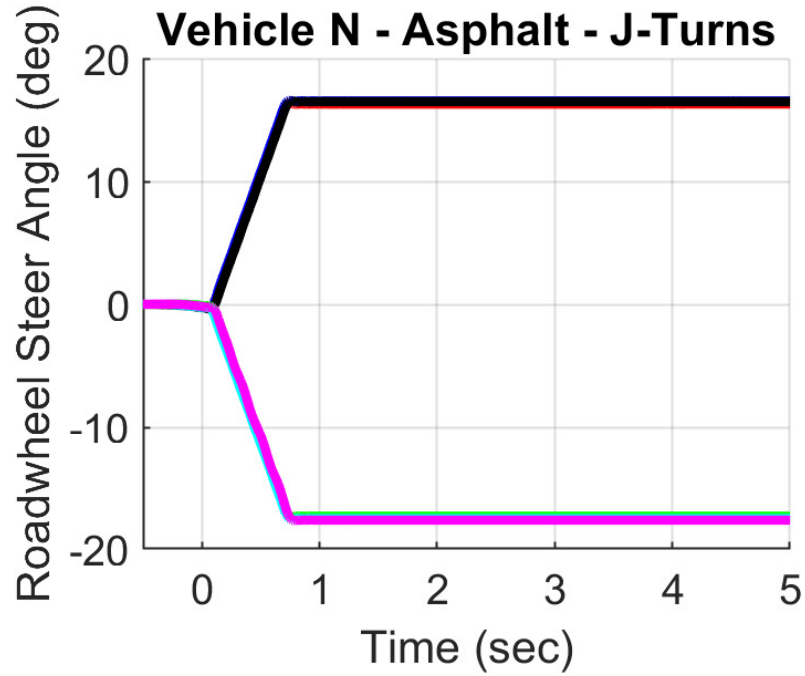

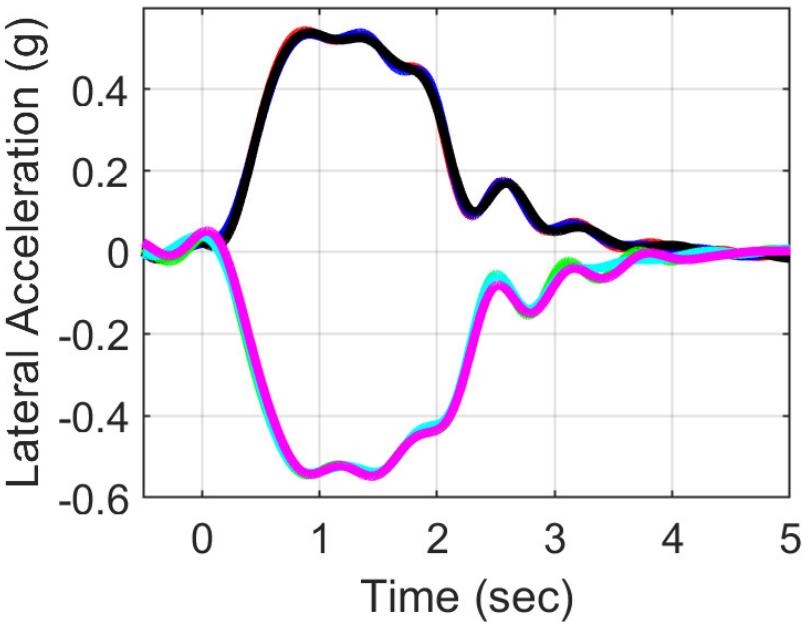

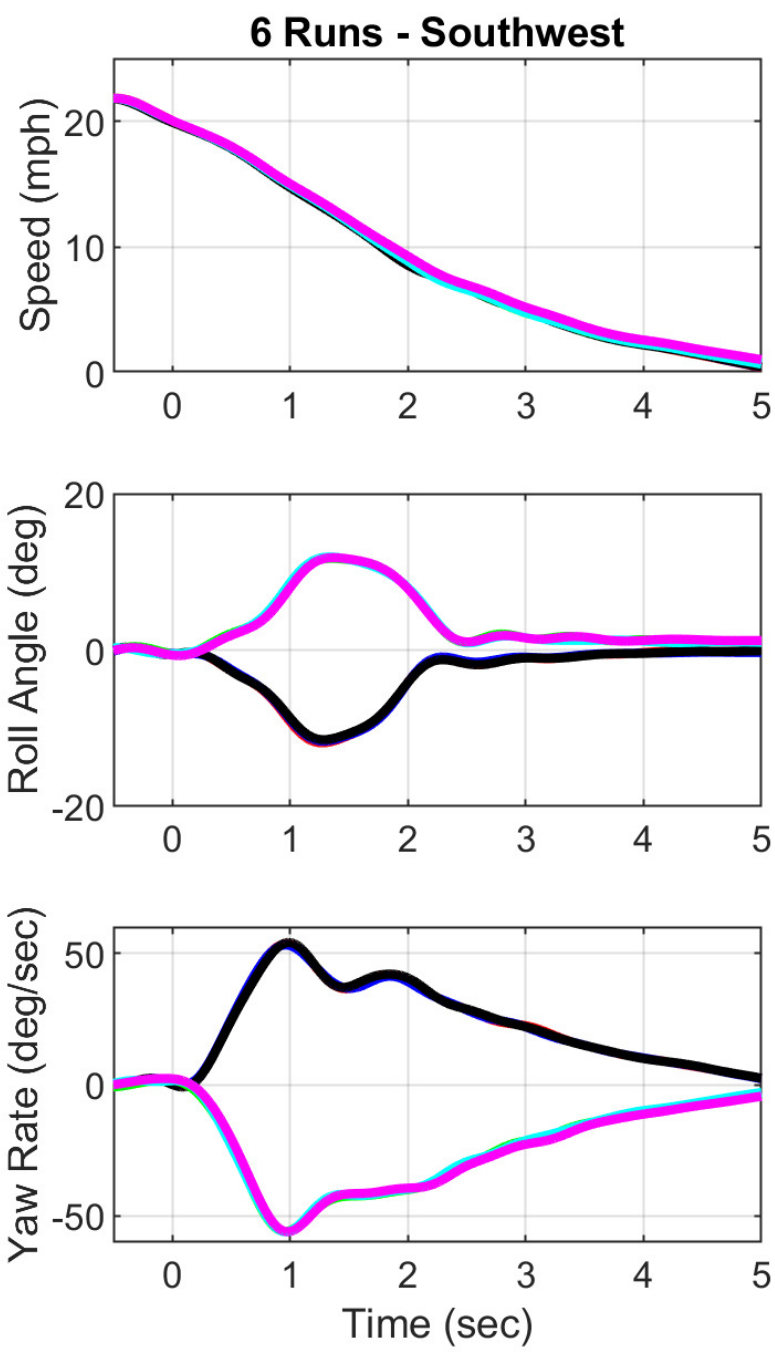

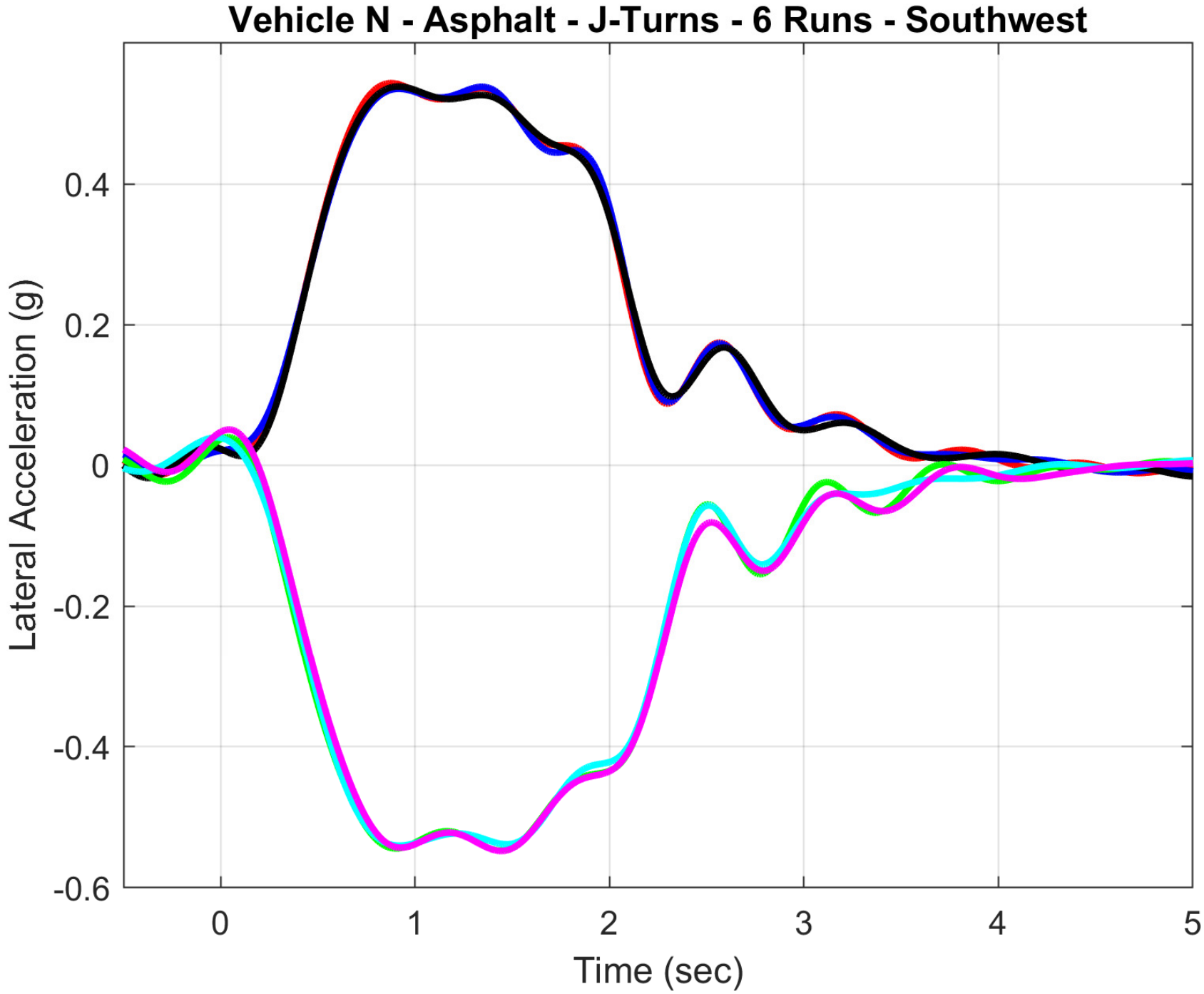

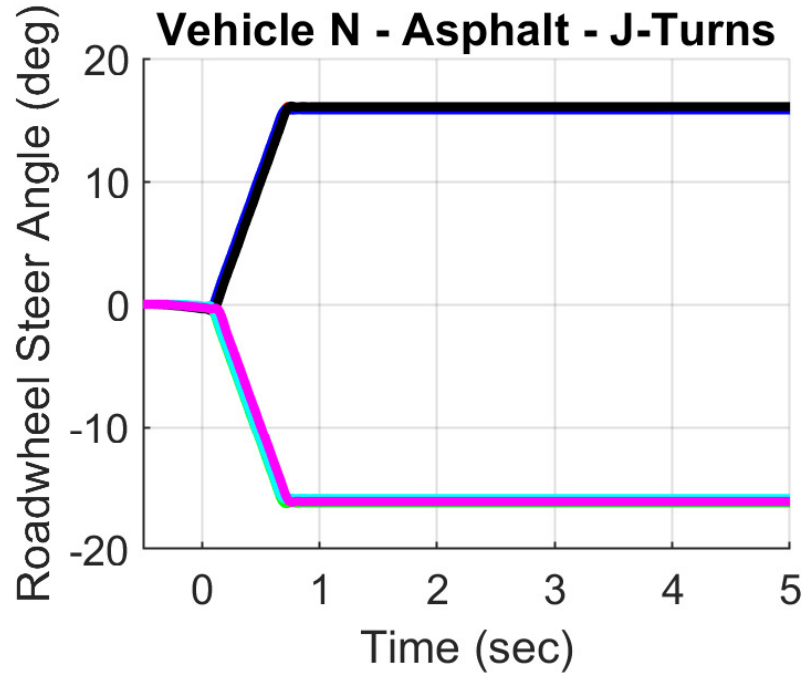

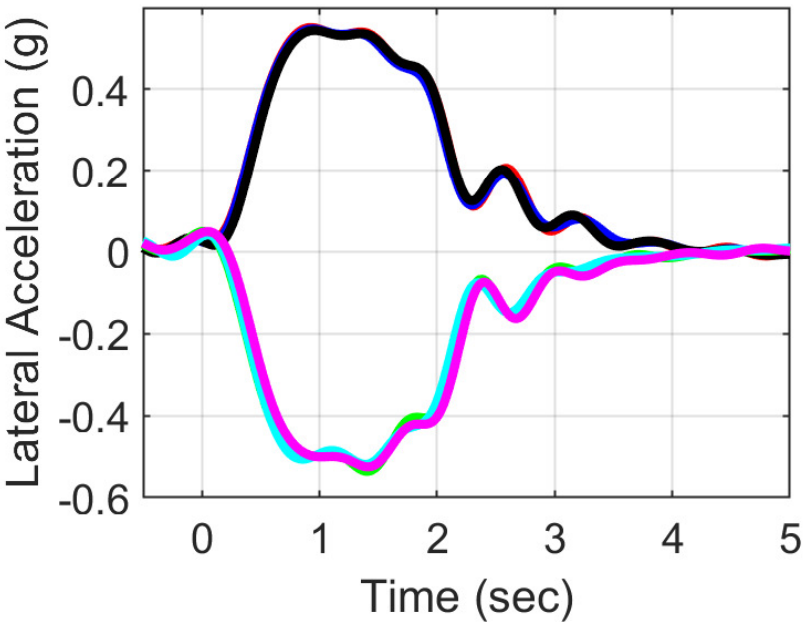

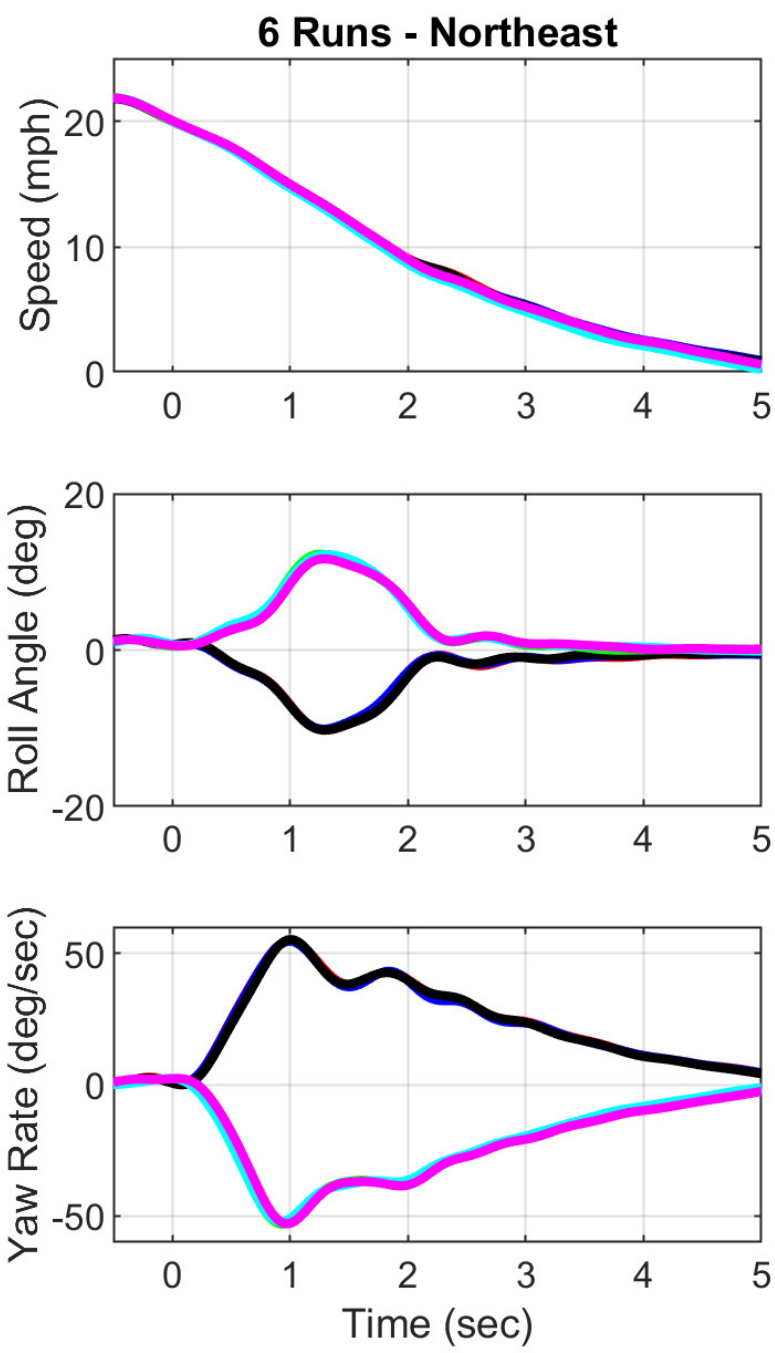

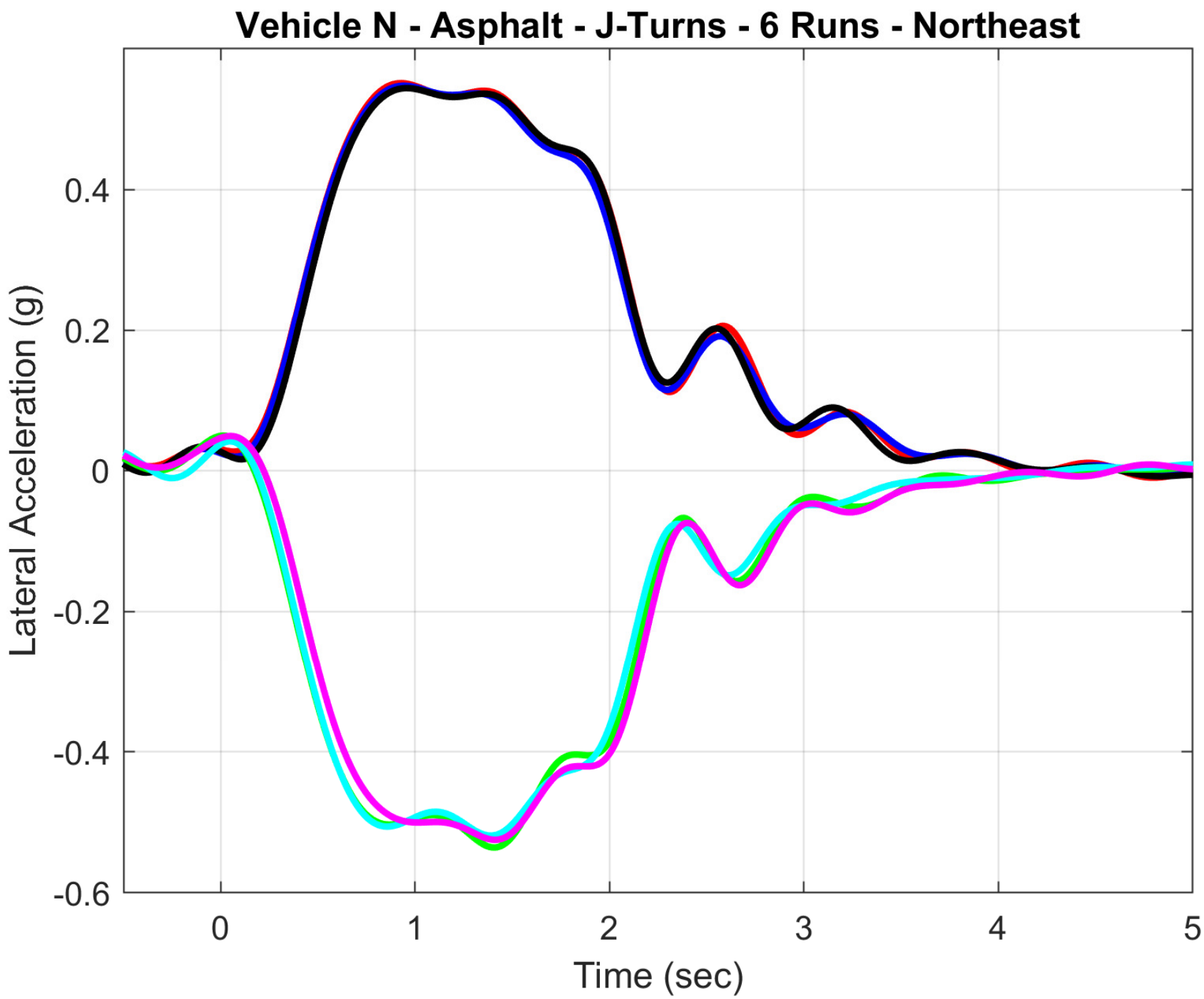

Vehicle N - Asphalt Results

Peak Lateral Accelerations During 2WL J-Turns - All Values in "g's"

Run Number	Northeast Right Turns	Northeast Left Turns
1	0.551	-0.536
2	0.548	-0.519
3	0.544	-0.525
Mean Value of 3 Runs	0.548	-0.526
Standard Deviation of 3 Runs	0.004	0.009

Average of 6 Northeast Runs

0.537

Run Number	Southwest Right Turns	Southwest Left Turns
1	0.543	-0.547
2	0.538	-0.540
3	0.539	-0.548
Mean Value of 3 Runs	0.540	-0.545
Standard Deviation of 3 Runs	0.003	0.004

Average of 6 Southwest Runs

0.543

Average of All 12 Runs

0.540

Threshold Ay

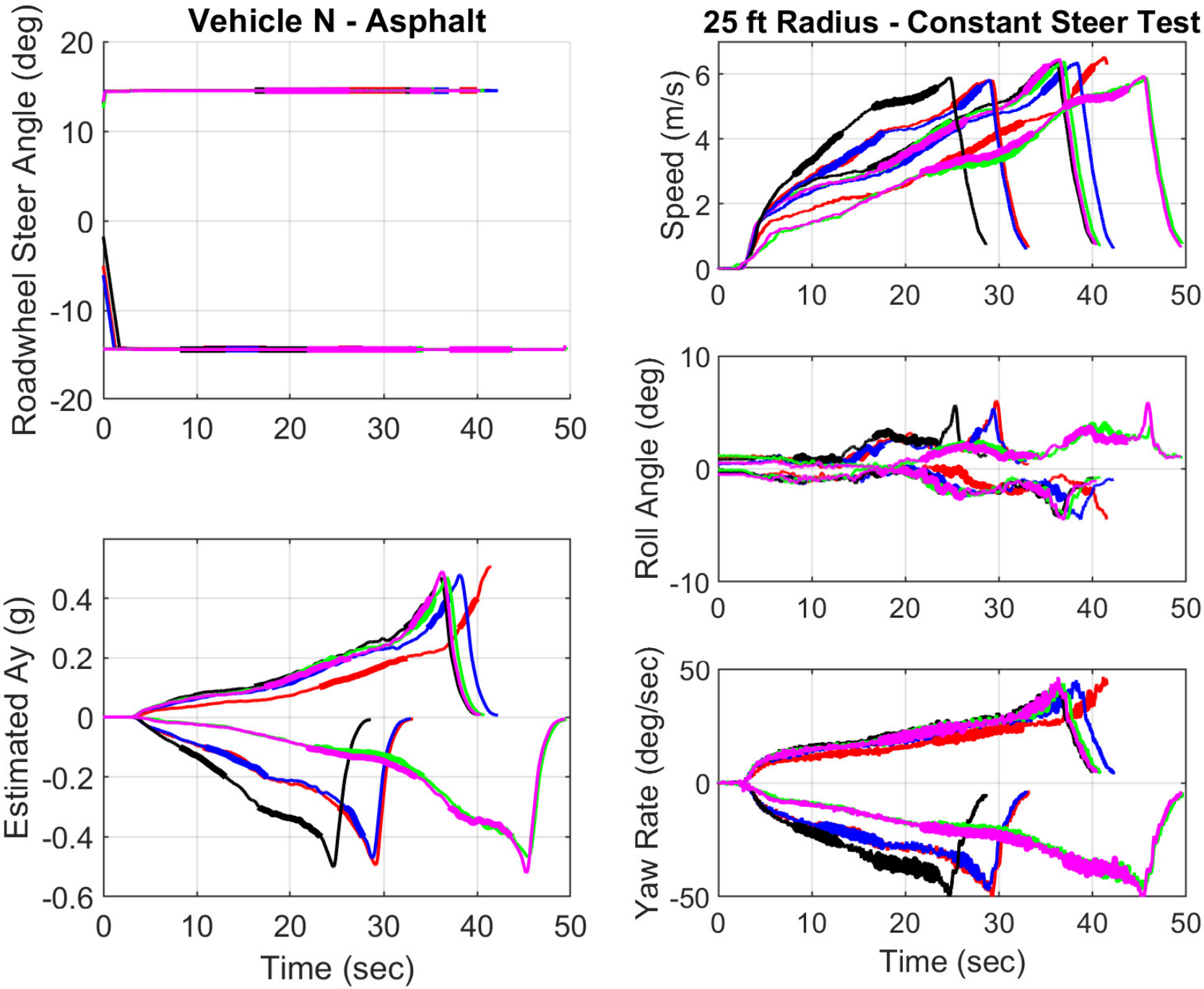

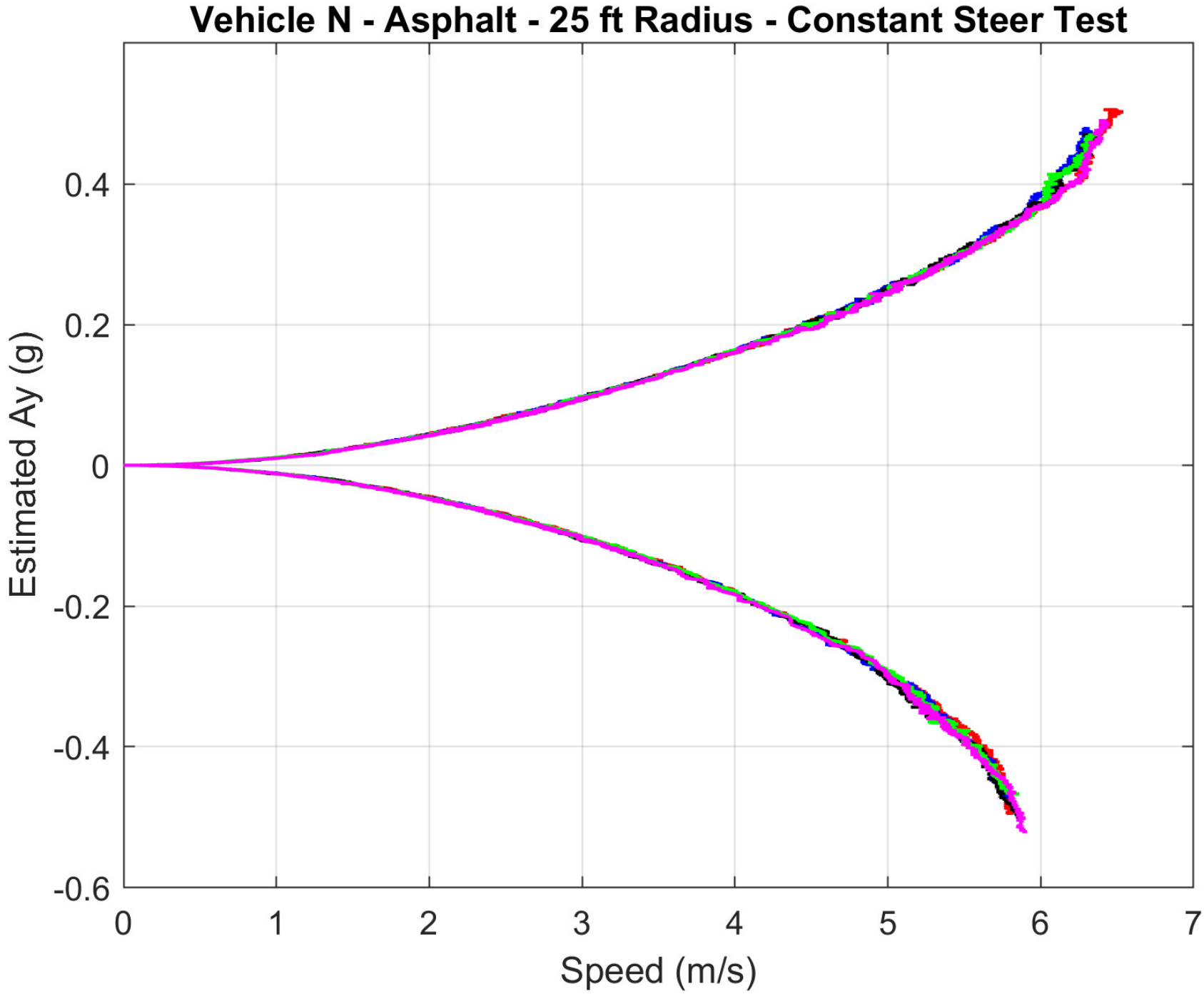

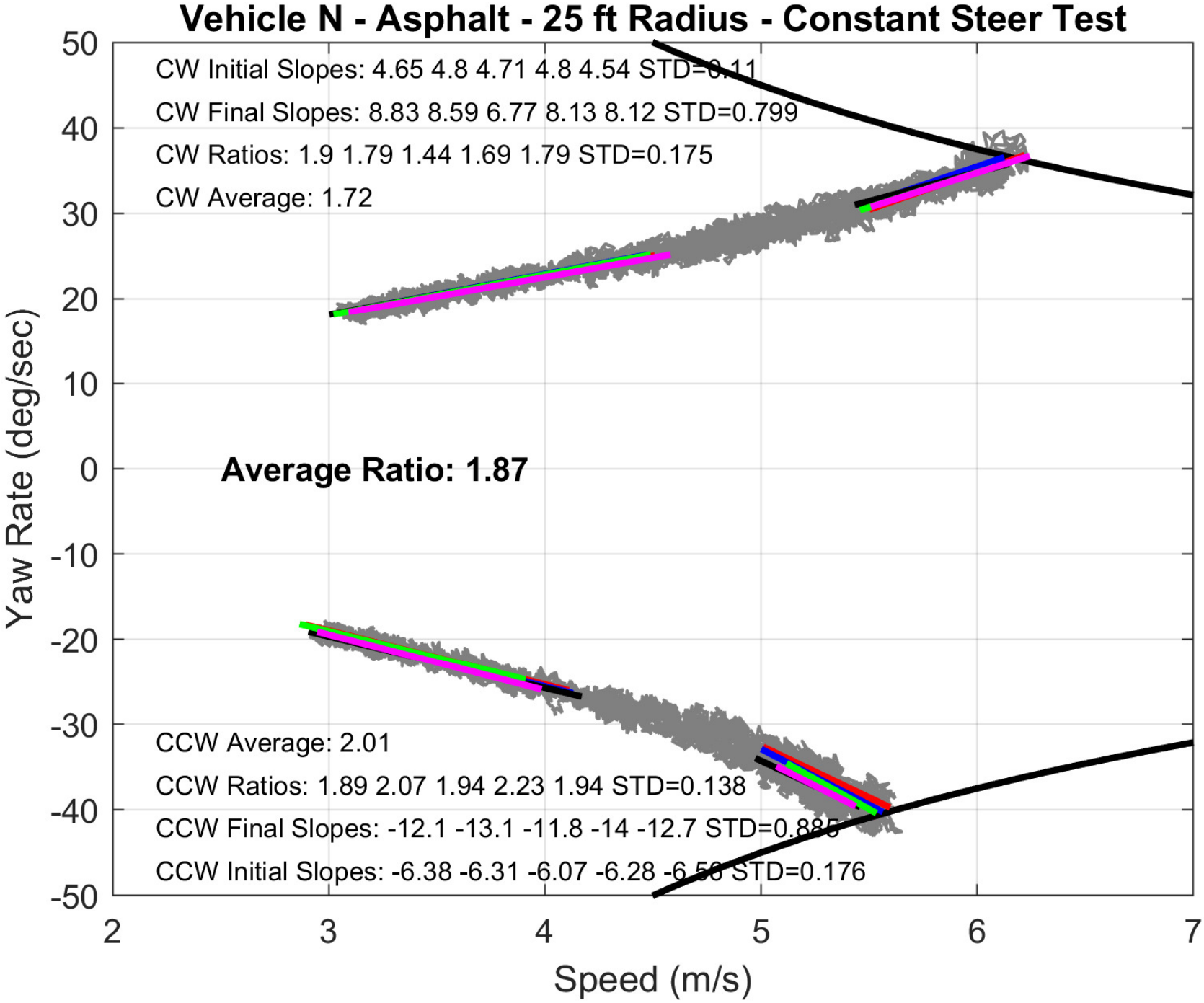

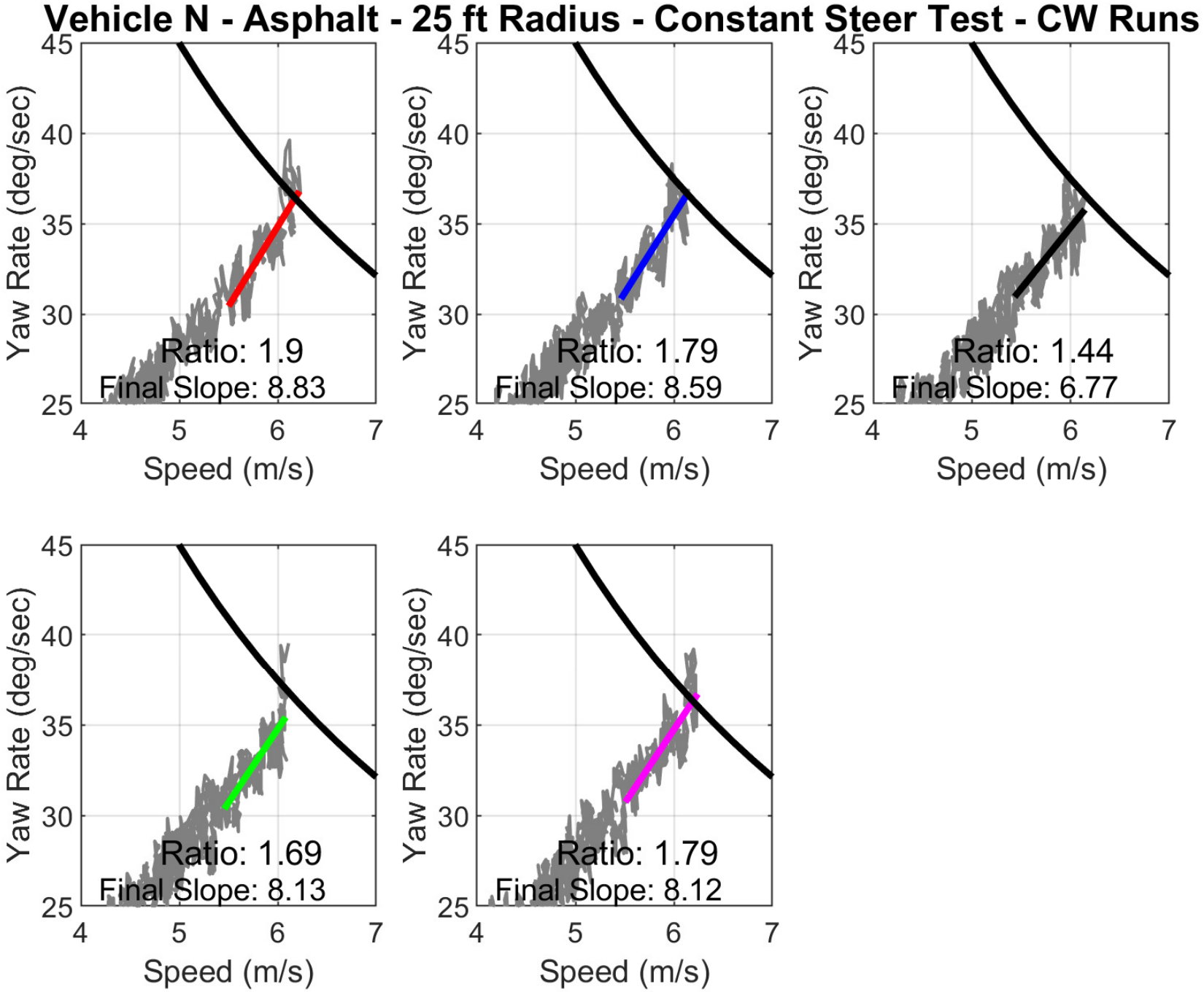

Vehicle N - Asphalt - 25 ft Radius - Constant Steer Test - CCW Runs

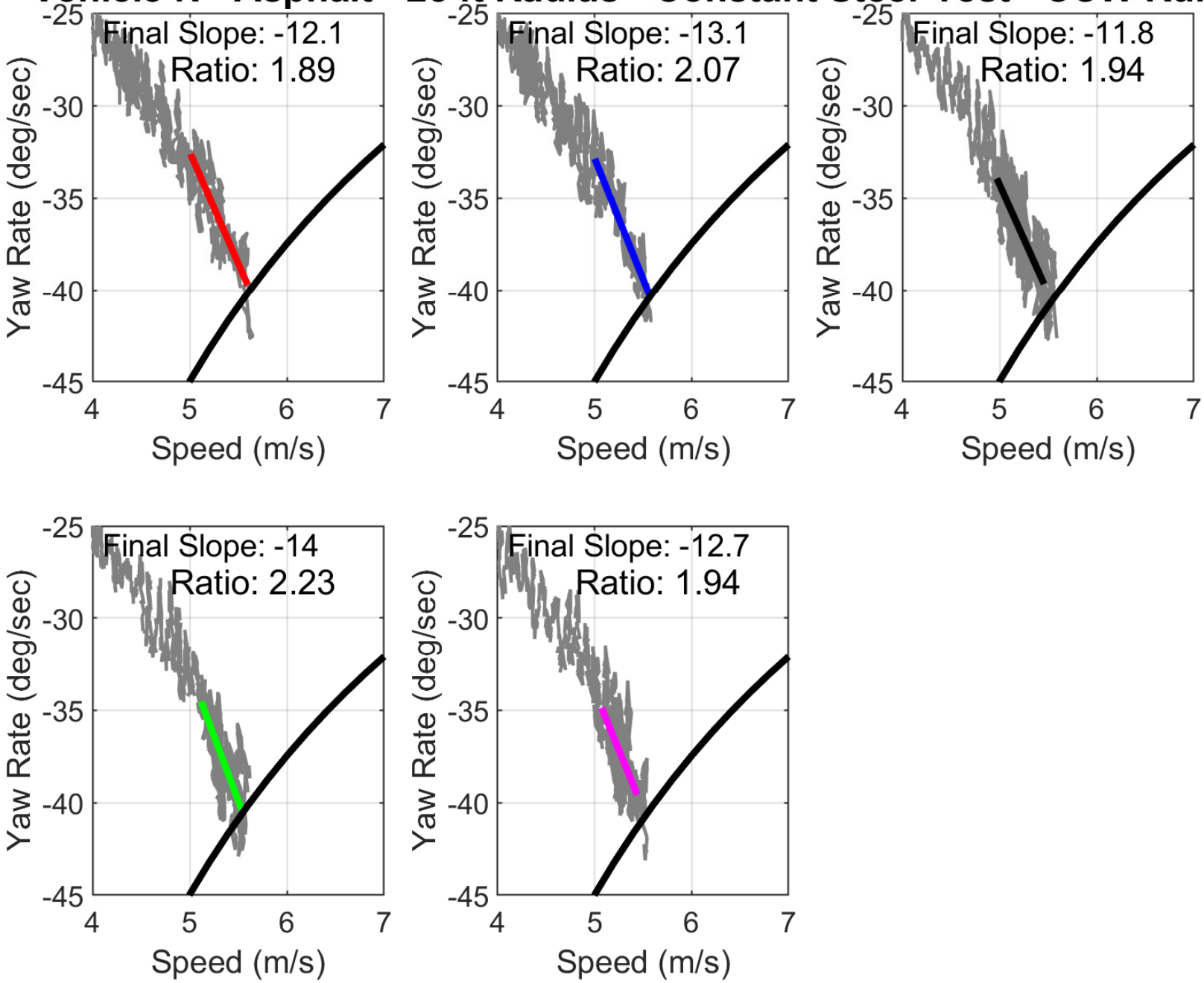

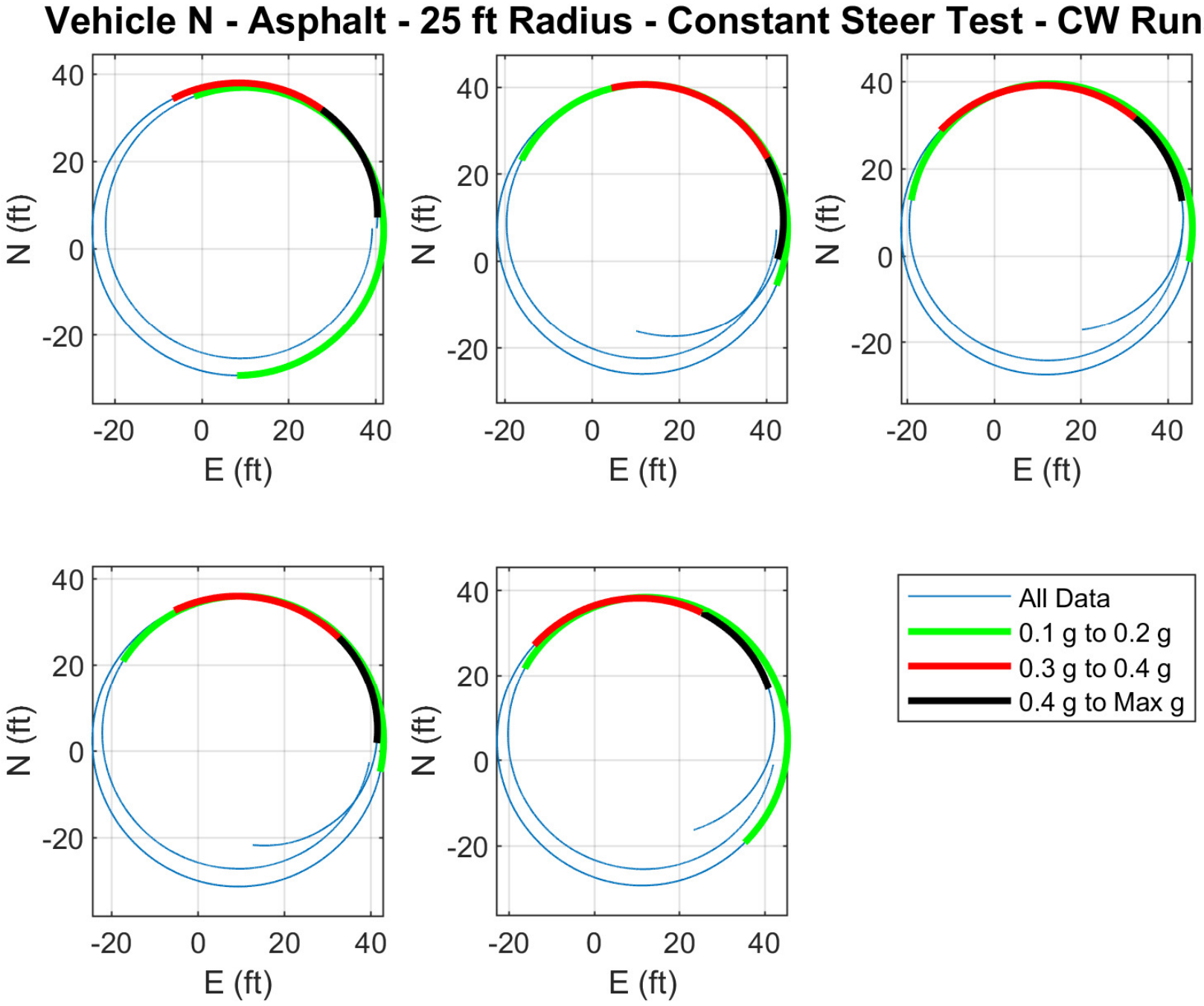

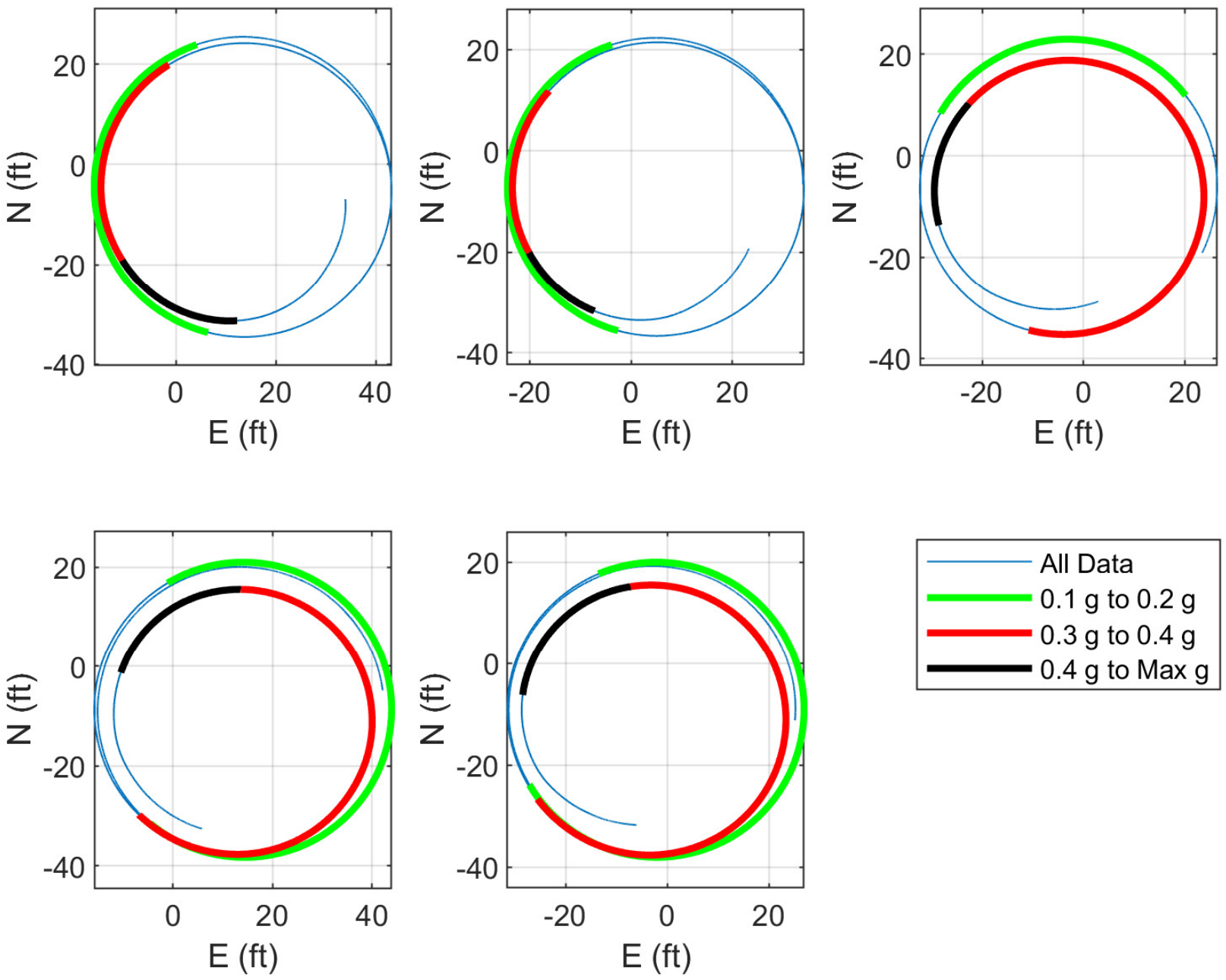

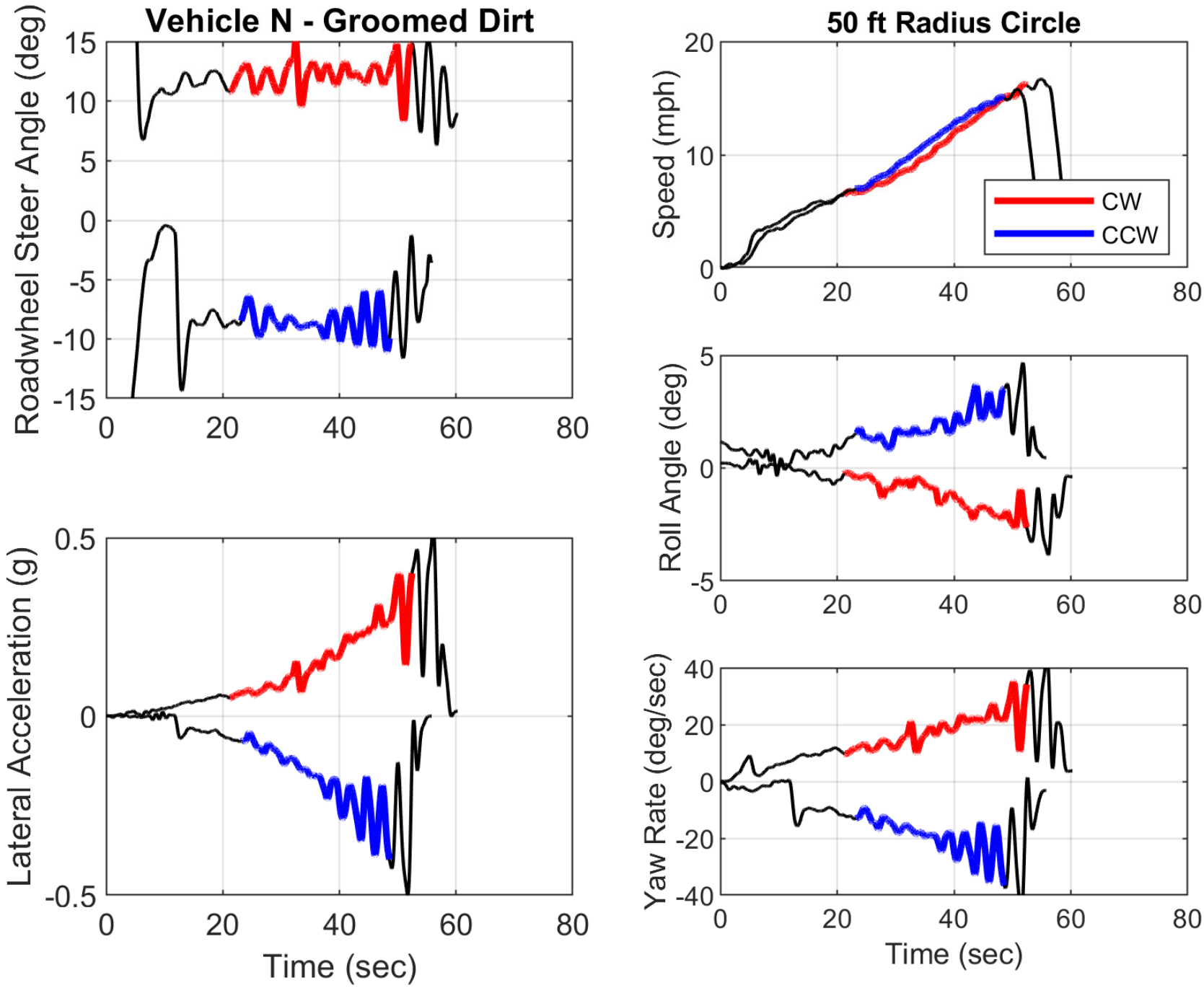

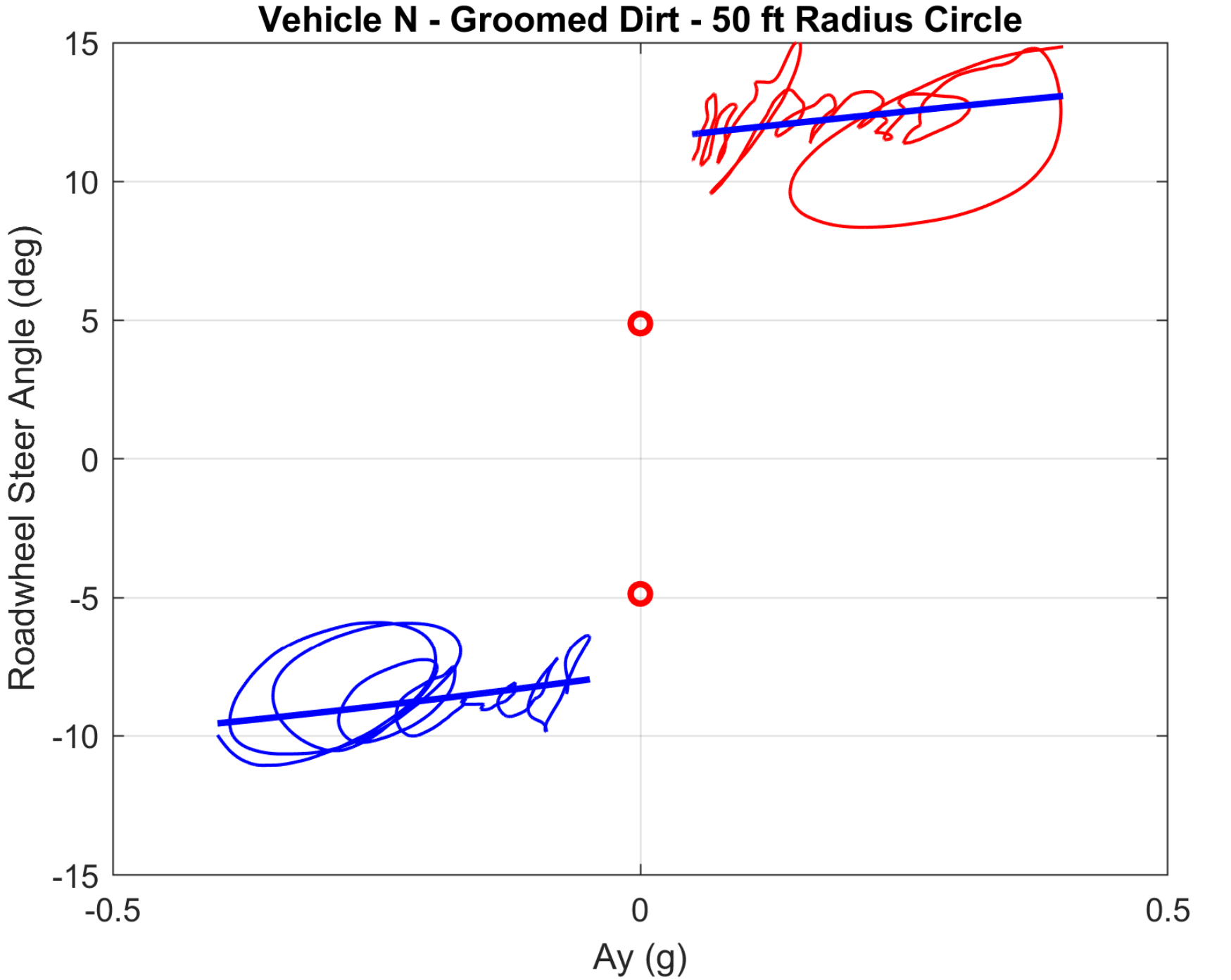

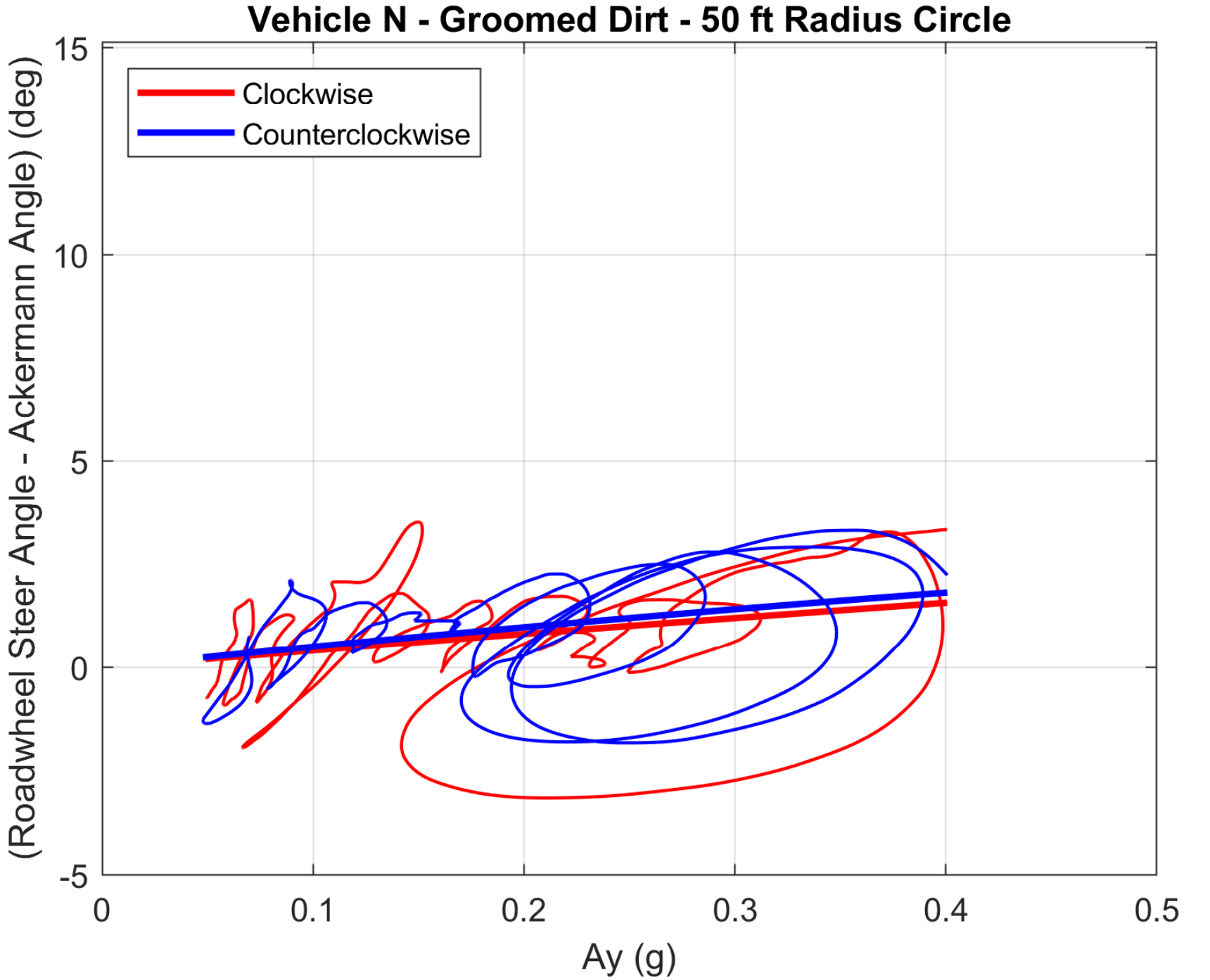

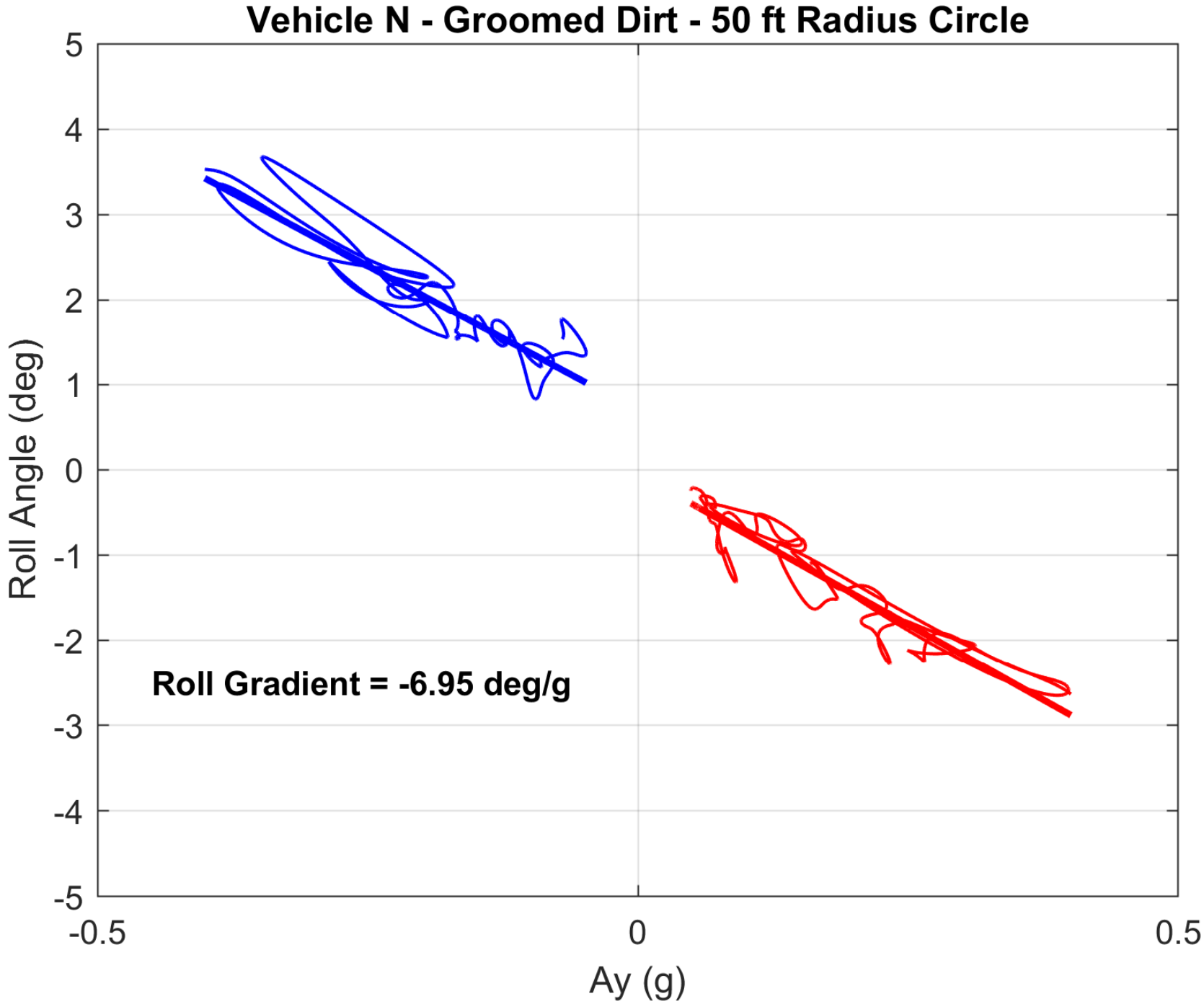

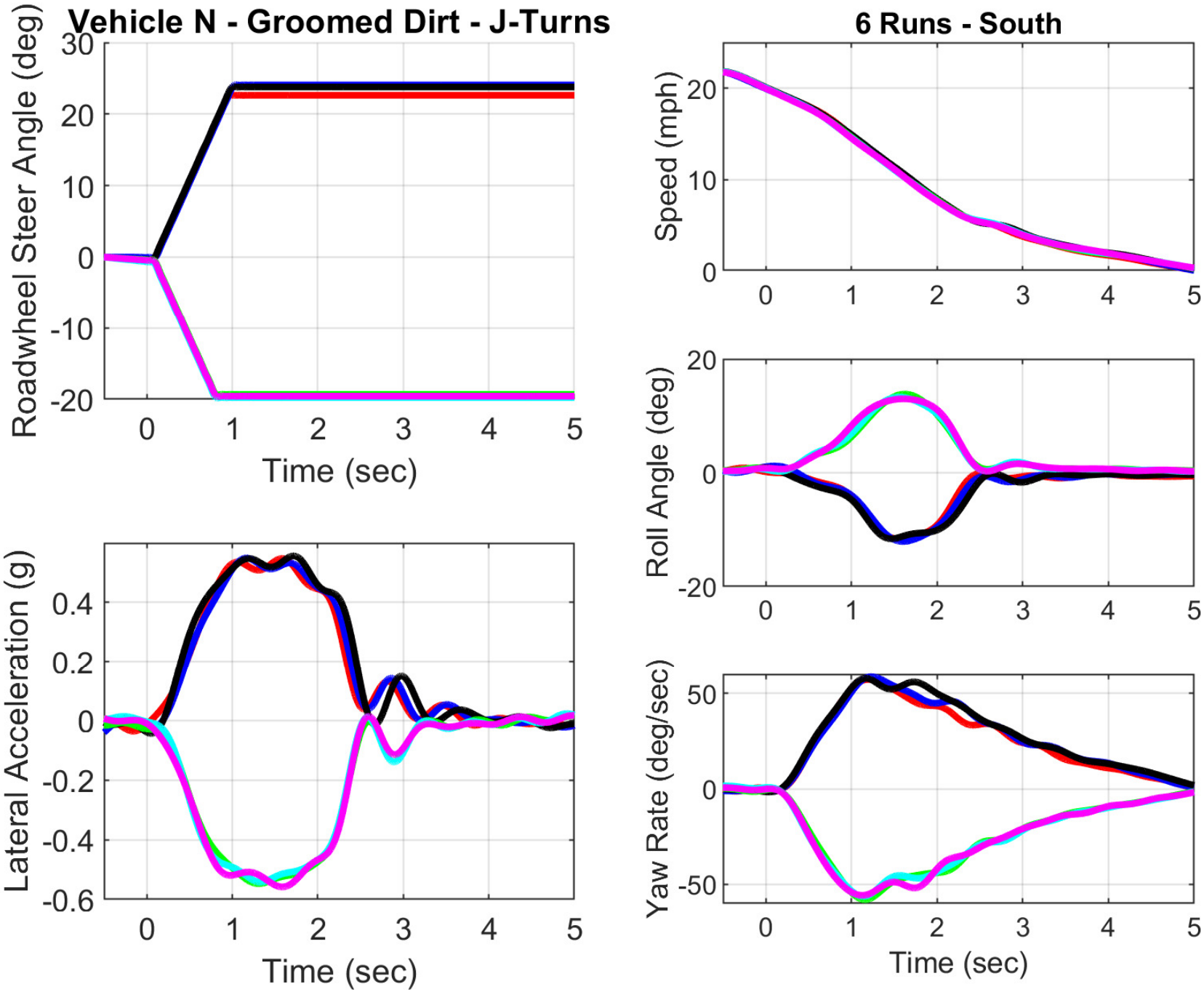

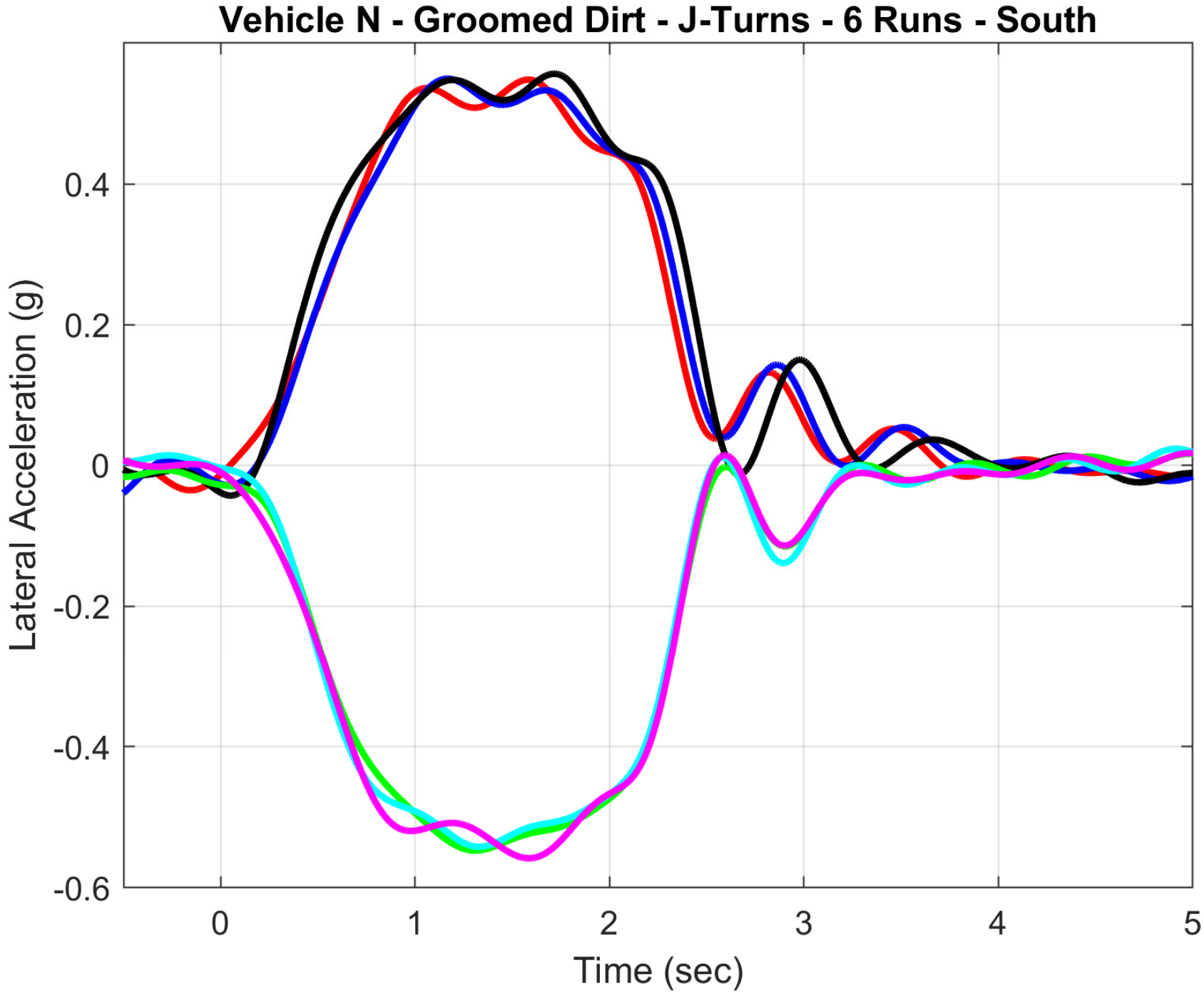

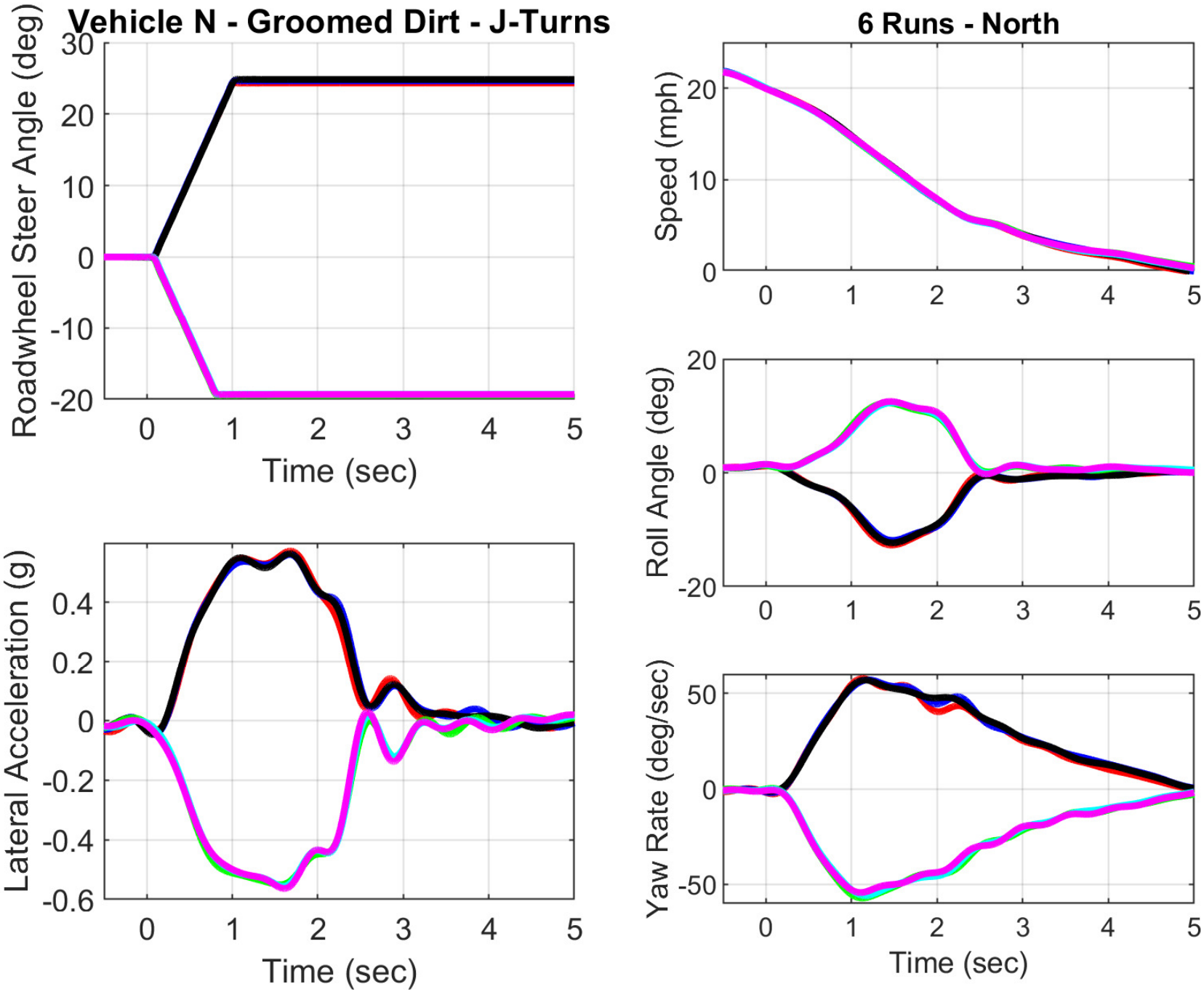

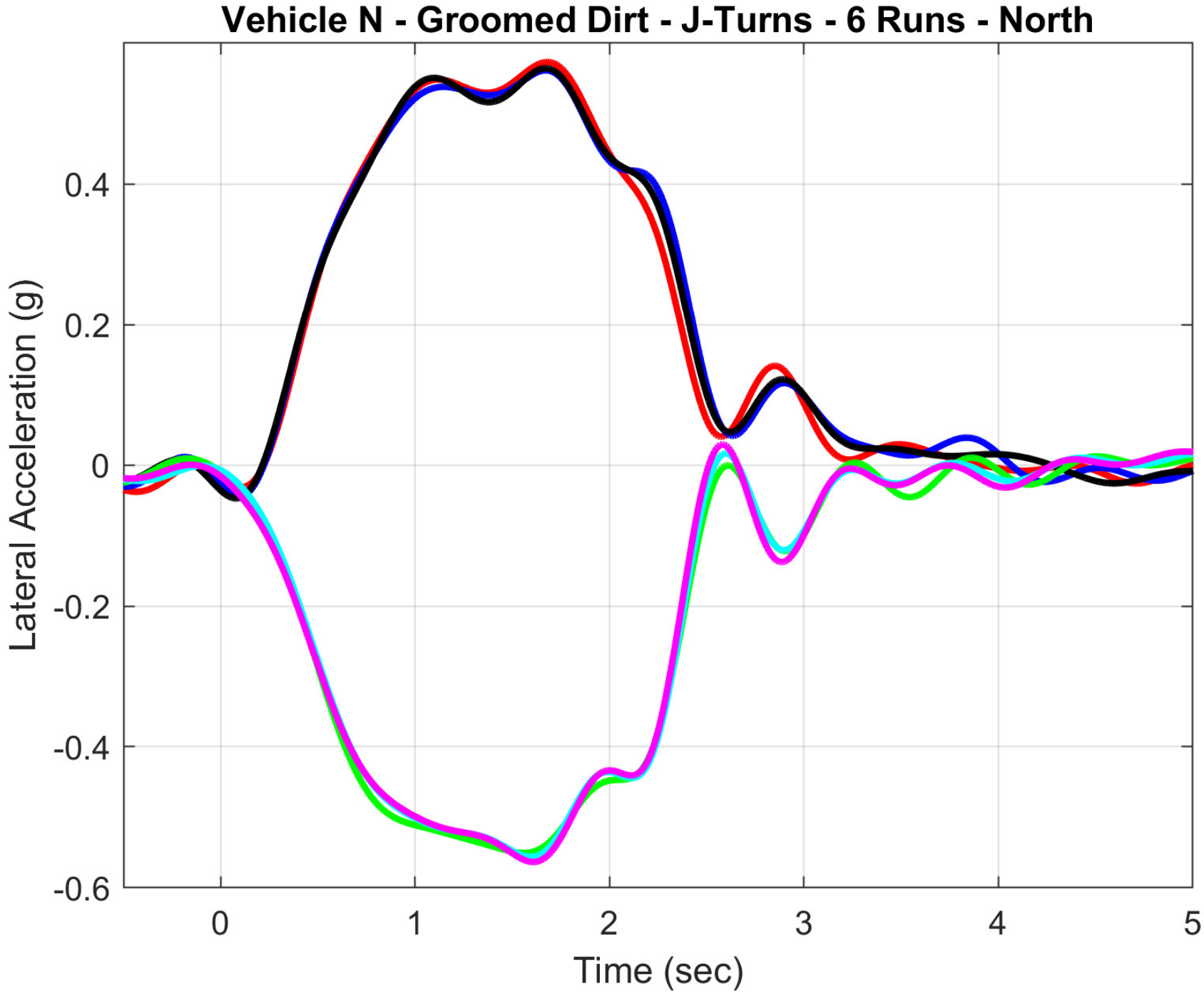

Vehicle N - Groomed Dirt Results

Peak Lateral Accelerations During 2WL J-Turns - All Values in "g's"

Run Number	North Right Turns	North Left Turns
1	0.573	-0.551
2	0.562	-0.556
3	0.565	-0.563
Mean Value of 3 Runs	0.566	-0.557
Standard Deviation of 3 Runs	0.006	0.006

Average of 6 North Runs

0.562

Run Number	South Right Turns	South Left Turns
1	0.548	-0.547
2	0.550	-0.542
3	0.557	-0.558
Mean Value of 3 Runs	0.552	-0.549
Standard Deviation of 3 Runs	0.004	0.008

Average of 6 South Runs

0.550

Average of All 12 Runs

0.556

Threshold Ay

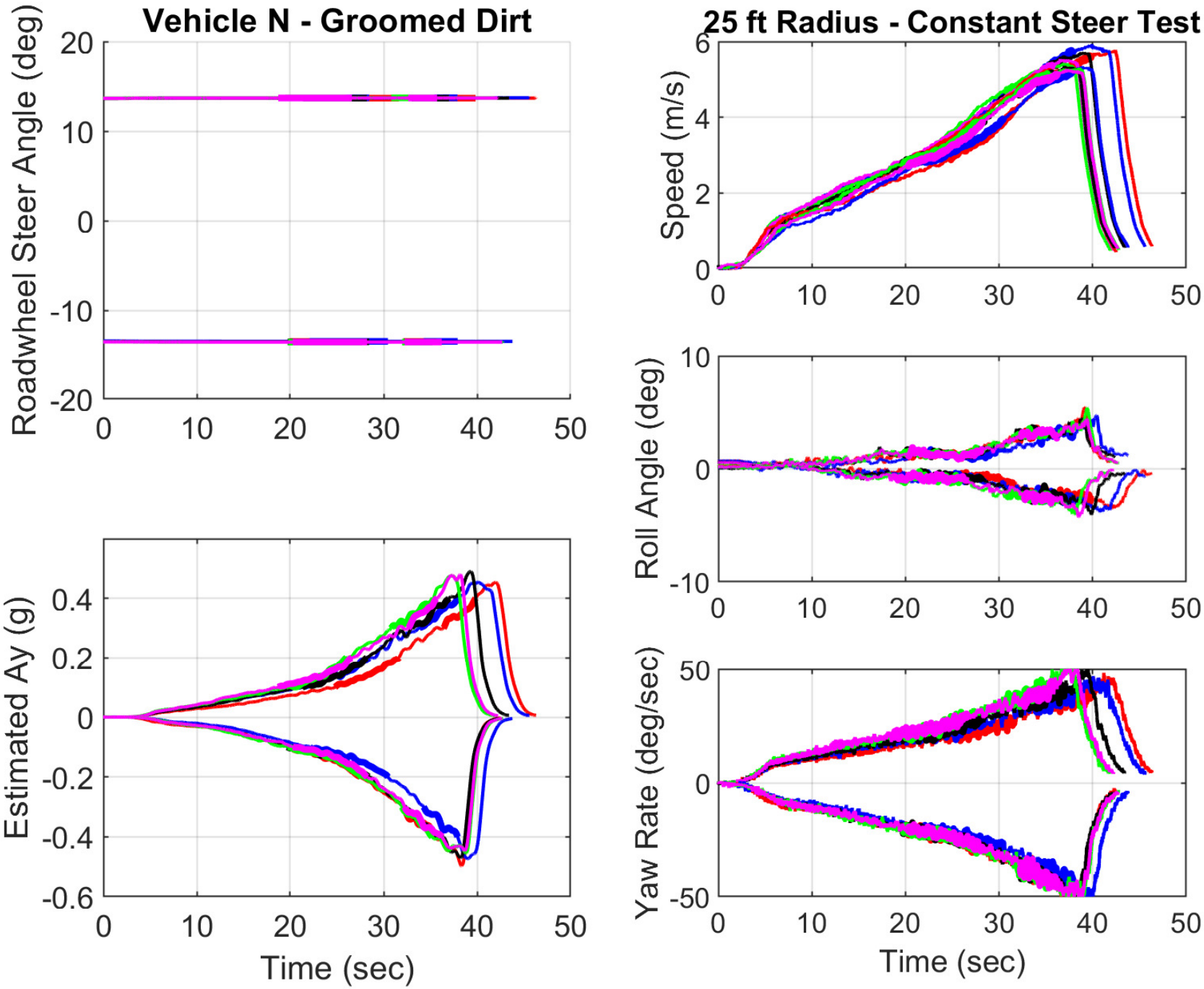

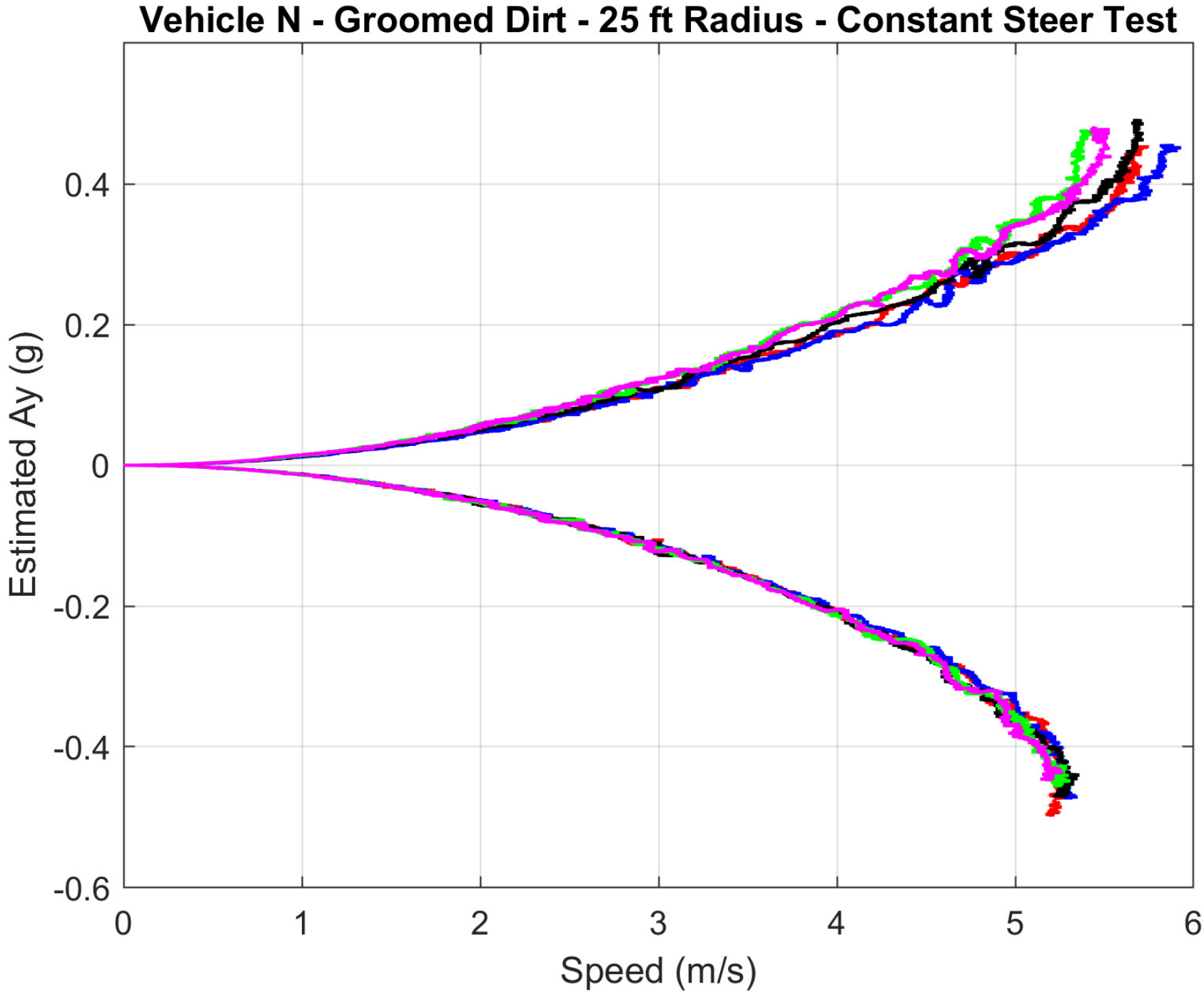

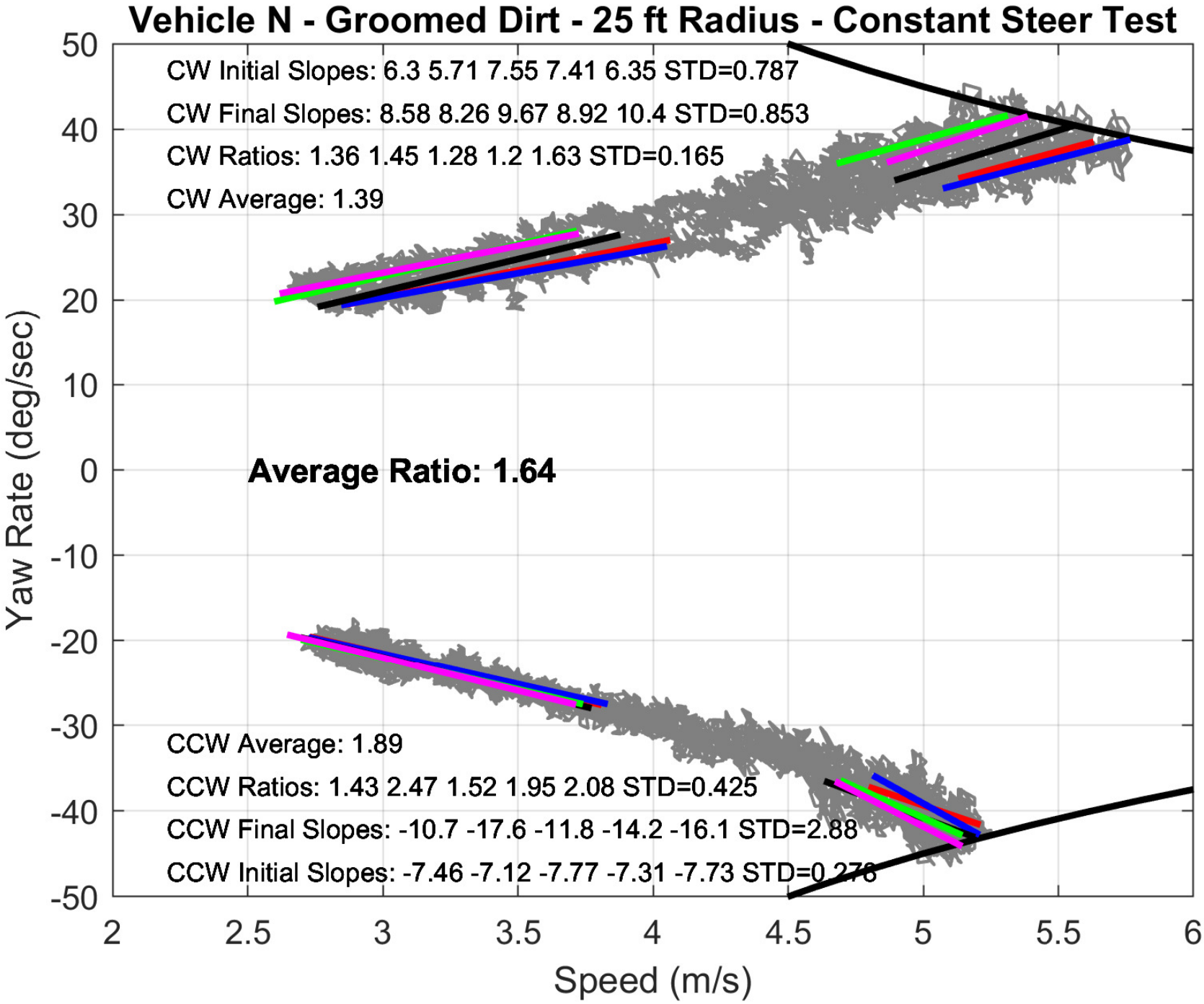

Vehicle N - Groomed Dirt - 25 ft Radius - Constant Steer Test - CW Runs

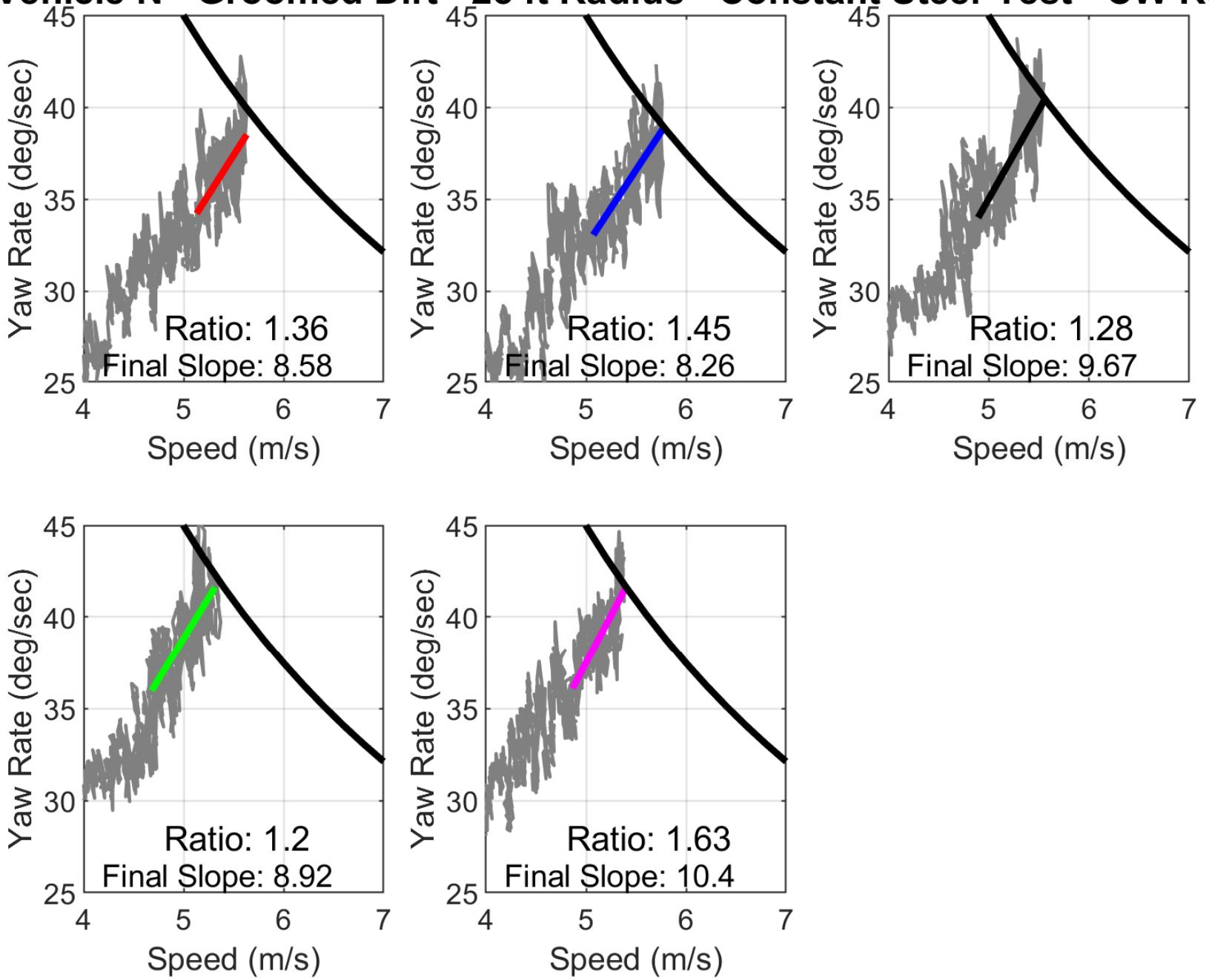

Vehicle N - Groomed Dirt - 25 ft Radius - Constant Steer Test - CCW Runs

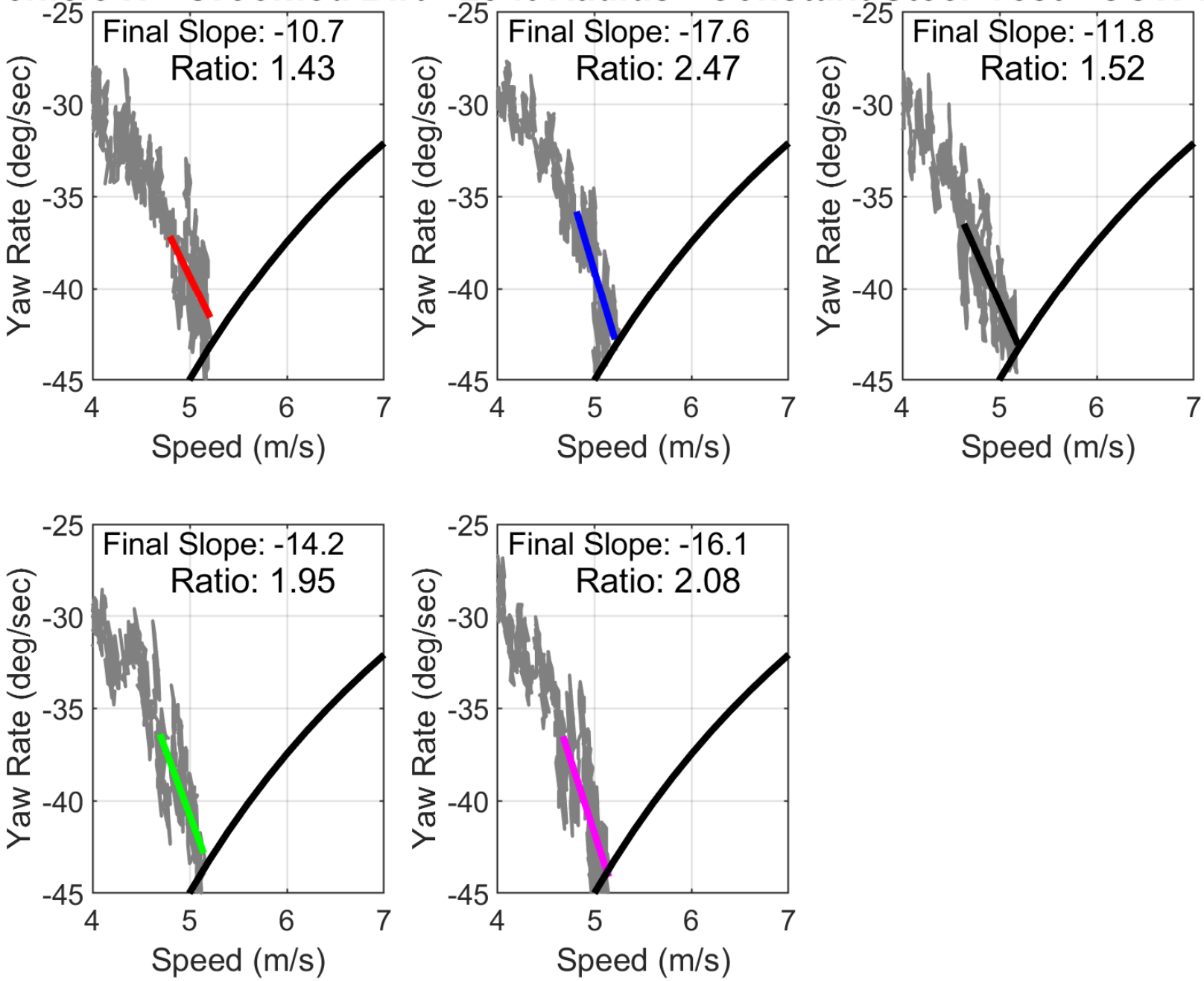

Vehicle N - Groomed Dirt - 25 ft Radius - Constant Steer Test - CW Runs

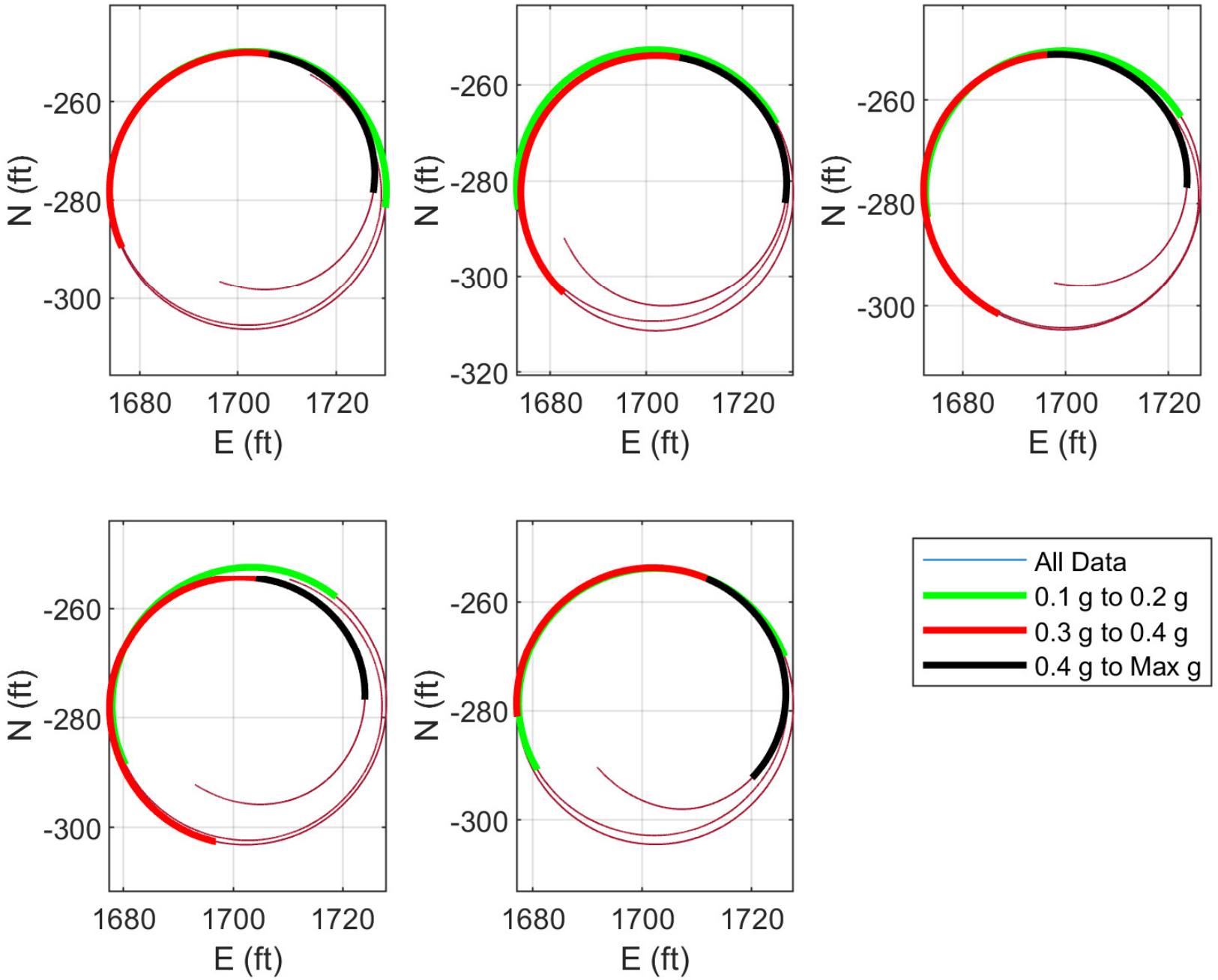

Vehicle N - Groomed Dirt - 25 ft Radius - Constant Steer Test - CCW Runs

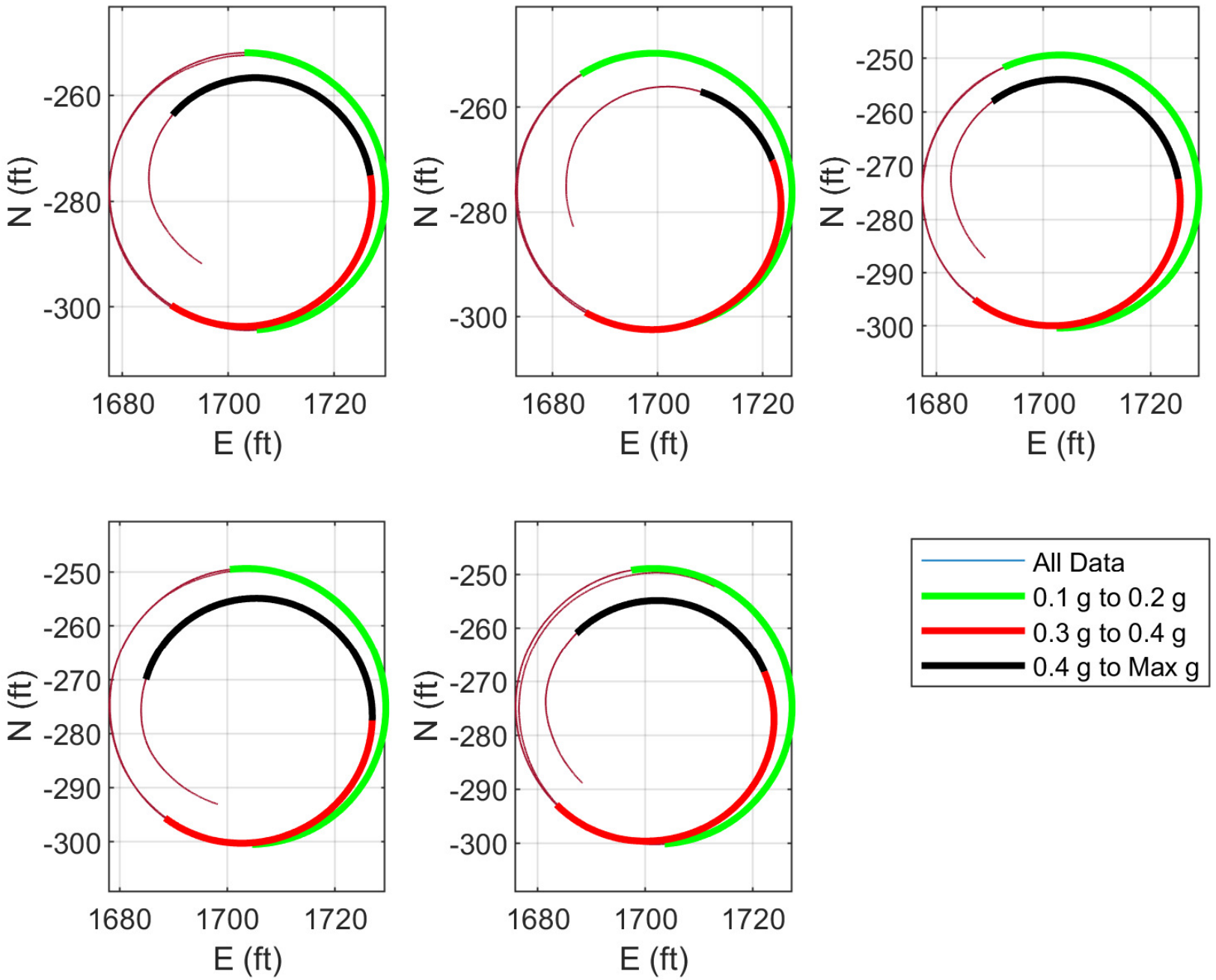

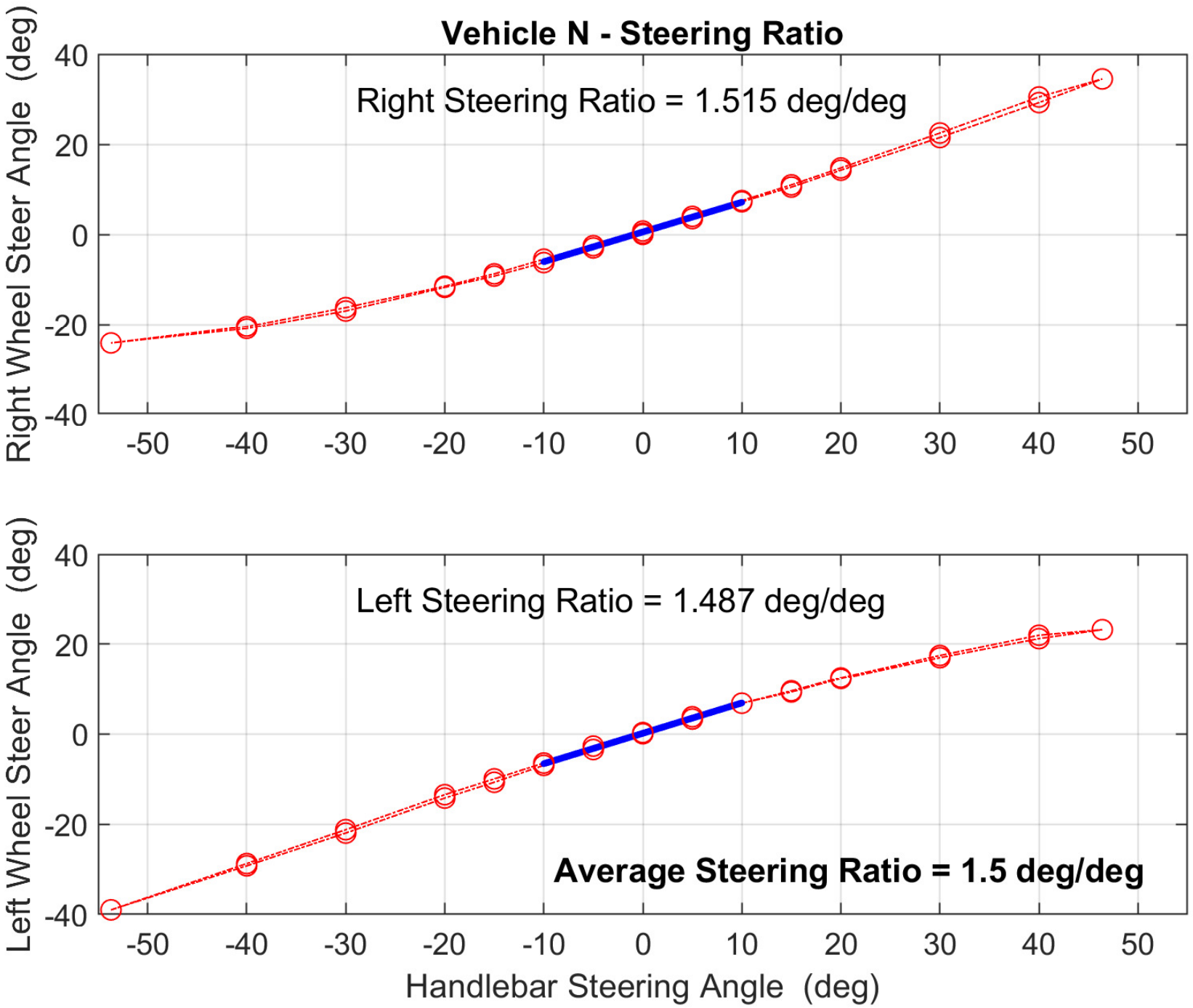

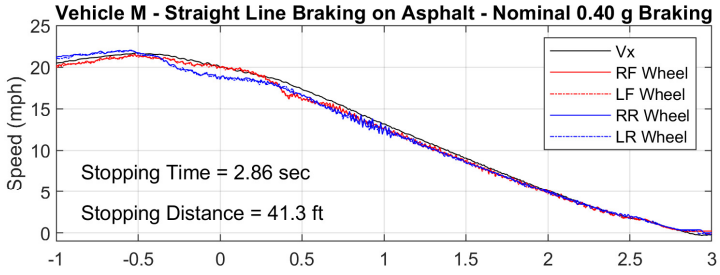

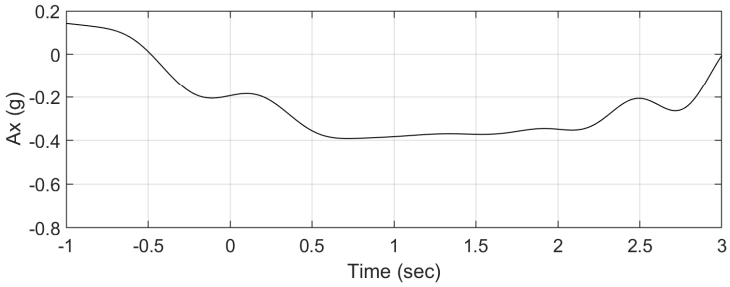

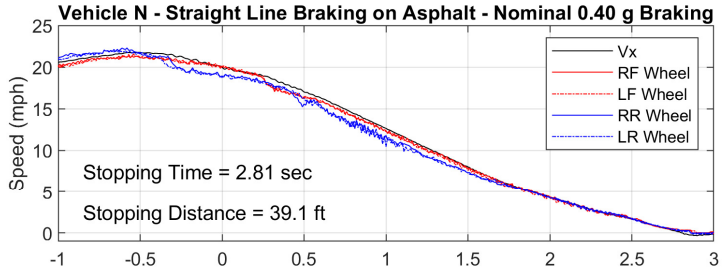

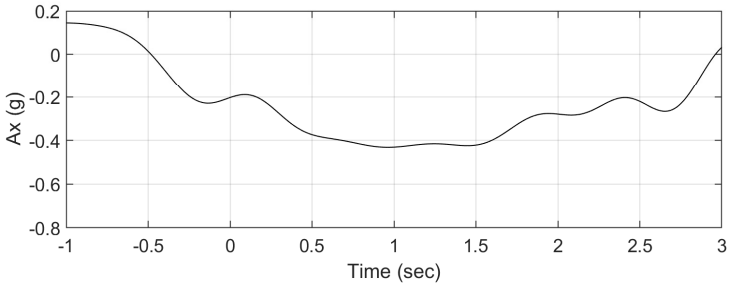

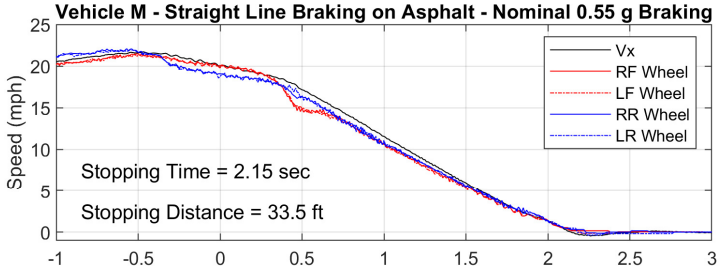

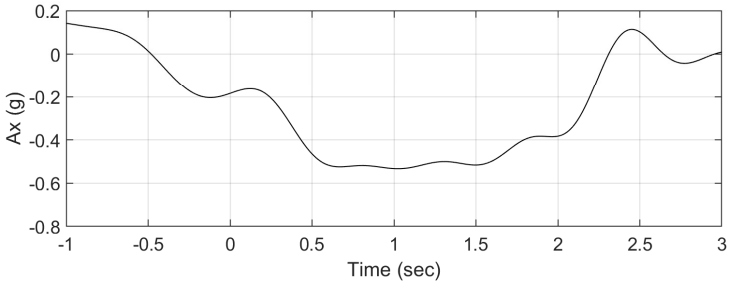

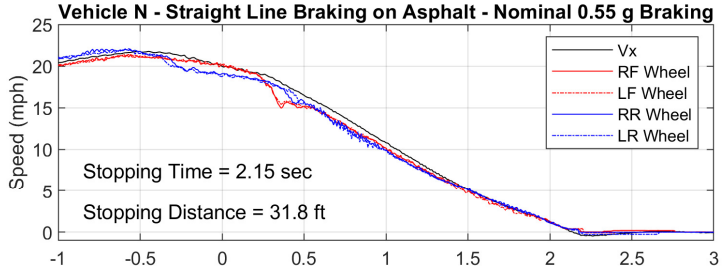

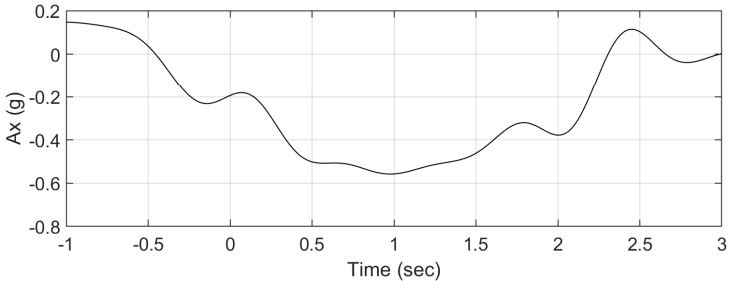

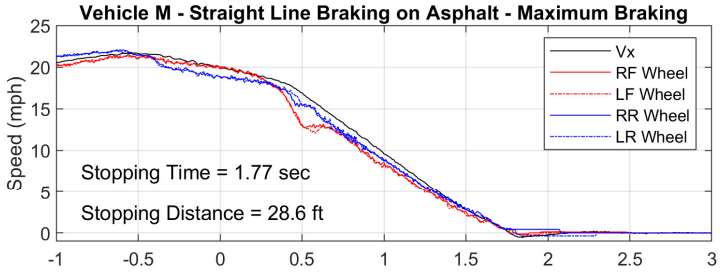

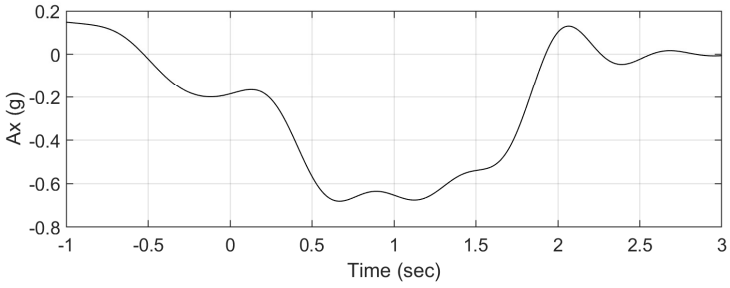

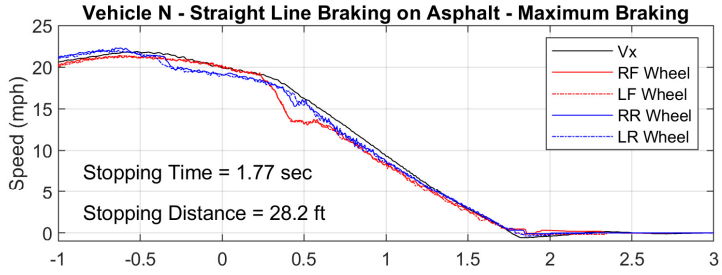

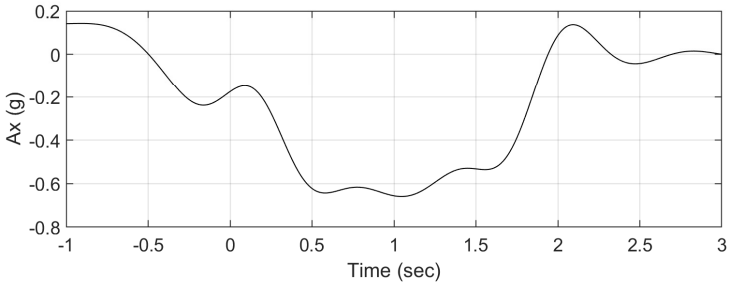

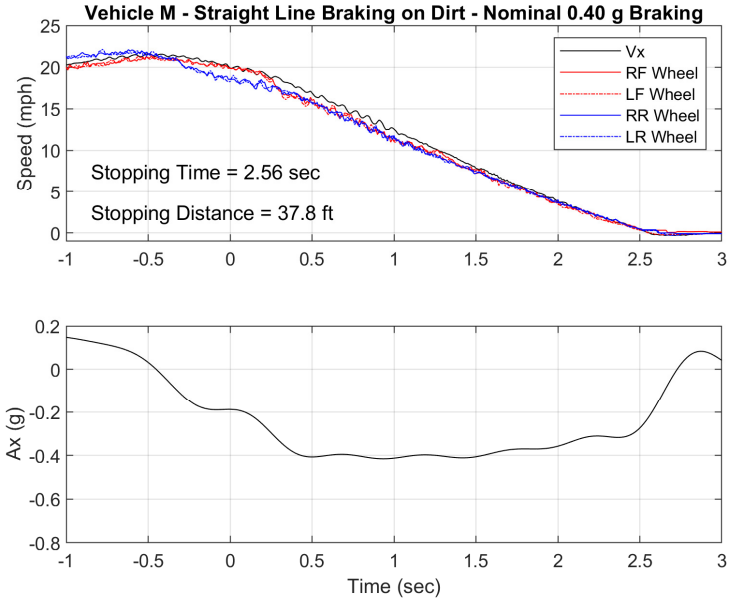

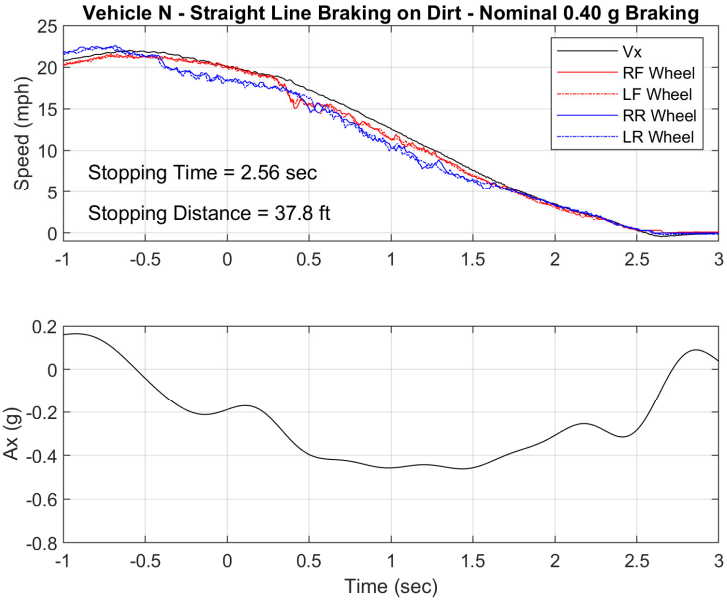

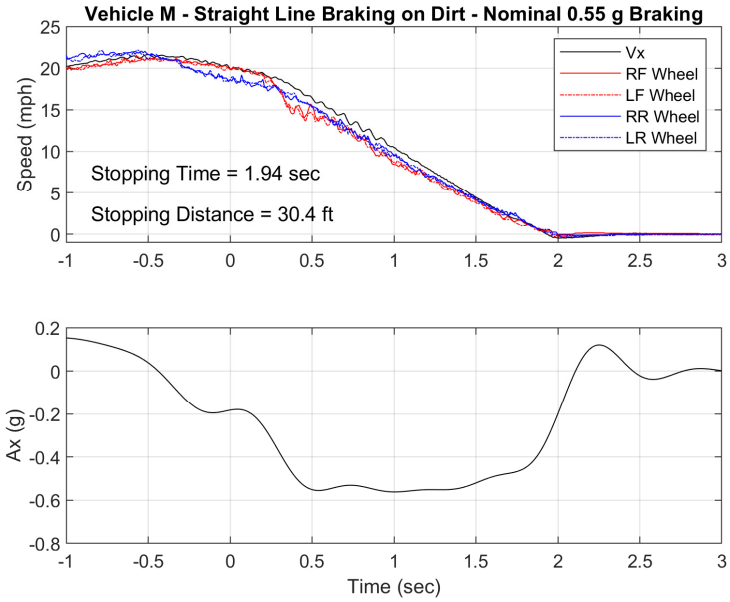

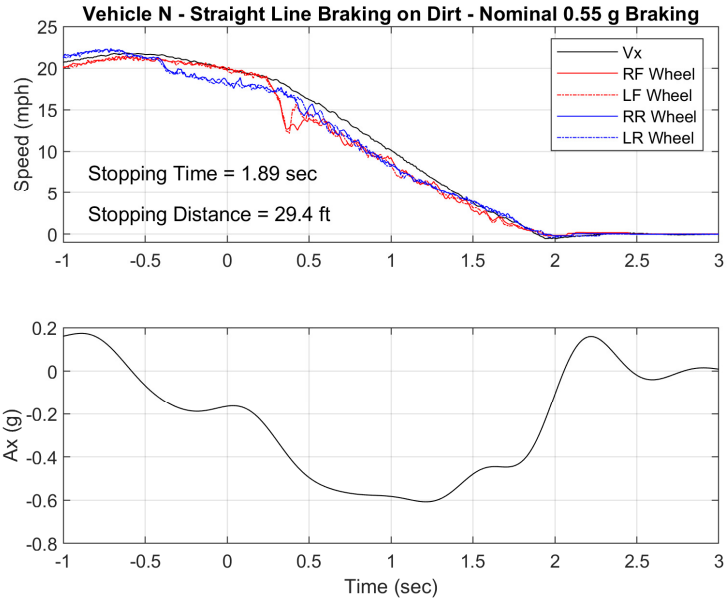

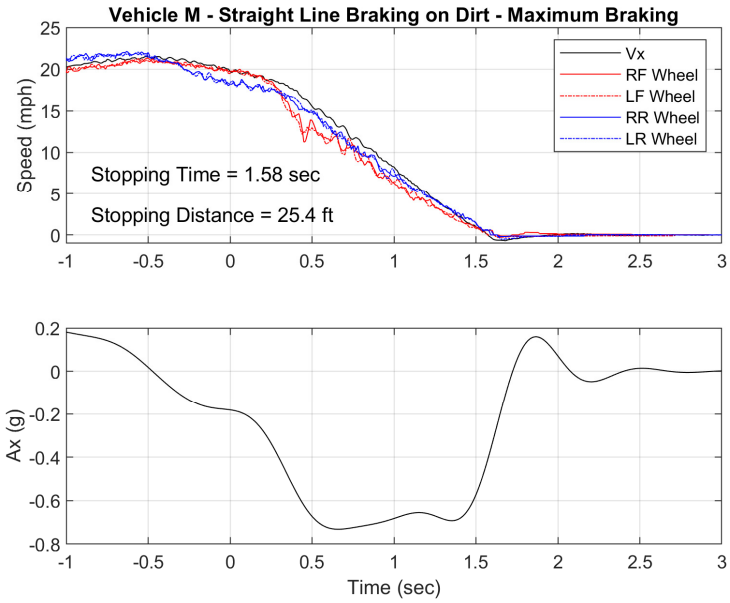

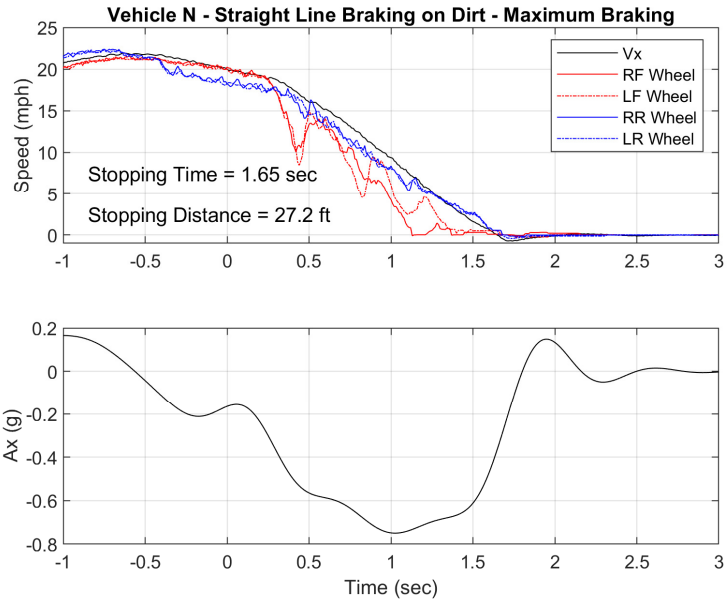

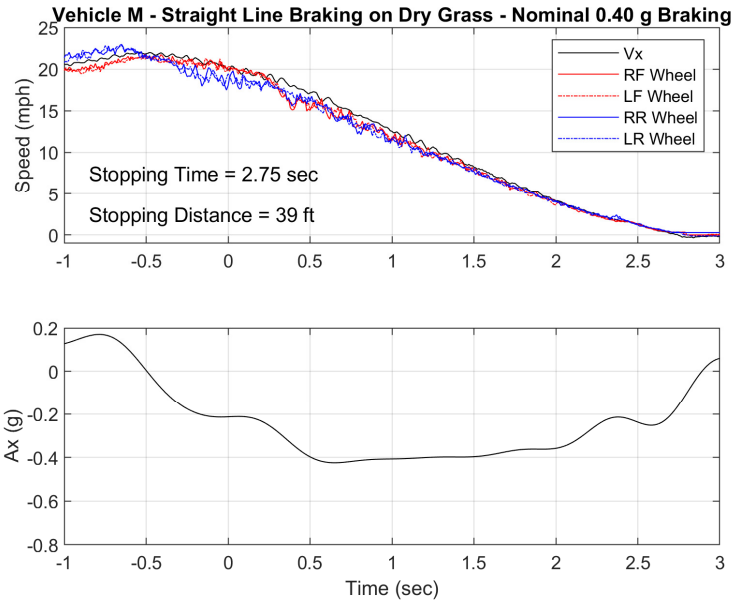

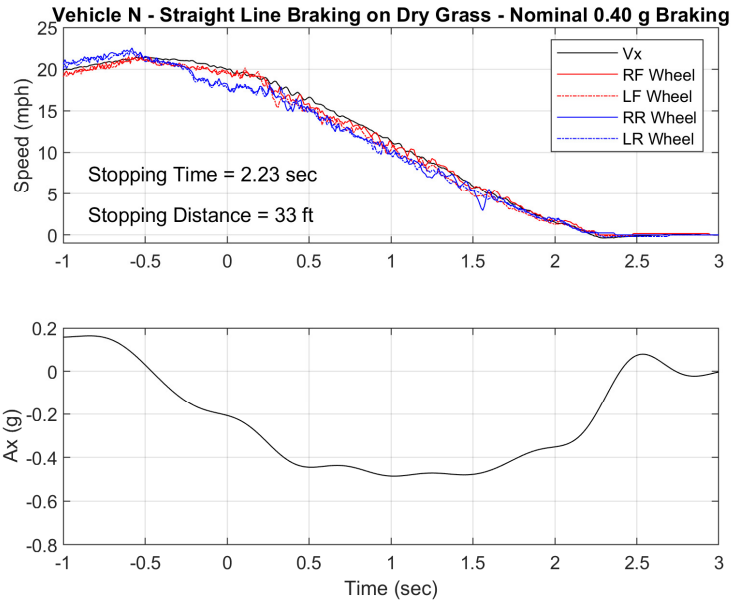

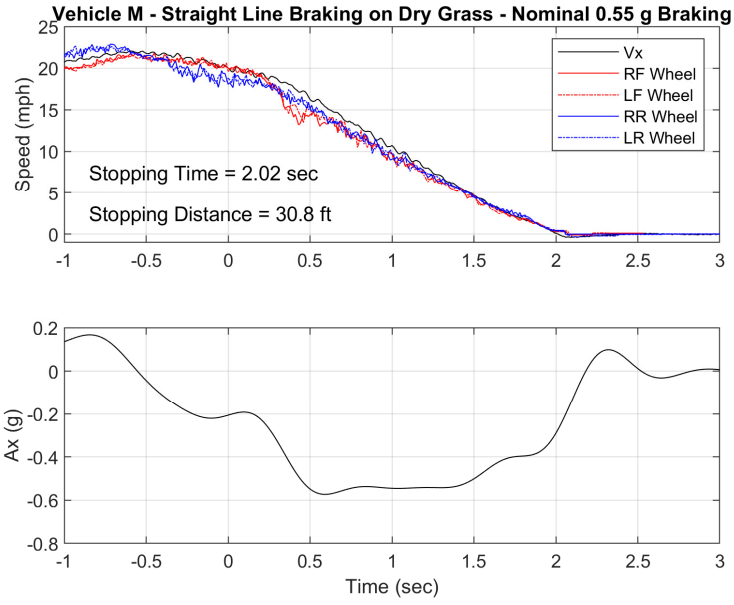

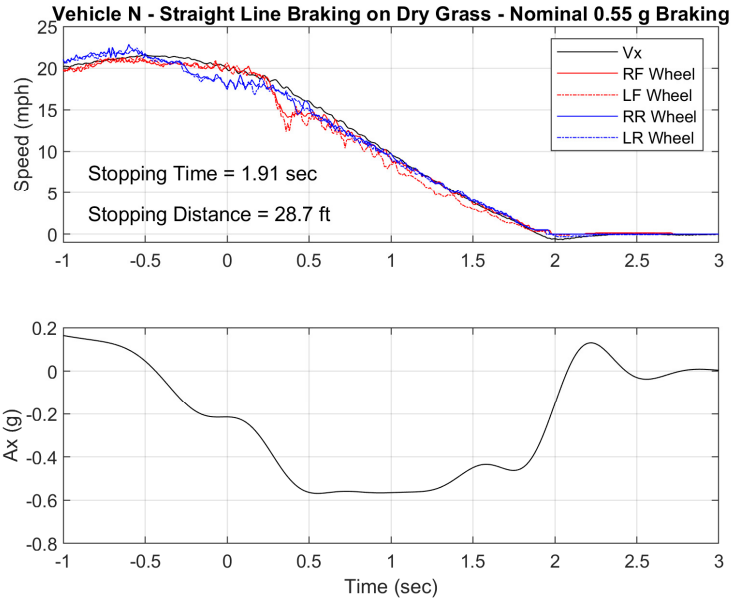

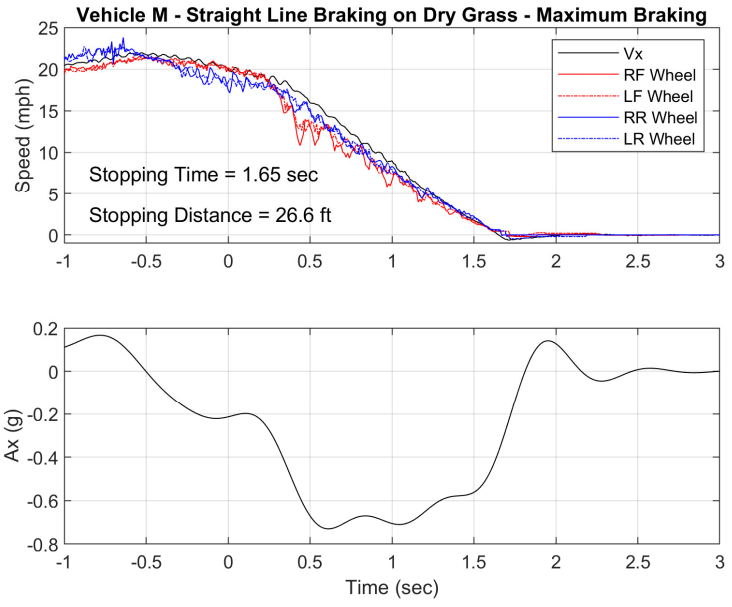

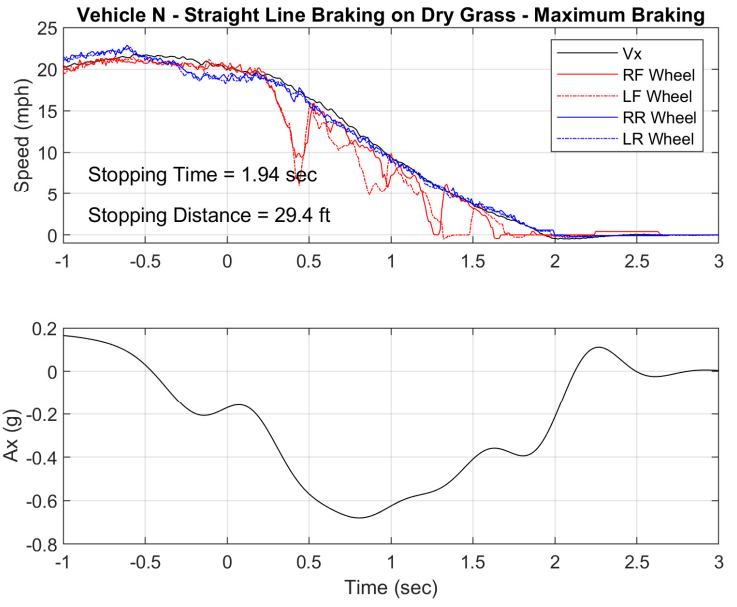

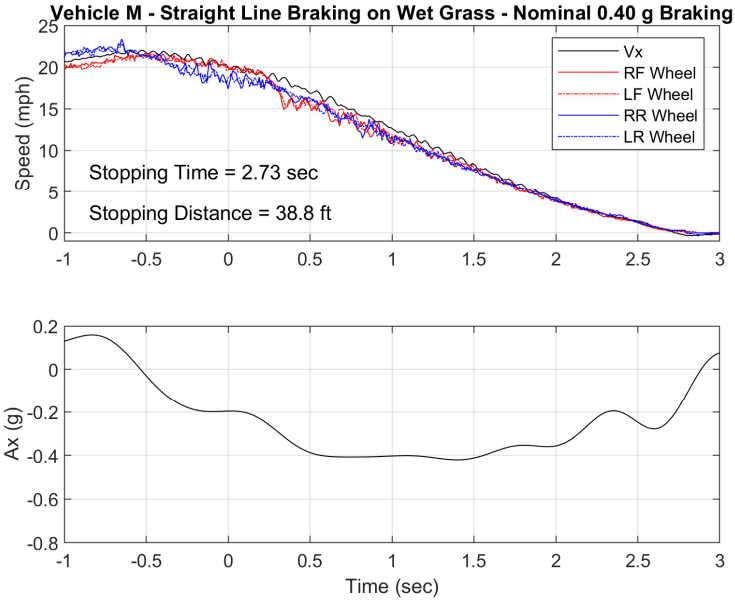

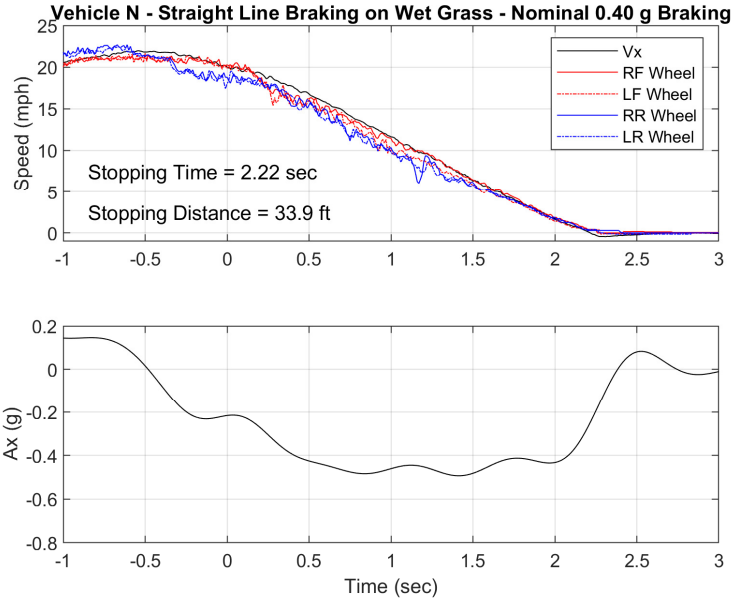

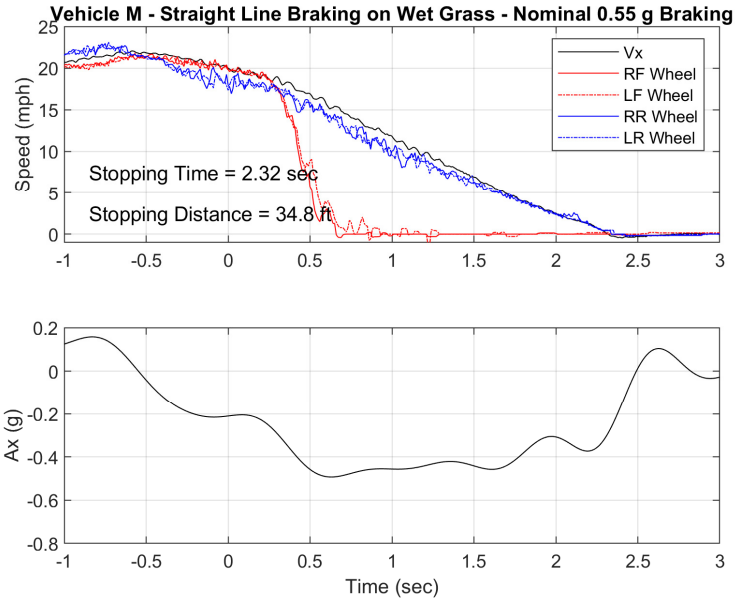

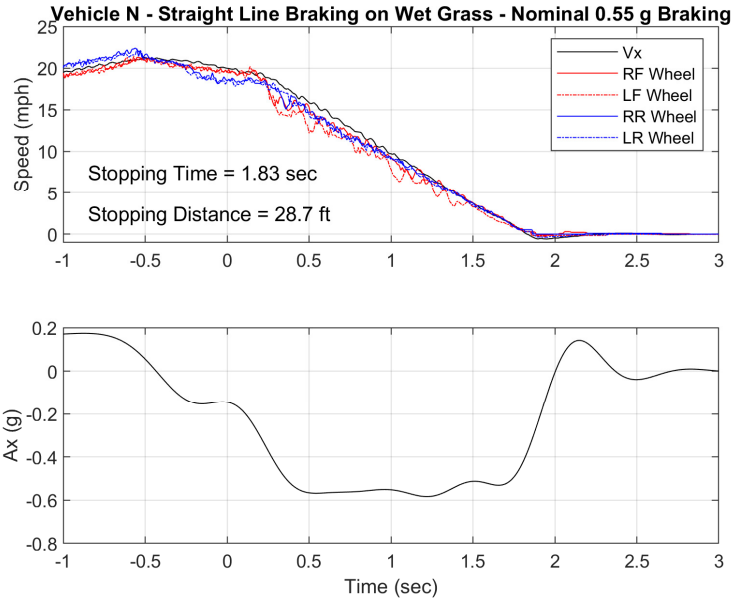

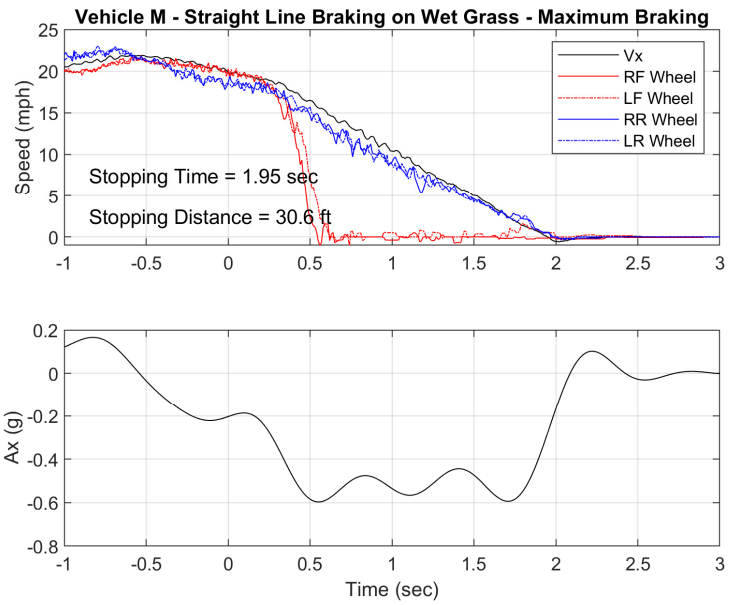

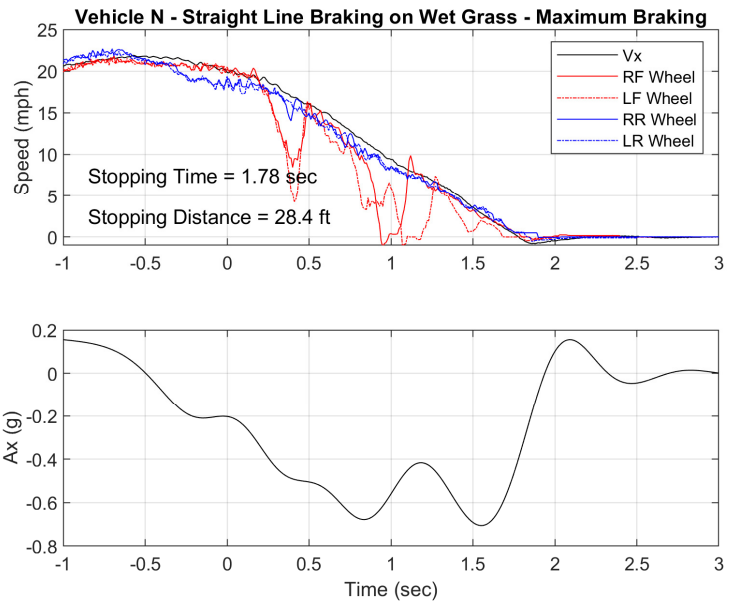

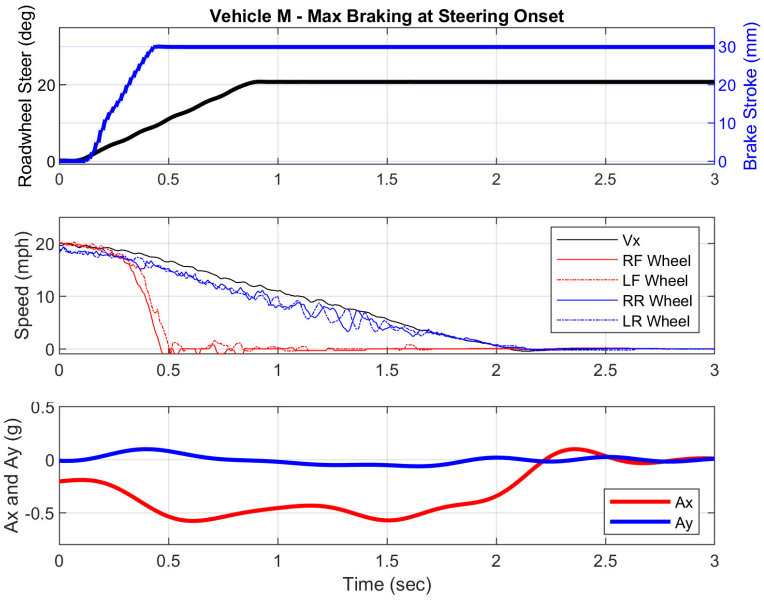

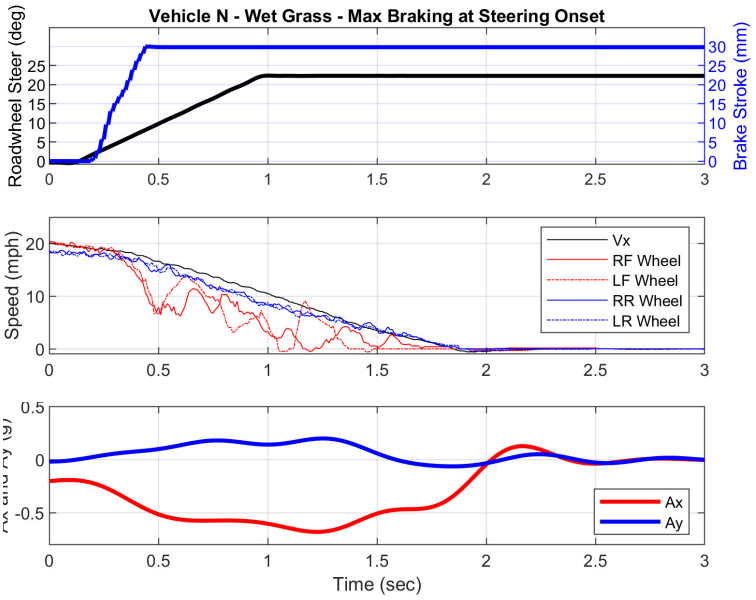

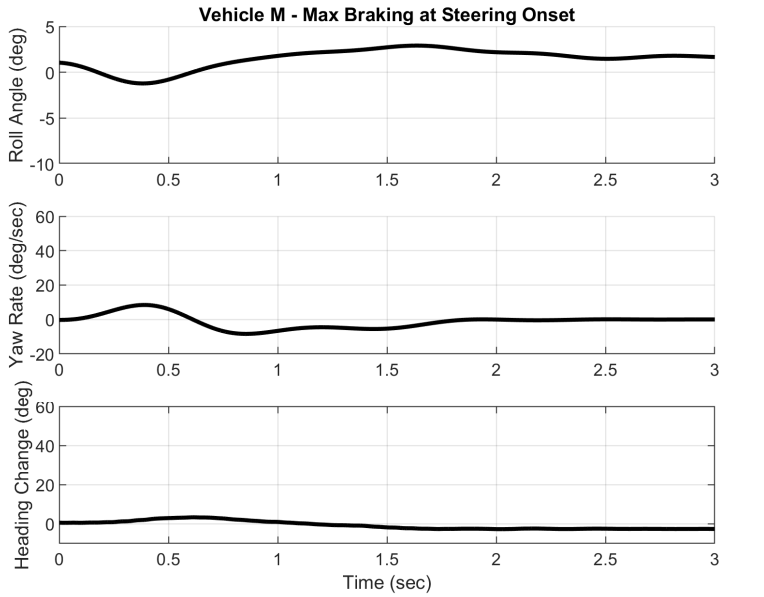

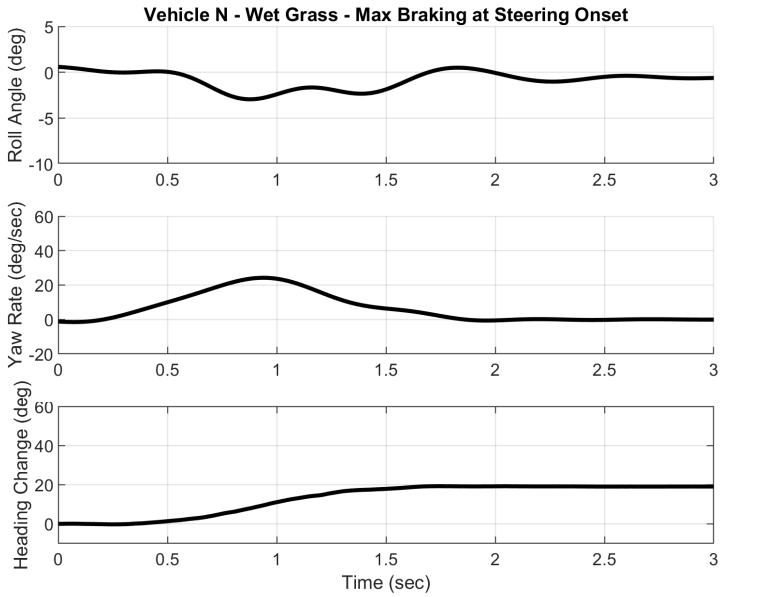

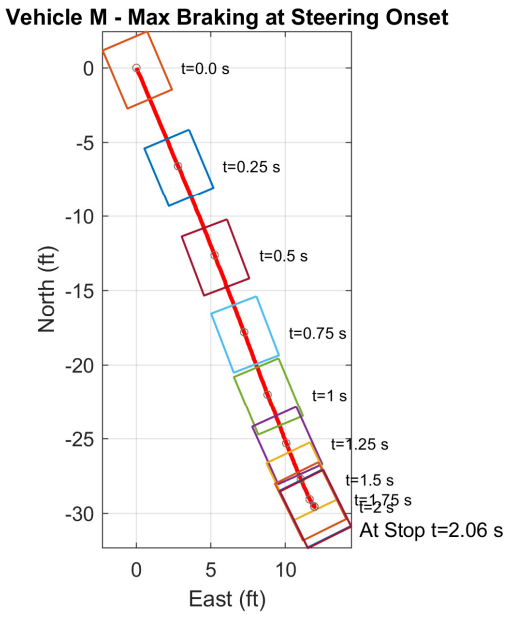

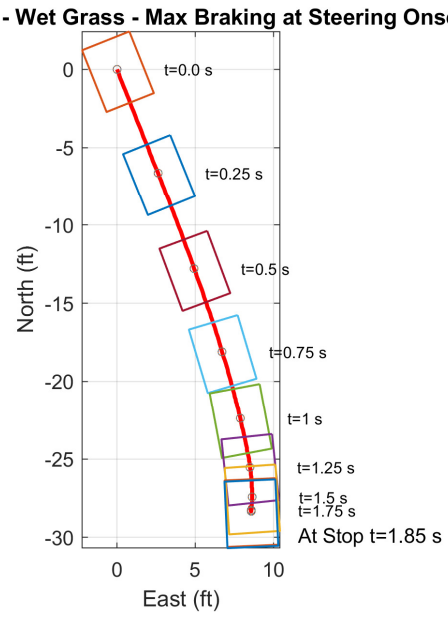

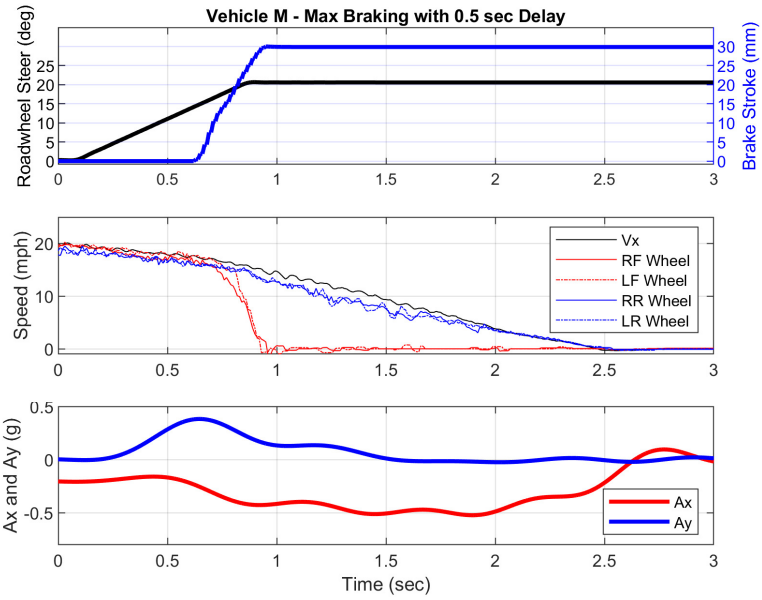

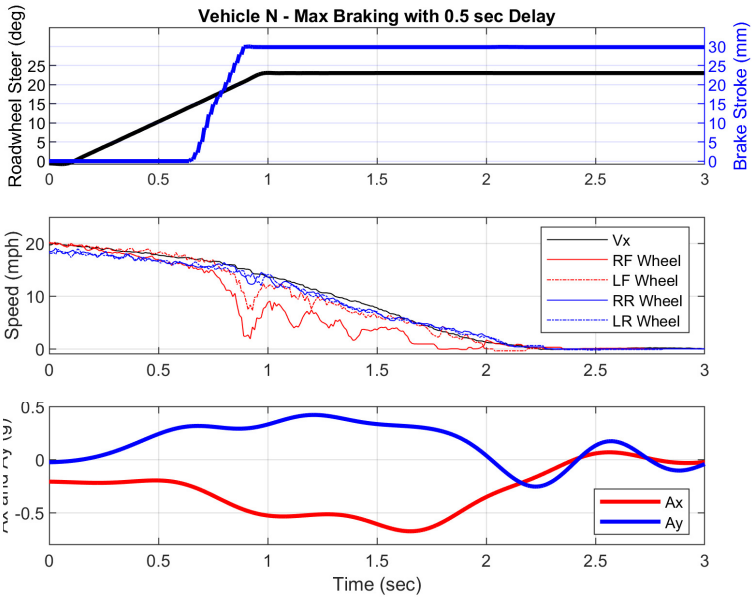

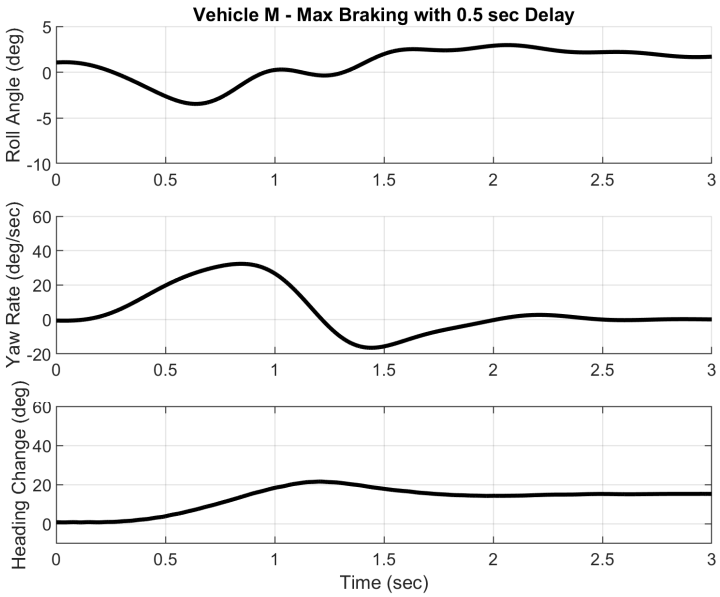

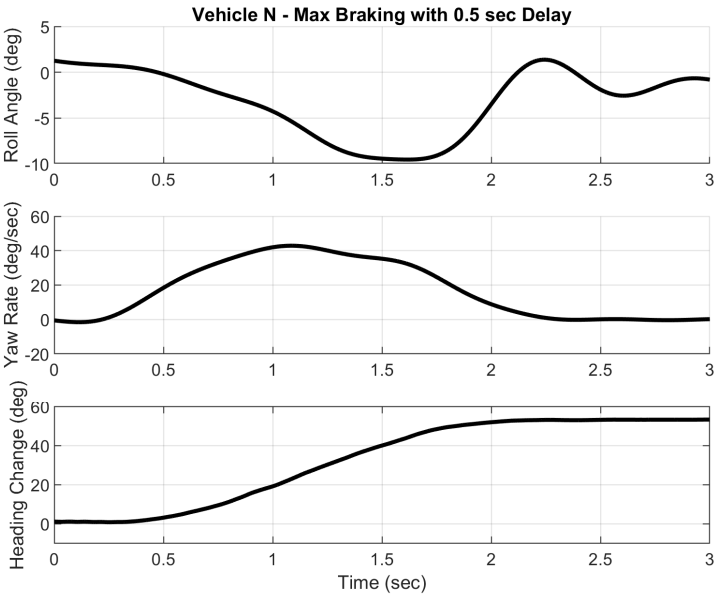

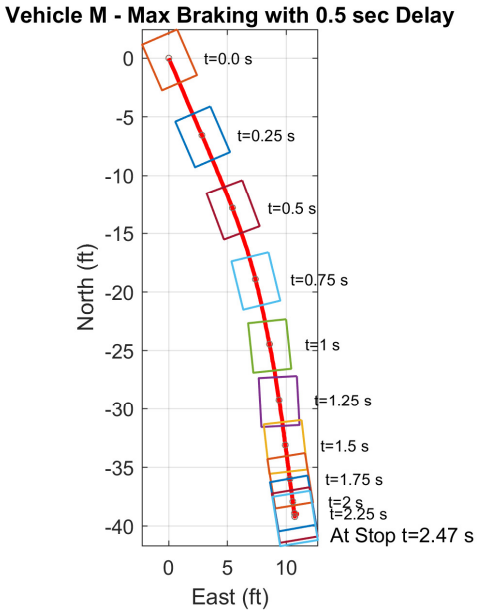

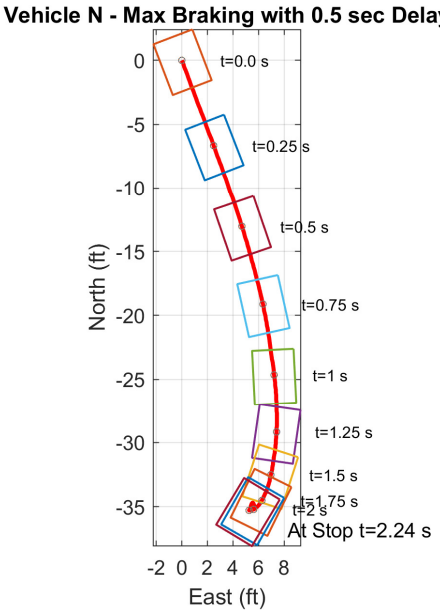

SEA Tilt Table

Side View of Test Vehicle

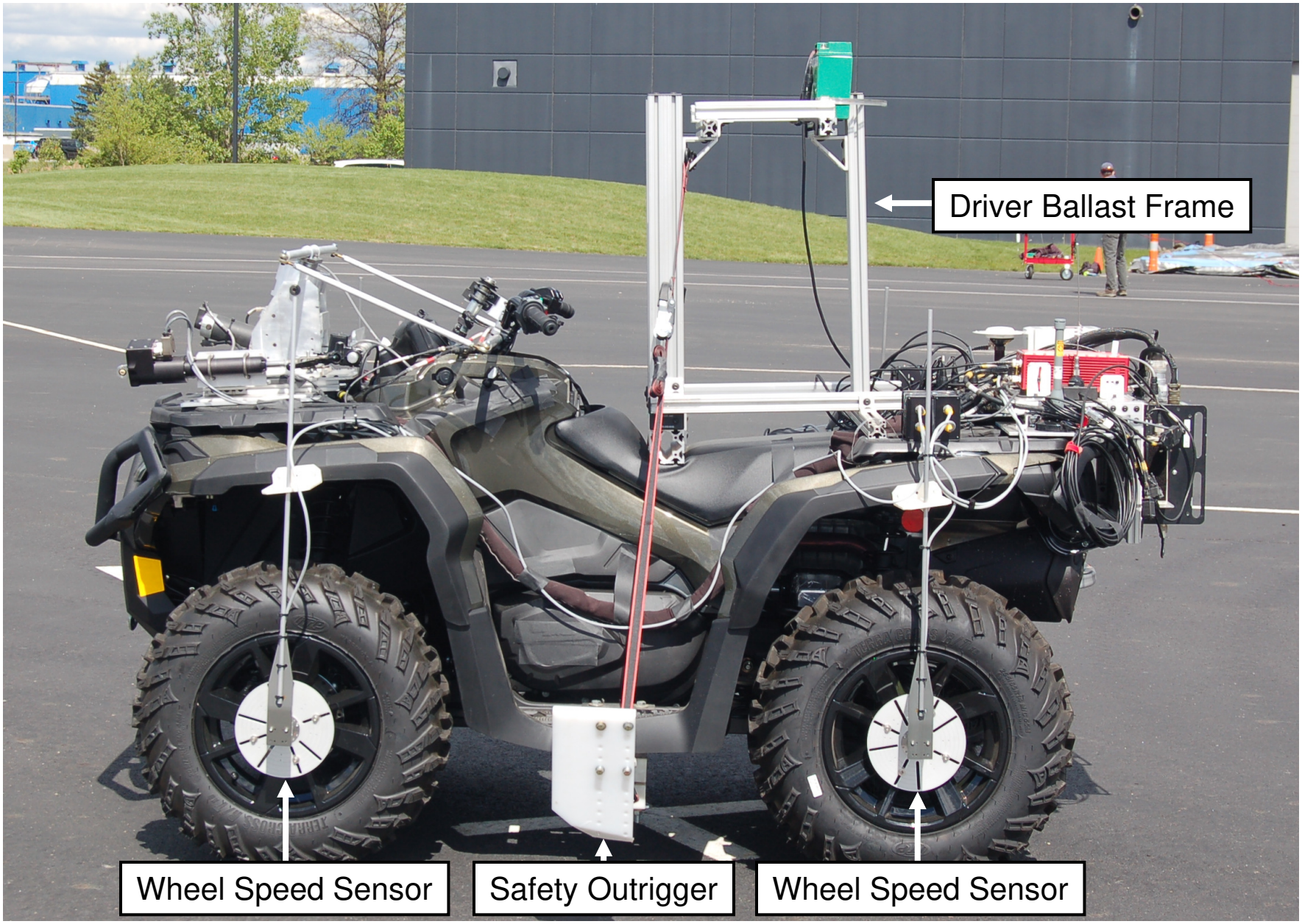

SEA ATV Robotic Test Driver (RTD) Components (Steer, Throttle, and Brake Actuators)

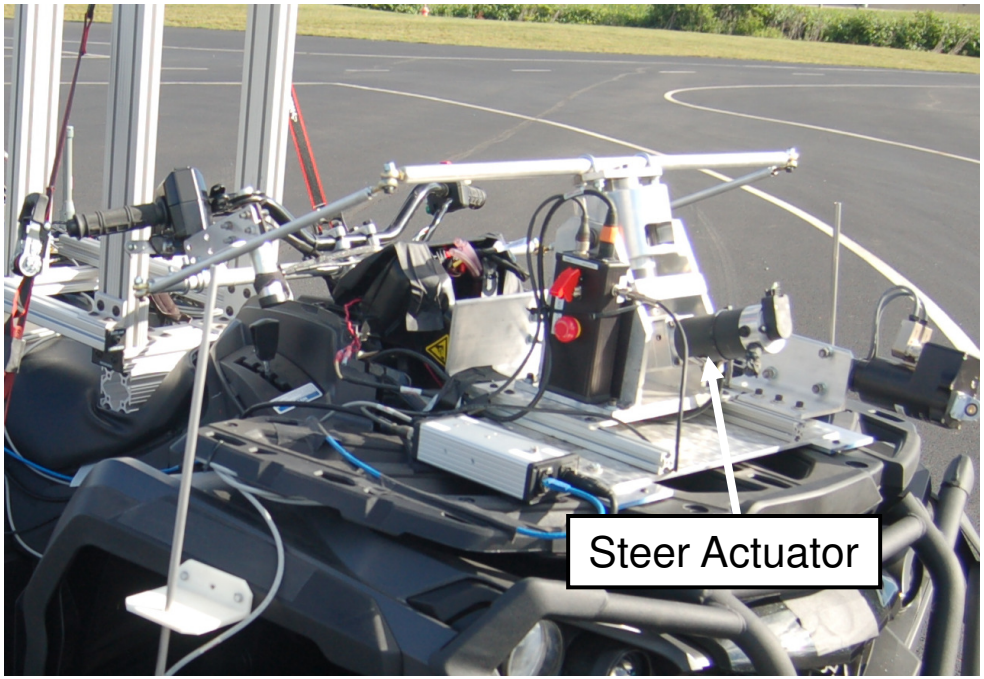

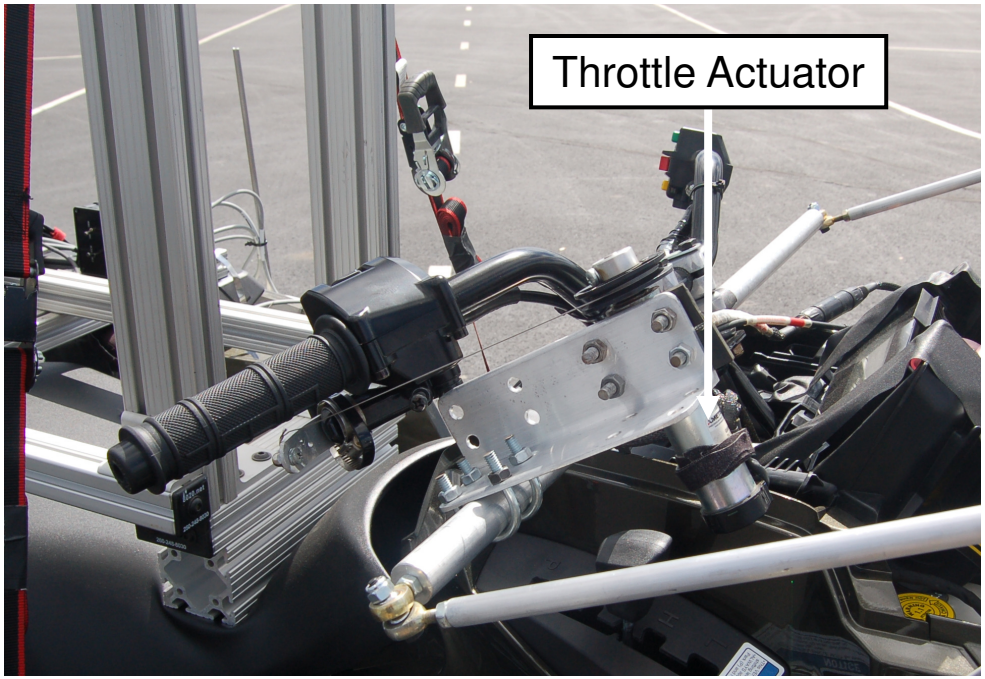

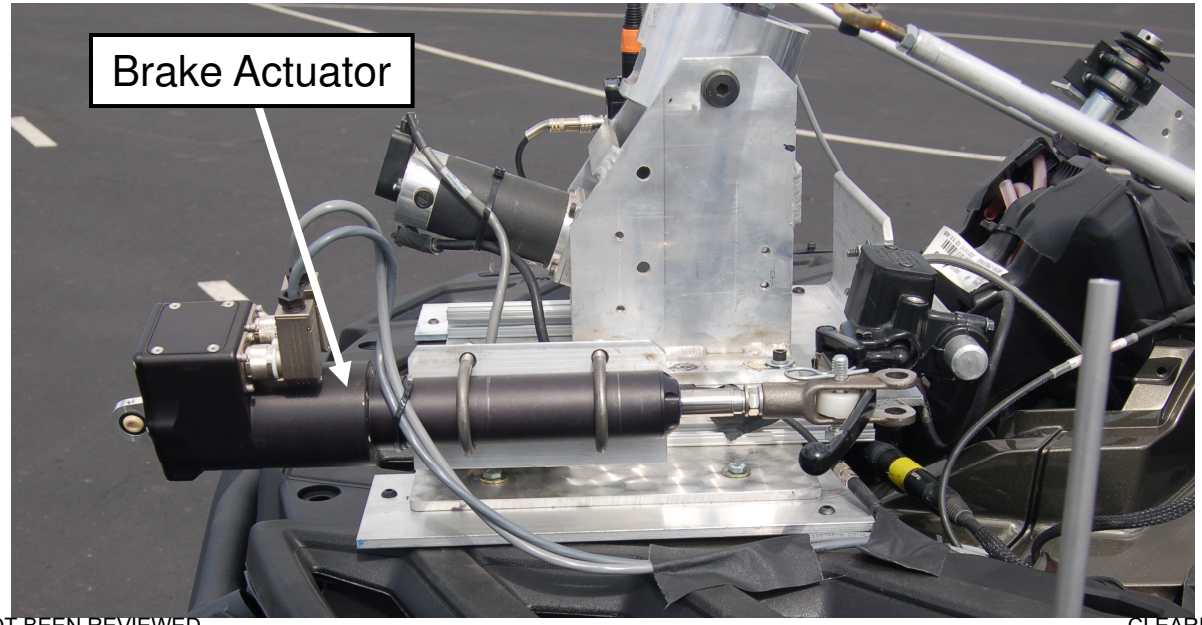

SEA ATV Robotic Test Driver (RTD) Components (GPS/IMU, Control Box, and Antennas)